Curriculum Vitae

NAME: Kerrick J. Nevels

DEGREE AND DATE TO BE CONFERRED: Ph.D., 2011

COLLEGIATE INSTITUTIONS ATTENDED:

2011 Ph.D., Pharmaceutical Sciences, University of Maryland, School of Pharmacy, Baltimore, MD

2000 Dual B.S., Biology/General Science Education, Rust College, Holly Springs, MS
Minor - Chemistry

PROFESSIONAL PUBLICATIONS

Jun Zhang, Taiji Oashi, Kerrick J. Nevels, Ramin Samadani, Kim Burkhard, U. Deva Priyakumar, Edvin Pozharskiy, Paul Shapiro, Alexander D. MacKerell, Jr. (2011). Chemical control of a signaling crossroad: ATP-independent ERK2 inhibitors targeting substrate docking domains. (submitted)

Venkataswarup Tiriveedhi, Kelly Kitchens, Kerrick J. Nevels, Hamid Ghandehari, Peter Butko. (2011). Kinetic analysis of the interaction between poly(amidoamine) dendrimers and model lipid membranes. *Biochim Biophys Acta*. **1808**(1): 209-18

Xiaochuan Li, Kerrick J. Nevels, Marianne Pusztai-Carey, Dexuan Xie, and Peter Butko. (2009). A molecular dynamics model of the Bt toxin Cyt1A and its validation by resonance energy transfer. *Biophysical Chemistry*. **144**: 53-61

Uwe Fass, Kiran Panickar, Katrina Williams, Kerrick Nevels, David Personett, and Michael McKinney. (2004). The role of glutathione in nitric oxide donor toxicity to SN56 cholinergic neuron-like cells. *Brain Research*. **1005**(1-2): 90-100

PRESENTATIONS

Kerrick Nevels, Paul Shapiro and Peter Butko (2010). Fluorescence resonance energy transfer (FRET) as a technique to study interactions of small-molecule inhibitors with MAP kinase ERK2. Poster presented at the Graduate Research Conference in Baltimore, MD.

Kerrick Nevels, Paul Shapiro and Peter Butko (2010). Binding of small-molecule inhibitors to MAP kinase ERK2, studied with resonance energy transfer (RET). Poster presented at the 54th Biophysical Society Meeting in San Francisco, CA.

Kerrick Nevels et. al. (2008). Site-directed mutagenesis of the Bt toxin Cyt1A for intramolecular distance determination by FRET. Poster presented at the 52nd Biophysical Society Meeting in Long Beach, CA.

Kerrick Nevels and Peter Butko (2007). Lipid specificity of the Bt toxin/membrane interactions. Poster presented at 2007 American Society for Biochemistry and Molecular Biology annual meeting in Washington, DC and at the 18th Annual Mississippi Academy of Sciences in Starksville, MS.

Kerrick Nevels and Peter Butko (2006). Determination of intramolecular distances in the Bt toxin Cyt1A by FRET and molecular dynamics simulation. Poster presented at the 50th Biophysical Society Meeting in Salt Lake City, UT.

Kerrick Nevels and Peter Butko (2006). Determination of intramolecular distances in the Bt toxin Cyt1A by FRET and molecular dynamics simulation. Oral presentation at the 17th Annual Mississippi Academy of Sciences in Vicksburg, MS.

Kerrick Nevels (1999). Computational modeling of a canine heart cell. Poster presented at the National Minority Science Symposium in Phoenix, AZ.

ASSOCIATION MEMBERSHIPS

Biophysical Society
Rho Chi Honor Society

HONORS AND AWARDS

2010 Graduate Student Association Travel Award
2009 Graduate Student Teaching Fellowship Award
2007 Minority Biophysicists Travel Grant recipient (2007)
2007 Wood-Whelan International Research Fellow (2007)
2007 Biotechnology Institute Minority Fellow (2007)
2004-2005 GK-12 Fellow
2002 Teacher of the Year
2000 Summa Cum Laude

COMMUNITY INVOLVEMENT

Served as News Editor for the UMB Campus Connection Newspaper
Mentored for Big Brothers/Big Sisters program
Mentored for National Guard Youth Challenge Program

Abstract

Title of Dissertation: Study of the Interactions Between Mitogen-Activated Protein Kinases and Small Molecule Inhibitors of Substrate Proteins Using Fluorescence Spectroscopy

Kerrick J. Nevels, Doctor of Philosophy, 2011

Dissertation Directed by:	Paul Shapiro, Ph.D. Associate Professor Pharmaceutical Sciences School of Pharmacy	Peter Butko, Ph.D. Professor Chemistry Graduate School of Science

The extracellular-signal-regulated kinase (ERK) proteins belong to the mitogen-activated protein kinase (MAPK) family. In addition to participating in important cell signaling pathways involved in normal cellular functions, unregulated activation of the ERK pathway promotes the proliferation and survival of cancer cells. As such, targeted inhibition of the ERK pathway is a goal in the development of new anti-cancer drugs. Given the importance of the ERK pathway in regulating normal cellular processes, we sought to identify small molecules that can selectively inhibit ERK interactions with protein substrates that promote cancer cell proliferation, but preserve ERK functions in normal cells. To accomplish this, computer-aided drug design (CADD) was used to identify low molecular weight compounds that are predicted to interact with specific substrate docking sites on ERK2. In addition, chemical modifications were made to explore structure-activity relationships. The results of the studies demonstrate how steady-state fluorescence spectroscopy methods can be used to rapidly identify ERK-targeted compounds, determine binding affinities, and evaluate the specificity for the ERK proteins as compared to the structurally related MAPK proteins.

Study of the Interactions Between Mitogen-Activated Protein Kinases and Small Molecule Inhibitors of Substrate Proteins using Fluorescence Spectroscopy

by
Kerrick J. Nevels

Dissertation submitted to the faculty of the Graduate School
of the University of Maryland, Baltimore in partial fulfillment
of the requirements for the degree of
Doctor of Philosophy
2011

Table of Contents

Chapter Page

Chapter Page

List of Tables

List of Figures

Figure Page

CHAPTER 1: General Introduction - Background into the MAP Kinase Family of Proteins

1.1 Mitogen-Activated Protein Kinase Signaling Pathway

The ERK family of proteins are mitogen-activated protein kinases (MAPK's). Multiple MAPK pathways exist in all eukaryotic cells [1]. The signaling pathways of MAPK's are involved in various cellular events such as cell differentiation, cell proliferation, and apoptosis [2, 3]. The signaling cascades of MAPK's generally follow a similar pattern as shown in Figure 1.1. MAPK kinase kinase (MAPKKK or MEKK) are activated when extracellular ligands bind to receptors on the surface of the cell [4]. Small GTP-binding proteins and/or adaptor proteins stimulate MAPKKK's to phosphorylate MAPK kinases (MAPKK or MEK) via threonine and tyrosine residues [1]. Active MAPKK in turn activate MAP kinases which in turn phosphorylate downstream substrates such as mitogen-activated protein-kinase-activated protein (MAPKAP) kinases and transcription factors [1]. MAPK's are activated by specific MAPKK's. However, each MAPKK can be phosphorylated by several different MAPKKK's. This allows for diversity in the phosphorylation of MAPK pathways upstream of the MAPKK [2].

Three well studied MAPK pathways include the extracellular signal-regulated kinase (ERK1/2), p38 MAPK, and the c-Jun N-terminal kinase (JNK also known as stress-activated protein kinase or SAPK) [5]. The MAPK's are 60-70% identical to each other; however, they have different activation loop sequences and sizes [6]. Also each group may be activated by different stimuli. ERK1/2 is often activated via growth factors and phorbol esters [5] whereas p38 is activated primarily in response to inflammation and stress [7]. ERK1 and ERK2 share 90% identity [8] and have been the focus of many studies [9-18].

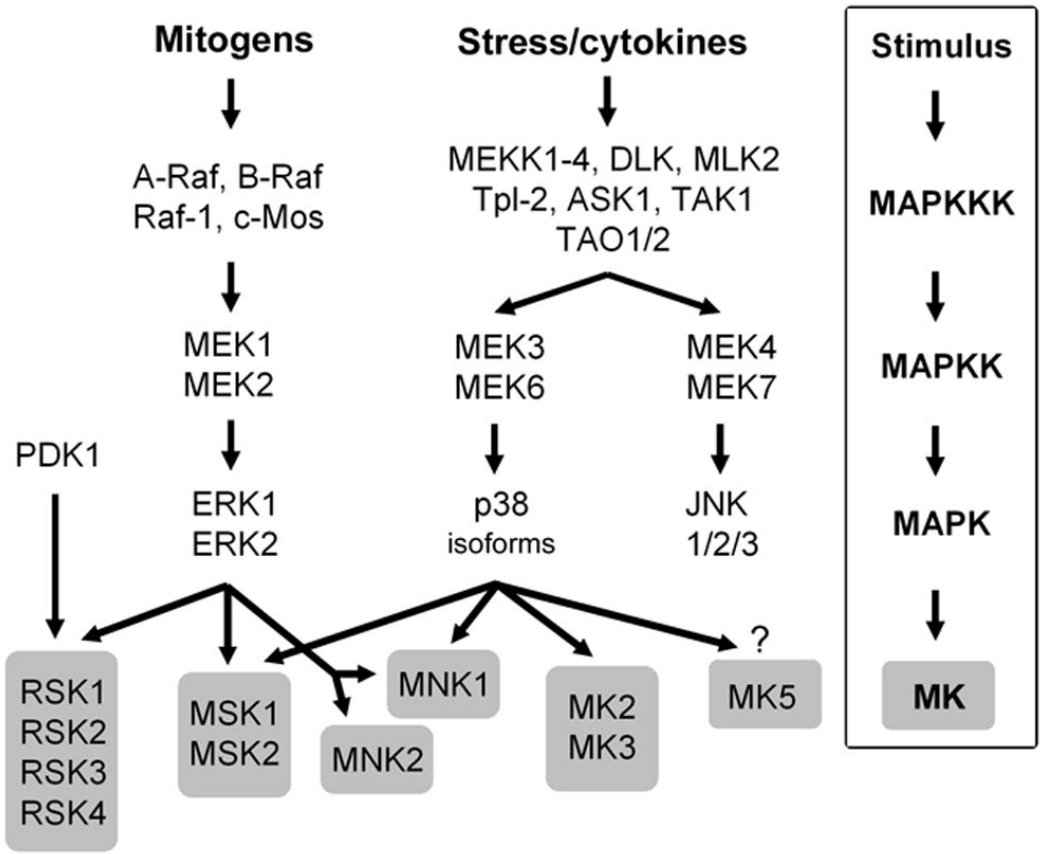

Figure 1.1. Overview of MAP kinase signaling cascade. In general, extracellular stimuli such as mitogens and/or cellular stresses lead to the activation of the ERK1/2, p38, and JNK pathways (for example) by signaling small GTP binding proteins to activate MAPKK kinases to phosphorylate MAPK kinases which in turn dually phosphorylate MAP kinases. Upon activation, MAP kinases regulate a variety of target substrates. This figure was reprinted from Roux et al. [1].

The ERK1 and ERK2 proteins participate in important cell signaling pathways involved in normal cellular functions. In addition, it has been shown that unregulated activation of the ERK pathway promotes the proliferation and survival of cancer cells. As such, targeted inhibition of the ERK pathway is a goal in the development of new anti-cancer drugs. Given the importance of the ERK pathway in regulating cellular processes in normal and disease tissue, an objective of the Shapiro lab is to identify inhibitors that can selectively prevent ERK regulation of substrates that promote diseases, such as cancer, but preserve ERK functions in normal cells.

1.1.1 ERK1/2 structure and activation

The ERK family of proteins consist of several members designated ERK1-8. ERK 1 and ERK 2 are the primary members of the ERK family and share 90% amino acid identity. The crystal structure of both the unphosphorylated and phosphorylated forms of ERK2 [19, 20] represents ERK as a bilobal structure similar to other protein kinases. The N-terminal domain is composed mostly of β-strands and two α-helices while the C-terminal domain is composed primarily of α-helices with four short β-strands. The β-strands of the C-terminal domain contain several residues involved in catalysis [21]. The active site of ERK1/2 is located at the interface of the two domains. ERK2 is activated via dual phosphorylation of the amino acids T183 and Y185, numbered according to the sequence of *Rattus norvegicus*. These two sites of phosphorylation are located in the activation loop. Both sites must be phosphorylated for ERK to be highly active, as a mutation of either amino acid results in a decrease in activity of ERK1 or ERK2 [15]. More specifically in ERK1/2, surface receptors on the plasma membrane are

activated by extracellular stimuli such as growth factors and hormones causing the recruitment of adapter proteins and the sequential phosphorylation of three kinase groups: Raf kinases, MAP or ERK kinases 1 and 2 (MEK1/2), and ERK1/2 [2, 21, 22]. An overview of the signaling cascade of ERK1/2 is shown in Figure 1.2. The small GTP binding protein, Ras, is stimulated to convert GDP to GTP which then interacts with Raf initiating its phosphorylation and subsequent activation. Once activated, Raf phosphorylates the dual specificity kinases MEK1/2. MEK1/2 are the only known MAPKK's to activate ERK1/2. MEK1/2 then phosphorylates the amino acid Y185 and in a subsequent reaction amino acid T183 within the conserved TXY motif within the activation loop of ERK1/2 [14, 23]. ERK1/2 is localized in the cytoplasm via interactions with scaffold proteins. About 60% of the ERK translocates to the nucleus upon stimulation [10, 24]. ERK1/2 then activates substrates downstream including nuclear substrates and transcription factors that are involved in various cellular responses such as cell growth, differentiation, and survival [1, 2]. ERK1/2 is involved in many normal cellular functions as suggested by the more than 160 substrates identified to interact with ERK1/2 [25, 26]. In addition, unregulated activation of the ERK pathway due to mutations in Ras and Raf proteins and receptor tyrosine kinases is thought to contribute to the proliferation, survival and metastasis of cancer cells [27]. Therefore, the development of pharmacologic inhibitors that selectively target ERK substrates involved in cell proliferation and survival of cancer cells without interfering with normal cell processes involving the ERK pathway would prove beneficial.

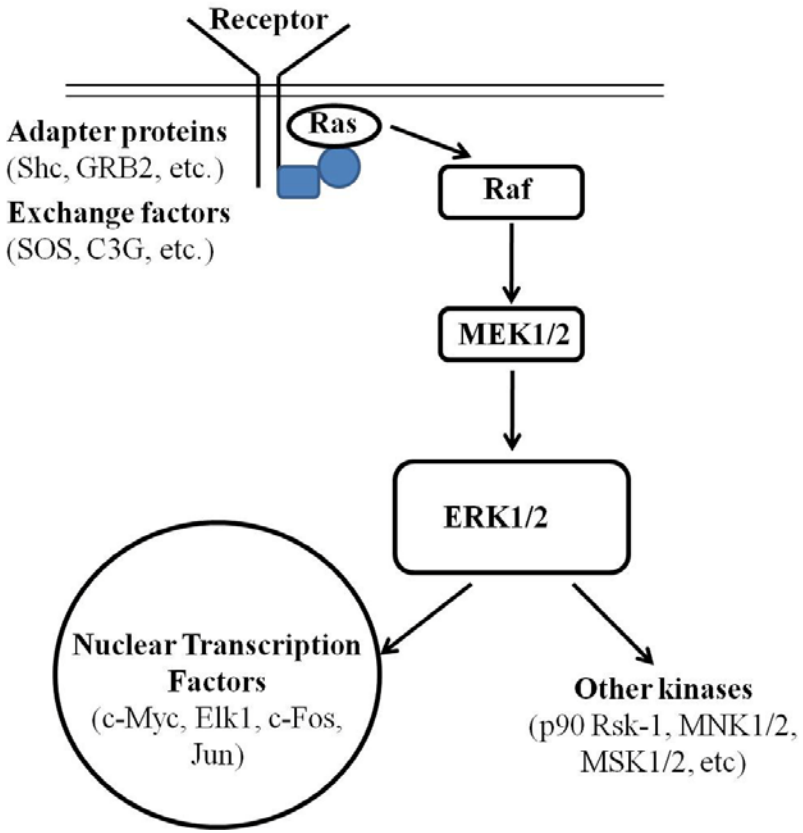

Figure 1.2. ERK 1/2 MAP kinase signaling pathway. Receptors involved in growth and differentiation (receptor tyrosine kinases (RTK's), integrins, etc.) initiate the MAPK/ERK signaling cascade. A set of adaptors (Shc, GRB2) and exchange factors (SOS, C3G) recruit small GTP binding proteins (Ras), which in turn activate a MAPKK kinase (Raf), followed by the phosphorylation of the MAPK kinase (MEK1/2) and then the MAP kinase (ERK1/2). ERK1/2 in turn regulates a number of cytosolic signaling proteins and kinases as well as translocates to the nucleus where it phosphorylates various transcription factors regulating gene expression.

1.1.2 ERK1/2 substrate docking domains.

ERK substrates contain two domains that have been shown to increase specificity to ERK. The first site is referred to as the D-domain and consists of a cluster of positively charged residues followed by a hydrophobic LXL (leucine/any amino acid/leucine) motif [28]. The D-domain is conserved in transcription factors, upstream regulatory proteins such as the MAPK kinase (MAPKK) MEK1/2 and the p90 ribosomal S6-kinase 1 substrate (p90Rsk1) as well as several phosphatases that interact with ERK1/2 such as the MAP kinase phosphatase 3 (MKP3) [1, 29, 30].

A second domain found on ERK substrates is the F-domain or DEF motif [31]. It is a hydrophobic pocket defined by the motif FXFP: two phenylalanines separated by a non-specific amino acid (X) and the second phenylalanine is followed by proline. ERK1/2 substrates containing this motif include the transcription factors Elk-1, LIN-1, SAP-1 and the anterior open protein (AOP or YAN) as well the kinase suppressor of RAS (KSR), A-Raf, c-Fos, c-Myc, phosphodiesterase 4D and nucleoporin proteins [10, 31-35]. The DEF motif is also found on substrates of p38 MAP kinase [33]. It has been suggested that the F-domain is necessary for efficient substrate phosphorylation and interaction with specific inactivators by ERK1/2 [1, 9, 32, 36]. It has been shown that the F-domain of MKP3 is necessary for the ERK2-induced MKP3 activation [37]. Furthermore, a peptide derived from Elk-1 containing the DEF motif and the phosphoacceptor sequence in part blocked the ERK2-induced activation of MKP3 [9], suggesting that the DEF motif interacts with a substrate binding region (F-site) on ERK2. In some substrates such as Elk-1 and the scaffold protein KSR-1, both ERK-substrate docking domains can be found and may act together to enhance protein interaction and

substrate phosphorylation [1]. It has been shown in our lab that protein interactions between ERK2 and Elk-1 was largely inhibited by mutations within the F-site of ERK2. Moreover, mutations in both the F-site and the CD/ED domain completely disrupted interactions between the ERK2 and Elk-1 [36].

1.1.3 ERK1/2 docking domains.

The D-domain of ERK substrates interacts with ERK via the common docking domain (CD-domain) located in the C-terminal lobe of ERK1/2 (Figure 1.3). The CD domain is also referred to as the D-recruitment site (DRS) and is located on the opposite face of ERK2 relative to the active site [38]. The CD-domain of ERK2 contains both acidic residues (D316 and D319) and hydrophobic residues that form electrostatic and hydrophobic interactions with the basic (lysine/arginine) and hydrophobic residues of the D-domain to facilitate protein-substrate interaction [9, 30, 39-42]. The CD domain is known to facilitate interactions with the upstream activating kinase MEK1, the regulatory MAP kinase phosphatase 3 (MKP-3) protein and the MAP kinase-interacting kinase 1 (Mnk1), the ERK1/2 effectors Elk1, p90 ribosomal S6 kinase-1 (RSK-1), caspase 9, and phosphatases such as the tyrosine phosphatase PTP-SL, all of which contain a D domain [21, 43-46]. The mitogen- and stress-activated protein kinases (MSKs) contain a D-domain and interact with the CD domain of both ERK1/2 and p38 kinase [47]. Adjacent to the CD-domain of ERK2 is the ED domain (named after E160 and D161 of p38α and the corresponding T157 and T158 residues of ERK2). Exchanging the threonine residues on ERK2 with the glutamate and aspartate residues of the ED domain of p38α enabled ERK2 to recognize and interact with the substrates of the p38 MAP kinase. This suggests

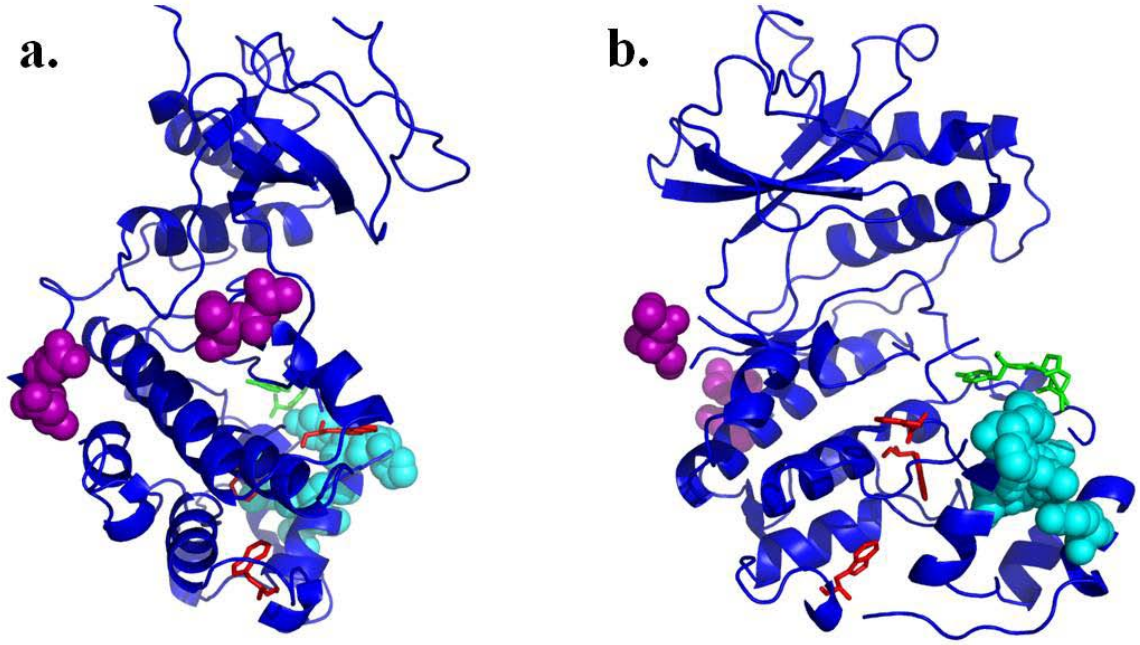

Figure 1.3. ERK2 structure and location of docking domains. The molecule in panel B is rotated around the vertical axis by 90° relative to panel A. The CD and ED domains are in purple. The F-recruitment site is in cyan. The three tryptophans (W190, W210, and W273) are colored red and the activating phosphorylation site (T183 and Y185) green.

that the ED domain of ERK2 confers specificity [41]. Mutating the amino acid residues of the ED domain of p38 with those of the ED domain of ERK2, however, did not alter specificity towards substrates of ERK2. This suggests that more amino acids together with the residues of the ED domain confer specificity of p38 MAP kinase for its substrates. Therefore, the CD and ED domain together confer substrate specificity with MAP kinases [28]. Both the ERK2 inactivator MKP3 and the substrate Elk-1 contain D domains (also referred to as kinase interaction motifs or KIM in several publications) with characteristic positively charged amino acids that interact with the CD domain of ERK2. It has been shown that the CD domain is important for high affinity target binding of ERK2 to its substrate Elk1 and the phosphatase highly specific for ERK2 inactivation MKP3 [9, 48, 49]. Zhang et al., showed that common amino acid residues in the CD/ED site are required for both MKP3 and Elk1 to bind efficiently; however, specific amino acid residues in the CD/ED site of ERK2 are necessary for MKP3 but not Elk1 binding (Y126 and N133) and in contrast necessary for Elk1 binding but does not interfere with MKP3 binding (T157 and T158) [9].

A second substrate recognition site on the ERK protein is the F-site recruitment site (FRS) which contains the residues L198, Y231, L232, L235, and Y261 [10, 31, 34, 35, 38, 50]. The FRS site is located adjacent to the catalytic cleft [38]. Studies have shown that the FRS interacts with the F-domain of ERK substrates. For instance, ERK2 phosphorylation of the DEF motif containing ERK substrate c-Fos was inhibited in the presence of F-domain peptide [51]. Moreover, it has recently been shown that a single residue within the FRS of ERK2 (L232) participates in ERK2 interactions with c-Fos [36].

1.2 Inhibitors of ERK Kinase pathway

1.2.1 Introduction

The MAP kinase signaling pathway is activated when extracellular ligands bind to receptors in the membrane. Stimulation of downstream effectors leads to the activation of RAS which in turn phosphorylates the RAF family of proteins. Activated RAF phosphorylates MEK1/2 which then phosphorylates ERK1/2. Upon activation, a portion of ERK1/2 translocates to the nucleus and signals responses from various downstream effectors, such as cell proliferation and survival mechanisms. Mutations in the receptor, RAS or RAF proteins have been found in many cancers that exhibit constitutive activation of the RAF-MEK-ERK pathway [52, 53]. Blocking the activity of ERK by blocking the Ras/Raf/MEK/ERK pathway is a target for human cancer treatment. Several inhibitors that target Ras, Raf, or MEK have been identified, are in clinical trials and have been or are on the market [27]. But some drawbacks include off target effects that lead to serious and sometimes dangerous side effects and reoccurrence of cancers due to compensatory pathways that restore ERK activity.

1.2.2 BRAF inhibitors

Mutations in BRAF have been reported in several types of cancers including melanoma, ovarian cancer, colorectal cancer, and thyroid cancer [54, 55]. Though there are more than 70 known BRAF mutations [56], most studies have focused on the mutation V600E, most likely because this mutation is one of the largest subgroups of melanomas (~70%).

BAY 43-9006, also known as sorafenib, was approved in 2005 by the Food and Drug Administration (FDA) for the treatment of renal cell carcinoma. Recently it has been used to study effectiveness against thyroid carcinomas and has been involved in phase I trials with patients diagnosed with acute leukemia [57]. It was originally designed to target Raf-1 [58]. Marketed as Nexavar, BAY 43-9006 is a multikinase inhibitor that targets RAF-1 and BRAF, as well as the tyrosine kinase receptors VEGFR-2, VEGFR-3, PDGFR-B, Flt-3, and KIT [58, 59]. The crystal structure of BAY 43-9006 in complex with BRaf was solved and showed that the compound was bound to the ATP pocket and prevented conformational changes of the kinase domain [56]. This led to non-specific inhibition of substrate binding and phosphorylation.

PLX4032, also known as RG7204, is used in the treatment of melanomas and has shown remarkable clinical activity [60]. Unlike MEK inhibitors which suppress ERK signaling in both normal and tumor cells, PLX4032 selectively inhibits the ERK pathway and cell growth in tumor cells harboring the BRaf mutation V600E [61]. Despite the success it has shown in increasing the survival rate of melanoma patients, resistance to PLX4032 has been observed. It was postulated that ERK signaling became insensitive to the therapy in the presence of increased RAF dimerization [61]. PLX4032 inhibits Raf activity in BRaf V600E melanomas because the levels of activated Ras are too low to initiate formation of Raf dimers. In the absence of dimer formation, the drug binds to the ATP site and inhibits the ERK signaling pathway [61]**.** This was supported when mutant Ras caused the ERK pathway to be insensitive to PLX4032 upon its introduction into mutant BRaf containing cells [62].

1.2.3 MEK inhibitors

U0126 is selective for MEK1 and MEK2 with an IC_{50} of 0.07 μM ± 0.02 and 0.06 μM ± 0.02, respectively [63]. MEK inhibition is noncompetitive with respect to ATP and its downstream effector ERK, and has been shown to inhibit production of a variety of cytokines and metalloproteinases involved in the inflammatory response [64, 65]. U0126 is used mostly in research due to it unsuitability for clinical trials.

PD98059 is a MEK inhibitor that binds to the inactive form of MEK1. It is a non-competitive inhibitor of ATP and has been shown to bind outside the active site [66, 67]. PD98059 was also found to bind to p38α with an IC_{50} of 24μM [67], however it was not found to inhibit p38α activity [66]. To locate the binding site, the crystal structure of PD98059 in complex with p38α was solved to a resolution of 2.6 Å. The crystal structure showed that the compound bound to the hinge point of the N-terminal and C-terminal lobe (referred to as the Backside binding site) [67].

AZD6244 is a selective MEK inhibitor that was found to inactivate ERK in a broad spectrum of human tumor xenograft models including breast and melanoma. It does not compete with ATP and prevents proliferation in Ras and BRaf mutated cells. AZD5244 was in phase II clinical trials. Studies showed that 12% of patients tested all with metastatic melanoma having the B-Raf mutation V600E experienced regression, though not complete [68].

1.2.4 ERK inhibitors

Inhibition of the ERK pathway via upstream activating kinases, though promising, has several drawbacks. The most problematic is that targeting receptor kinases, Raf and

MEK inhibits the entire ERK signaling pathway usually in both normal and abnormal cells. Because all information that travels through the ERK signaling cascade is funneled through ERK, it is beneficial to develop inhibitors that interact specifically with ERK. Inhibitors of ERK have been identified that compete with ATP. One such compound, FR180204 was identified via a high-throughput phosphorylation assay in which ERK-mediated phosphorylation of myelin basic protein (MBP) was inhibited. This compound was found to inhibit the transforming growth factor β (TGFβ)-induced AP-1 activation [69]. Because it competes with ATP for the active site, high doses of compound are required which can lead to increased toxic effects. Also, ATP binding sites are conserved amongst kinases, thus reducing specificity. An alternative approach that is currently being pursued in our lab is to target substrate specific ERK interactions, thereby vastly reducing off-target effects.

1.3 Previous Studies

The overall goal of the Shapiro lab as it relates to this project is to identify compounds that can selectively prevent ERK regulation of substrates that promote diseases, such as cancer, but preserve ERK functions in normal cells. In that more than 160 substrates are thought to interact with ERK, compounds that can block some of these substrate interactions can be used as research tools to better understand protein-substrate interactions and their roles in signaling pathways of normal and diseased cells. Using knowledge of ERK2 docking domains and substrate specificity, computer-aided drug design (CADD) was used to identify novel low molecular weight compounds that interact with the ERK2 kinase and disrupt substrate docking interactions [11, 12, 21]. The CADD screening approach was developed in Dr. Alexander Mackerell's lab in which the pre-determined crystal structure of the protein of interest served as a model to perform high-throughput screening of low molecular weight compounds predicted to target specific binding domains on the protein [70]. Initially, the CD and ED domains of ERK2 (more specifically, a groove located between the two domains) were chosen as a target for CADD to identify potential binding sites [41]. As an example of a lead compound targeting the ERK2, Figure 1.4 provides structural characterization of an active compound (designated **2.3.2**) in complex with ERK2 [71]. X-ray crystallography data was generated by Jun Zhang in our lab. Compound **2.3.2** was predicted by CADD to interact with two putative binding sites of ERK2 (designated site 2 and site 3); however, the data illustrates the interaction of compound **2.3.2** with the FRS substrate docking site of ERK2 [71]. Nevertheless, the primary purpose of this illustration is to visualize what we are trying to achieve in identifying compounds that target and bind to ERK2 substrate

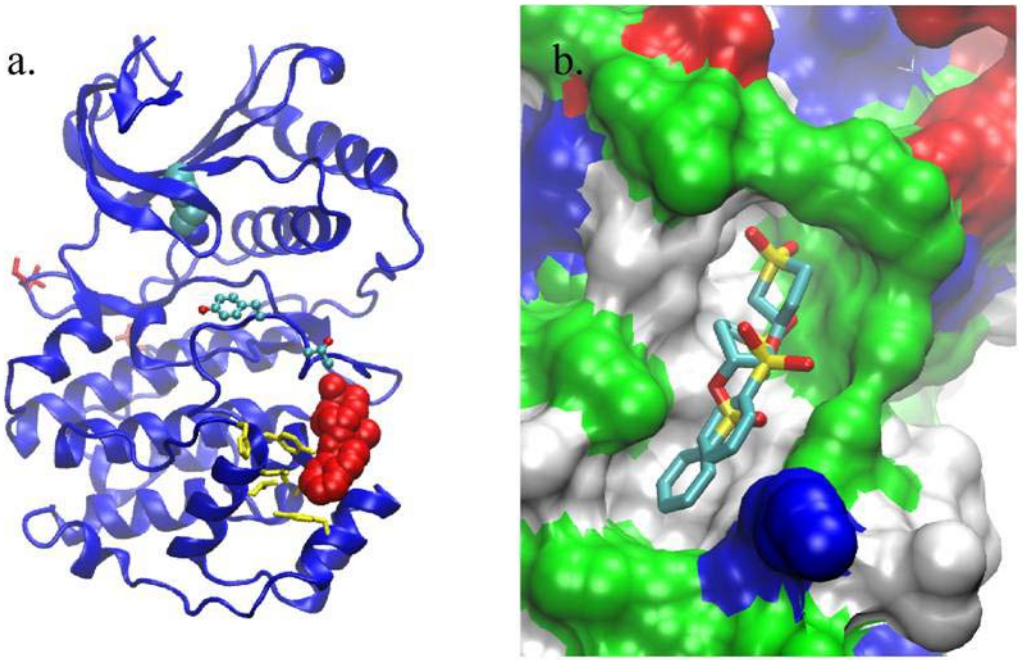

Figure 1.4. X-ray crystallographic structure of the ERK2-**2.3.2** complex. (**a**) Overall structure of the ERK2-**2.3.2** complex including **2.3.2** (red, vdW spheres), FRS, site 5 residues Leu198, His230, Tyr231, Leu232, Leu235, Tyr261 (yellow, licorice), Thr183 and Tyr185 (atom-based color, CPK), Lys52 indicating the ATP binding site (atom-based color, vdW spheres) and CD/ED domain residues Thr157, Thr158, Asp316, Asp319 (red, licorice). (**b**) The cavity on the surface of C-terminal domain of ERK2 with two conformers of **2.3.2**. Residue coloring by polarity. Molecular representations were rendered in PyMOL (www.pymol.org) or VMD[49].

docking domains. The Shapiro lab identified several lead compounds that interacted with ERK2 and inhibited the phosphorylation of substrates without affecting the overall activity of ERK as shown by fluorescence experiments and biological assays. The structures of the compounds initially tested are shown in the following reference [11].

The experiments illustrated in Figure 1.5 were performed by Dr. Chad Hancock. As shown by the titration curve in Figure 1.5A, two test compounds designated **76** and **36** directly interacted with ERK2. The chemical structure of **76 (**Figure 1.6) consists of a thiazolidine-2,4,dione core with both a phenyl group and an ethylamine group attached. When observing the inhibitory effects of the compounds on cell proliferation of HeLa cells, a colony formation assay showed that both compounds **76** and **81** completely inhibited cell proliferation (Figure 1.5B) [11]. Direct interaction of **76** with ERK2 likely led to its biological activity. Though **36** was shown to directly interact with ERK2, the compound produced only slight changes in HeLa cell growth [11]. The inhibitory effects of **81** may target another signaling pathway in that this compound does not quench ERK2 fluorescence. In addition to binding and inhibiting HeLa cell proliferation, several compounds were shown to inhibit ERK-mediated substrate phosphorylation but not phosphorylation of ERK. Immunoblot for p90RSK-1 phosphorylation in the presence of **76** and **81** was quantified by densitometry as shown in Figure 1.5C. Data showed that these compounds caused greater than 50% inhibition of p90RSK-1 phosphorylation [11]. There was no inhibitory effect of ERK phosphorylation by these compounds, thus showing that the compounds are working on the level of ERK-substrate phosphorylation. Former graduate student Dr. Fengming Chen showed that **76** inhibited the interaction of

Figure 1.5. Identification of lead compounds targeting ERK2 substrate docking sites. A) Fluorescence titration of ERK2 was done with selected compounds. The fluorescence (F) is plotted against the log concentration in moles/liter (Log [M]) for each compound is shown. Data are included for compounds **81** (open squares), **67** (closed triangles), **76** (open circles), and **36** (closed circles). B) Inhibition of cell proliferation with test compounds. The number of cell colonies that formed after incubation with varying concentrations of test compounds **76** (closed squares) or **81** (open squares) were graphed. C) Effects of test compounds on Rsk-1 phosphorylation. HeLa cells were preincubated with 100 μM of test compounds and then stimulated for 5 min with EGF (50 ng/mL). Controls included untreated (-) and EGF-only treated cells. The relative amount of Rsk-1 phosphorylation in the immunoblot (not shown) quantified by densitometry and normalized as a fraction of the R-tubulin levels. The pRsk-1 to tubulin ratio for the EGF only treatment was set at 100% and the pRsk-1 values for all other treatments were expressed as percentage of the EGF only control.

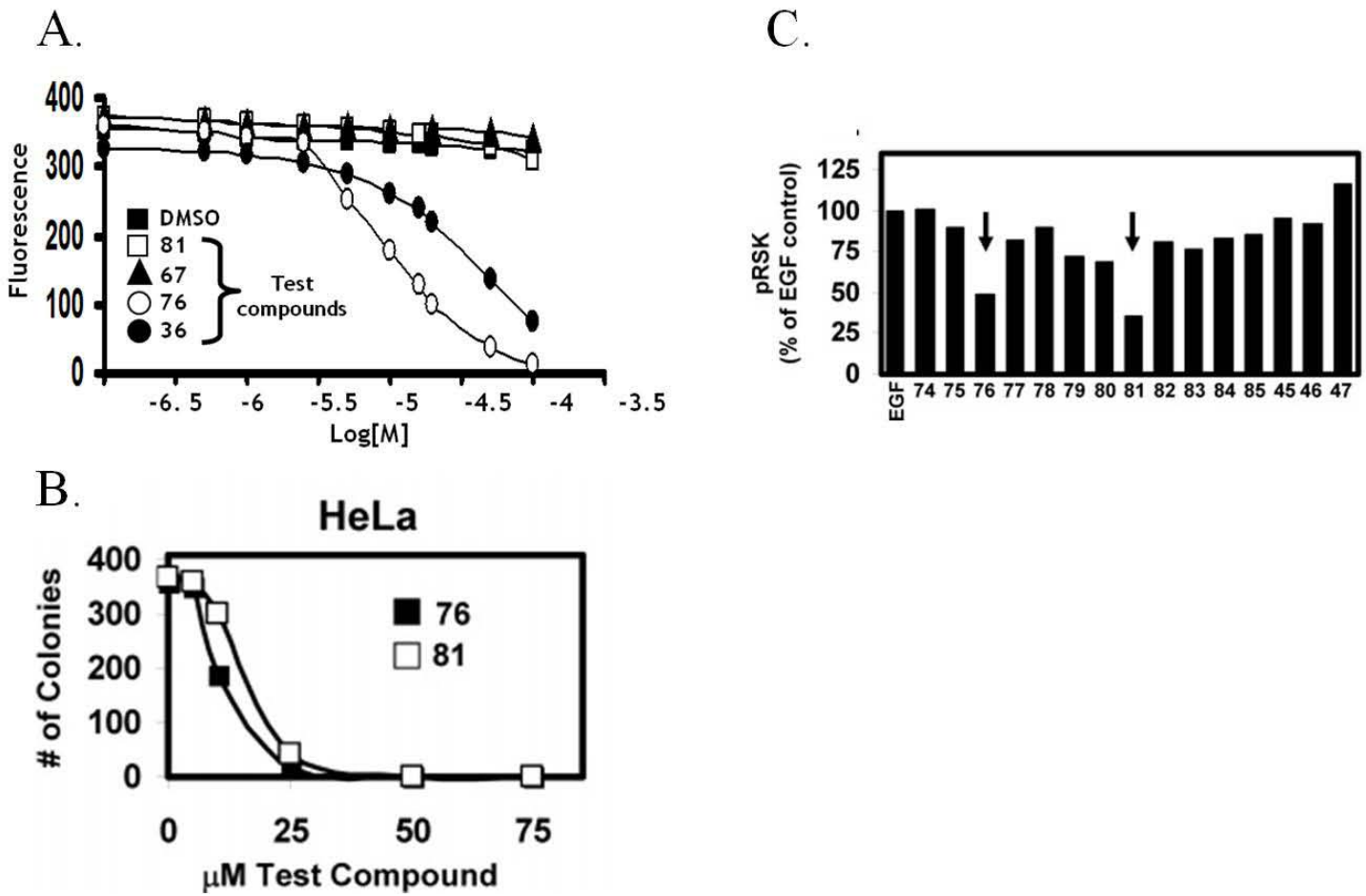

Hancock, C.N., et al. Journal of medicinal chemistry, 2005. 48(14): p. 4586-95.

MPK-1, a homolog to human ERK2, with its substrate LIN-1 in a *C. elegans* model [72]. It is important to note that the CD and ED docking domains of ERK2 and MPK-1 share identical amino acid sequences important for substrate recognition. Binding of **76** to ERK2 was quantified yielding a K_D of 5 μM [11].

Using **76** as a lead compound, CADD was again used to identify structurally similar compounds based on subtle changes in chemical structure and these compounds were obtained [72, 73]. The computational search was based on the chemical similarity using the MAC-BITS fingerprints in conjunction with the Tanimoto Similarity index to search a virtual database of over 1 million commercially available compounds as described [74]. The chemical structures are shown in Figure 1.6. These and a few additional compounds were evaluated for their effects on cell proliferation of HeLa cells [73]. Of the compounds identified, **76.2, 76.3, and 76.4** were previously reported by former graduate student Dr. Sarice Boston to inhibit cell proliferation and induce apoptosis of HeLa cells [73]. She showed that compounds **76.2**, **76.3** and **76.4** inhibited cell proliferation of HeLa cells similar to the parent compound **76**. As will be discussed in a later chapter, several of these compounds, including the three aforementioned in addition to **76.1** and **76.8**, were shown to directly interact with ERK2 via fluorescence quenching experiments. However, **76.1** and **76.8** appeared to have relatively little or no effect as inhibitors of cell proliferation. In the context of these five compounds, the chemical structures all consist of a common core (thiazolidinedione core). The difference in the structures is that the three compounds that exhibit biological effect - **76.2, 76.3**, and **76.4 -** have an ethylamine group attached, suggesting this moiety may contribute to the functionality of these compounds. In addition, **76.3** was reported to have improved

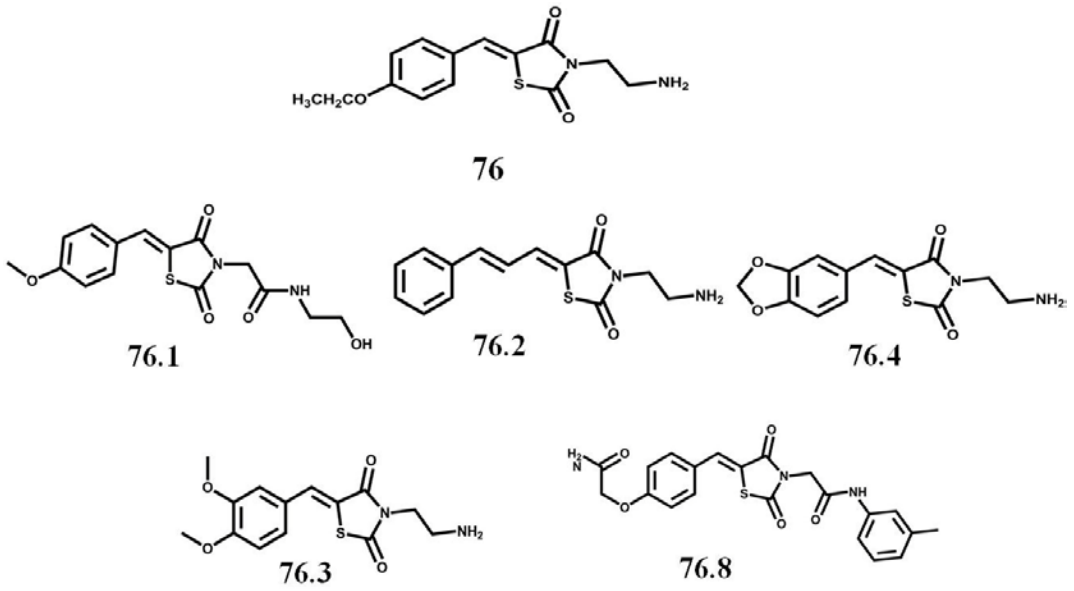

Figure 1.6. Chemical structures of **76** and structurally similar compounds.

potency over the parent compound **76** as shown via cell based and *in vitro* kinase assays. Data showed that **76.3** was significantly more potent at inhibiting phosphate incorporation into the ERK2 substrate p90RSK-1 than **76** [73]. It is important to note that ERK activation from upstream kinases was unaffected [73]. As a result it has been shown that structurally similar compounds that have similar biological effects and chemical features may indeed have increased selectivity and potency as compared to the parent compound **76**.

One of my research goals was to evaluate the binding interactions and the selectivity of the low molecular weight compounds structurally similar to lead compound **76** to the common docking domain of ERK2 as well as its selectivity for structurally similar MAP kinases. Fluorescence spectroscopy was one tool used to determine the binding affinity of the test compounds to ERK2. The rationale is that structurally similar compounds will exhibit improved potency and selectivity. As previously stated, the **76** family of compounds contain a thiazolidindione core with both a phenyl group and an ethylamine group attached. It appeared from the molecular model of ERK2 and **76** that the ethylamine group may be interacting with the aspartic acid residues of the CD domain. Combined with the fact that compounds lacking the ethylamine moiety (**76.1** and **76.8**) had little or no inhibitory effect on cell proliferation, a second research goal was to assess the effect chemical modifications made to the amino group of **76** has on the structure-activity relationship (SAR) of compounds with ERK2. The CADD approach discussed previously used a database of over 1 million commercially available compounds to select structurally similar compounds based on chemical similarity. Expanding upon this technology, specific modifications were made to lead compound **76**

via CADD-directed medicinal chemistry in collaboration with Dr. Steven Fletcher. Using chemical synthesis to add new groups and/or remove groups to modify the biological activity and potency of the compounds presented a more direct approach to understanding SAR of these compounds. This technique allowed for specific changes to be made to the lead compound such as but not limited to increasing or decreasing basicity, adding more hydrophobic or less hydrophobic groups, and introducing hydrogen bond donors. The compounds were synthesized based on predicted outcomes, purified, and screened for interactions with ERK2. Ultimately, a better understanding is gained of which groups are responsible for the compound's activity and how to improve upon the compound's bioactivity.

1.4 List of References

1. Roux, P.P. and J. Blenis, *ERK and p38 MAPK-activated protein kinases: a family of protein kinases with diverse biological functions.* Microbiol Mol Biol Rev, 2004. **68**(2): p. 320-44.
2. Lewis, T.S., P.S. Shapiro, and N.G. Ahn, *Signal transduction through MAP kinase cascades.* Adv Cancer Res, 1998. **74**: p. 49-139.
3. Kohno, M. and J. Pouyssegur, *Targeting the ERK signaling pathway in cancer therapy.* Ann Med, 2006. **38**(3): p. 200-11.
4. Kolch, W., *Meaningful relationships: the regulation of the Ras/Raf/MEK/ERK pathway by protein interactions.* Biochem J, 2000. **351 Pt 2**: p. 289-305.
5. Pearson, G., et al., *Mitogen-activated protein (MAP) kinase pathways: regulation and physiological functions.* Endocr Rev, 2001. **22**(2): p. 153-83.
6. Schindler, J.F., J.B. Monahan, and W.G. Smith, *p38 pathway kinases as anti-inflammatory drug targets.* J Dent Res, 2007. **86**(9): p. 800-11.
7. Cuadrado, A. and A.R. Nebreda, *Mechanisms and functions of p38 MAPK signalling.* Biochem J, 2010. **429**(3): p. 403-17.
8. Boulton, T.G., et al., *An insulin-stimulated protein kinase similar to yeast kinases involved in cell cycle control.* Science, 1990. **249**(4964): p. 64-7.
9. Zhang, J., et al., *A bipartite mechanism for ERK2 recognition by its cognate regulators and substrates.* J Biol Chem, 2003. **278**(32): p. 29901-12.
10. Ahn, N.G., *PORE-ing over ERK substrates.* Nat Struct Mol Biol, 2009. **16**(10): p. 1004-5.

11. Hancock, C.N., et al., *Identification of novel extracellular signal-regulated kinase docking domain inhibitors.* Journal of medicinal chemistry, 2005. **48**(14): p. 4586-95.

12. Chen, F., et al., *Characterization of ATP-independent ERK inhibitors identified through in silico analysis of the active ERK2 structure.* Bioorg Med Chem Lett, 2006. **16**(24): p. 6281-7.

13. Shapiro, P.S., et al., *Extracellular signal-regulated kinase activates topoisomerase IIalpha through a mechanism independent of phosphorylation.* Mol Cell Biol, 1999. **19**(5): p. 3551-60.

14. Robbins, D.J. and M.H. Cobb, *Extracellular signal-regulated kinases 2 autophosphorylates on a subset of peptides phosphorylated in intact cells in response to insulin and nerve growth factor: analysis by peptide mapping.* Mol Biol Cell, 1992. **3**(3): p. 299-308.

15. Robbins, D.J., et al., *Regulation and properties of extracellular signal-regulated protein kinases 1 and 2 in vitro.* J Biol Chem, 1993. **268**(7): p. 5097-106.

16. Satoh, Y., et al., *Deletion of ERK1 and ERK2 in the CNS causes cortical abnormalities and neonatal lethality: Erk1 deficiency enhances the impairment of neurogenesis in Erk2-deficient mice.* J Neurosci. **31**(3): p. 1149-55.

17. Chan, S.H., E.Y. Sun, and A.Y. Chang, *Extracellular signal-regulated kinase 1/2 plays a pro-life role in experimental brain stem death via MAPK signal-interacting kinase at rostral ventrolateral medulla.* J Biomed Sci. **17**: p. 17.

18. Yang, Y. and C. Han, *GDNF stimulates the proliferation of cultured mouse immature Sertoli cells via its receptor subunit NCAM and ERK1/2 signaling pathway.* BMC Cell Biol. **11**: p. 78.

19. Zhang, F., et al., *Atomic structure of the MAP kinase ERK2 at 2.3 A resolution.* Nature, 1994. **367**(6465): p. 704-11.

20. Canagarajah, B.J., et al., *Activation mechanism of the MAP kinase ERK2 by dual phosphorylation.* Cell, 1997. **90**(5): p. 859-69.

21. Chen, Z., et al., *MAP kinases.* Chem Rev, 2001. **101**(8): p. 2449-76.

22. Ullrich, A. and J. Schlessinger, *Signal transduction by receptors with tyrosine kinase activity.* Cell, 1990. **61**(2): p. 203-12.

23. Ferrell, J.E., Jr. and R.R. Bhatt, *Mechanistic studies of the dual phosphorylation of mitogen-activated protein kinase.* J Biol Chem, 1997. **272**(30): p. 19008-16.

24. Lenormand, P., et al., *Growth factors induce nuclear translocation of MAP kinases (p42mapk and p44mapk) but not of their activator MAP kinase kinase (p45mapkk) in fibroblasts.* J Cell Biol, 1993. **122**(5): p. 1079-88.

25. Yoon, S. and R. Seger, *The extracellular signal-regulated kinase: multiple substrates regulate diverse cellular functions.* Growth Factors, 2006. **24**(1): p. 21-44.

26. Hong, S.K., et al., *Noncatalytic function of ERK1/2 can promote Raf/MEK/ERK-mediated growth arrest signaling.* J Biol Chem, 2009. **284**(48): p. 33006-18.

27. Roberts, P.J. and C.J. Der, *Targeting the Raf-MEK-ERK mitogen-activated protein kinase cascade for the treatment of cancer.* Oncogene, 2007. **26**(22): p. 3291-310.

28. Tanoue, T. and E. Nishida, *Molecular recognitions in the MAP kinase cascades.* Cell Signal, 2003. **15**(5): p. 455-62.

29. Camps, M., et al., *Catalytic activation of the phosphatase MKP-3 by ERK2 mitogen-activated protein kinase.* Science, 1998. **280**(5367): p. 1262-5.

30. Enslen, H. and R.J. Davis, *Regulation of MAP kinases by docking domains.* Biol Cell, 2001. **93**(1-2): p. 5-14.

31. Jacobs, D., et al., *Multiple docking sites on substrate proteins form a modular system that mediates recognition by ERK MAP kinase.* Genes Dev, 1999. **13**(2): p. 163-75.

32. Fantz, D.A., et al., *Docking sites on substrate proteins direct extracellular signal-regulated kinase to phosphorylate specific residues.* J Biol Chem, 2001. **276**(29): p. 27256-65.

33. Galanis, A., S.H. Yang, and A.D. Sharrocks, *Selective targeting of MAPKs to the ETS domain transcription factor SAP-1.* J Biol Chem, 2001. **276**(2): p. 965-73.

34. Murphy, L.O., et al., *Molecular interpretation of ERK signal duration by immediate early gene products.* Nat Cell Biol, 2002. **4**(8): p. 556-64.

35. MacKenzie, S.J., et al., *ERK2 mitogen-activated protein kinase binding, phosphorylation, and regulation of the PDE4D cAMP-specific phosphodiesterases. The involvement of COOH-terminal docking sites and NH2-terminal UCR regions.* J Biol Chem, 2000. **275**(22): p. 16609-17.

36. Burkhard, K.A., F. Chen, and P. Shapiro, *Quantitative analysis of ERK2 interactions with substrate proteins: roles for kinase docking domains and activity in determining binding affinity.* J Biol Chem, 2011.

37. Zhou, B., et al., *Multiple regions of MAP kinase phosphatase 3 are involved in its recognition and activation by ERK2.* J Biol Chem, 2001. **276**(9): p. 6506-15.

38. Lee, T., et al., *Docking motif interactions in MAP kinases revealed by hydrogen exchange mass spectrometry.* Mol Cell, 2004. **14**(1): p. 43-55.

39. Tanoue, T., et al., *A conserved docking motif in MAP kinases common to substrates, activators and regulators.* Nat Cell Biol, 2000. **2**(2): p. 110-6.

40. Tanoue, T., et al., *Identification of a docking groove on ERK and p38 MAP kinases that regulates the specificity of docking interactions.* Embo J, 2001. **20**(3): p. 466-79.

41. Tanoue, T., et al., *Identification of a docking groove on ERK and p38 MAP kinases that regulates the specificity of docking interactions.* The EMBO journal, 2001. **20**(3): p. 466-79.

42. Bardwell, A.J., M. Abdollahi, and L. Bardwell, *Docking sites on mitogen-activated protein kinase (MAPK) kinases, MAPK phosphatases and the Elk-1 transcription factor compete for MAPK binding and are crucial for enzymic activity.* Biochem J, 2003. **370**(Pt 3): p. 1077-85.

43. Gavin, A.C., et al., *A p90(rsk) mutant constitutively interacting with MAP kinase uncouples MAP kinase from p34(cdc2)/cyclin B activation in Xenopus oocytes.* Mol Biol Cell, 1999. **10**(9): p. 2971-86.

44. Smith, J.A., et al., *Identification of an extracellular signal-regulated kinase (ERK) docking site in ribosomal S6 kinase, a sequence critical for activation by ERK in vivo.* J Biol Chem, 1999. **274**(5): p. 2893-8.

45. Martin, M.C., et al., *The docking interaction of caspase-9 with ERK2 provides a mechanism for the selective inhibitory phosphorylation of caspase-9 at threonine 125.* J Biol Chem, 2008. **283**(7): p. 3854-65.

46. Zuniga, A., et al., *Interaction of mitogen-activated protein kinases with the kinase interaction motif of the tyrosine phosphatase PTP-SL provides substrate specificity and retains ERK2 in the cytoplasm.* J Biol Chem, 1999. **274**(31): p. 21900-7.

47. Anjum, R. and J. Blenis, *The RSK family of kinases: emerging roles in cellular signalling.* Nat Rev Mol Cell Biol, 2008. **9**(10): p. 747-58.

48. Camps, M., A. Nichols, and S. Arkinstall, *Dual specificity phosphatases: a gene family for control of MAP kinase function.* Faseb J, 2000. **14**(1): p. 6-16.

49. Keyse, S.M., *Protein phosphatases and the regulation of mitogen-activated protein kinase signalling.* Curr Opin Cell Biol, 2000. **12**(2): p. 186-92.

50. Polychronopoulos, S., et al., *The transcriptional ETS2 repressor factor associates with active and inactive Erks through distinct FXF motifs.* J Biol Chem, 2006. **281**(35): p. 25601-11.

51. Dimitri, C.A., et al., *Spatially separate docking sites on ERK2 regulate distinct signaling events in vivo.* Curr Biol, 2005. **15**(14): p. 1319-24.

52. Sharma, A., et al., *Mutant V599EB-Raf regulates growth and vascular development of malignant melanoma tumors.* Cancer Res, 2005. **65**(6): p. 2412-21.

53. Hingorani, S.R., et al., *Suppression of BRAF(V599E) in human melanoma abrogates transformation.* Cancer Res, 2003. **63**(17): p. 5198-202.

54. Davies, H., et al., *Mutations of the BRAF gene in human cancer.* Nature, 2002. **417**(6892): p. 949-54.

55. Nikiforova, M.N., et al., *BRAF mutations in thyroid tumors are restricted to papillary carcinomas and anaplastic or poorly differentiated carcinomas arising from papillary carcinomas.* J Clin Endocrinol Metab, 2003. **88**(11): p. 5399-404.

56. Wan, P.T., et al., *Mechanism of activation of the RAF-ERK signaling pathway by oncogenic mutations of B-RAF.* Cell, 2004. **116**(6): p. 855-67.

57. Pratz, K.W., et al., *A pharmacodynamic study of sorafenib in patients with relapsed and refractory acute leukemias.* Leukemia. **24**(8): p. 1437-44.

58. Lyons, J.F., et al., *Discovery of a novel Raf kinase inhibitor.* Endocr Relat Cancer, 2001. **8**(3): p. 219-25.

59. Wilhelm, S.M., et al., *BAY 43-9006 exhibits broad spectrum oral antitumor activity and targets the RAF/MEK/ERK pathway and receptor tyrosine kinases involved in tumor progression and angiogenesis.* Cancer Res, 2004. **64**(19): p. 7099-109.

60. Flaherty, K.T., et al., *Inhibition of mutated, activated BRAF in metastatic melanoma.* N Engl J Med. **363**(9): p. 809-19.

61. Solit, D.B. and N. Rosen, *Resistance to BRAF inhibition in melanomas.* N Engl J Med. **364**(8): p. 772-4.

62. Poulikakos, P.I., et al., *RAF inhibitors transactivate RAF dimers and ERK signalling in cells with wild-type BRAF.* Nature. **464**(7287): p. 427-30.

63. Duncia, J.V., et al., *MEK inhibitors: the chemistry and biological activity of U0126, its analogs, and cyclization products.* Bioorg Med Chem Lett, 1998. **8**(20): p. 2839-44.

64. DeSilva, D.R., et al., *Inhibition of mitogen-activated protein kinase kinase blocks T cell proliferation but does not induce or prevent anergy.* J Immunol, 1998. **160**(9): p. 4175-81.

65. Favata, M.F., et al., *Identification of a novel inhibitor of mitogen-activated protein kinase kinase.* J Biol Chem, 1998. **273**(29): p. 18623-32.

66. Dudley, D.T., et al., *A synthetic inhibitor of the mitogen-activated protein kinase cascade.* Proc Natl Acad Sci U S A, 1995. **92**(17): p. 7686-9.

67. Akella, R., T.M. Moon, and E.J. Goldsmith, *Unique MAP Kinase binding sites.* Biochim Biophys Acta, 2008. **1784**(1): p. 48-55.

68. Adjei, A.A., et al., *Phase I pharmacokinetic and pharmacodynamic study of the oral, small-molecule mitogen-activated protein kinase kinase 1/2 inhibitor AZD6244 (ARRY-142886) in patients with advanced cancers.* J Clin Oncol, 2008. **26**(13): p. 2139-46.

69. Ohori, M., et al., *Identification of a selective ERK inhibitor and structural determination of the inhibitor-ERK2 complex.* Biochem Biophys Res Commun, 2005. **336**(1): p. 357-63.

70. Zhong, S., A.T. Macias, and A.D. MacKerell, Jr., *Computational identification of inhibitors of protein-protein interactions.* Curr Top Med Chem, 2007. **7**(1): p. 63-82.

71. Zhang, J., et al., *Chemical control of a signaling crossroad: ATP-independent ERK2 inhibitors targeting substrate docking domains.* 2011.

72. Chen, F., et al., *Using Caenorhabditis elegans as a model organism for evaluating extracellular signal-regulated kinase docking domain inhibitors.* J Cell Commun Signal, 2008. **2**(3-4): p. 81-92.

73. Boston, S.R., et al., *Characterization of ERK docking domain inhibitors that induce apoptosis by targeting Rsk-1 and caspase-9.* BMC cancer, 2011. **11**: p. 7.

74. Macias AT, et al., *Lead validation and SAR development via chemical similarity searching; application to compounds targeting the pY+3 site of the SH2 domain of p56lck.* . J Chem Inf Model, 2005. **45**: p. 1759-1766.

CHAPTER 2: Using Fluorescence Spectroscopy to Determine Selectivity of Small Molecule Inhibitors that Target the ERK2 Common Docking (CD) Substrate Binding Site.

2.1 Introduction

Taking advantage of the naturally occurring tryptophan residues, fluorescence spectroscopy was used to determine direct binding of test compounds to ERK2. The quenching of tryptophan (Trp) fluorescence occurs upon interaction with polar ligands. Changes in Trp fluorescence intensity upon increase of test compound concentration suggest a protein conformational change in the region where Trp resides caused by interaction of the test compounds with the protein. As such, binding can be monitored and quantified by observing changes in Trp fluorescence due to quenching as a function of concentration increase [2-4]. It is important to consider the spectral properties of the test compounds as well. Care must be taken to measure absorbance and/or fluorescence of the test compounds in solution at the excitation and emission wavelength range of the protein [1]. A correction procedure may be applied depending on the degree of absorbance and/or fluorescence of the compound [1, 3, 5]. The concentration of solvent must be considered. In this case, the DMSO solvent for each titration was maintained constant. It was found that many of the structurally similar compounds to **76** caused quenching of ERK2 tryptophan fluorescence. The selectivity of some of the more active compounds was compared to p38α and data suggested that several compounds showed greater quenching of ERK2. To determine whether the test compounds interacted with specific residues of the CD and ED domains, binding interactions of the test compounds to ERK2 mutants harboring amino acid substitutions located in the CD and/or ED domain were evaluated. These ERK mutants contain changes in specific amino acid residues

located in the CD/ED domain that have been shown to interact with specific substrates of the ERK2 kinase and to be necessary for interactions with specific substrates to occur. Several studies have demonstrated the importance of docking domains to determining specificity of substrate interactions with MAP kinases [6-10]. Replacing only two amino acids within the ED domain of ERK2 altered its binding specificity and enabled the kinase to interact with a p38 specific substrate, MK3 [10]. Studies in our lab showed that mutations in the ED and FRS domain of ERK2 inhibited interactions with the ERK2 substrate c-Fos [6]. Thus, specificity of ERK substrate domains to docking domains of ERK2 will allow for the selective inhibition of specific substrates of ERK2 involved in abnormal cellular functions by low-molecular weight compounds.

In this study, the aspartate residue in position 319 is located in the CD domain and likely participates in ionic interactions with basic residues of the D domain of various ERK substrates. The aspartate residue was replaced by asparagine (D319N) which has a net neutral charge. Threonine 157, located in the ED domain, was replaced by alanine. These sites were chosen because the compounds being tested were designed to target the CD/ED domain. As stated previously, these amino acids have been suggested to play a significant role in interactions with certain substrates. The selected mutations allowed us to quantify the importance of each domain in interactions with the test compounds. The goal is to identify compounds that interact with the docking sites and ultimately interfere with and/or weaken ERK-substrate interactions, thereby inhibiting the selected substrate responses without interfering with the overall ERK signaling pathway. Cancer cells may be sensitized making them more susceptible to apoptosis at lower concentrations of chemotherapeutics, minimizing toxic effects.

Selectivity for the CD and/or ED domain of ERK2 was determined by monitoring changes in fluorescence quenching upon interaction of the test compounds with ERK2 containing mutations in the CD/ED domains: ERK2 CD mutant (T157A) and ED mutant (D319N) and CD/ED mutant (T157A/D319N). Moreover binding of test compounds to ERK2, p38α and ERK2 CD/ED domain mutants was quantified.

2.2 Fluorescence Spectroscopy

2.2.1 The Basics of Fluorescence

Luminescence is the emission of photons from electronic excitation states. Fluorescence is one category of luminescence characterized by the nature of the electrons in the ground state and the excited state. Often times referred to as the father of fluorescence spectroscopy, Alexander Jablonski illustrated the absorption and emission of light in the energy level diagram commonly known as the Jablonski diagram (Figure 2.1). The electronic energy levels are designated S_0 (ground state) and S_1 (first energy level). The excited vibrational states are also shown. When light strikes the molecule, a photon of energy ($h\nu_A$) is absorbed and creates an excited electronic singlet state. Photon absorption ranges in the order of 10^{-15} seconds. The internal conversion of energy resulting in fast, nonradiative transitions from the second to the first excited singlet state is also known as vibrational relaxation. This conversion usually occurs in 10^{-12} seconds and involves the release of energy usually as heat. The electron then returns to the ground state and emits energy as photons (fluorescence). Quantum yield is the ratio of the number of photons emitted to the number of photons absorbed. The expression for quantum yield is

$$\mathbf{Q = k_f / (k_f + k_{nr})} \qquad \mathbf{(1)}$$

where k_f is the emissive rate of the fluorophore and k_{nr} is the nonradiative decay to the ground state. It represents the fraction of fluorophores which decay through emission.

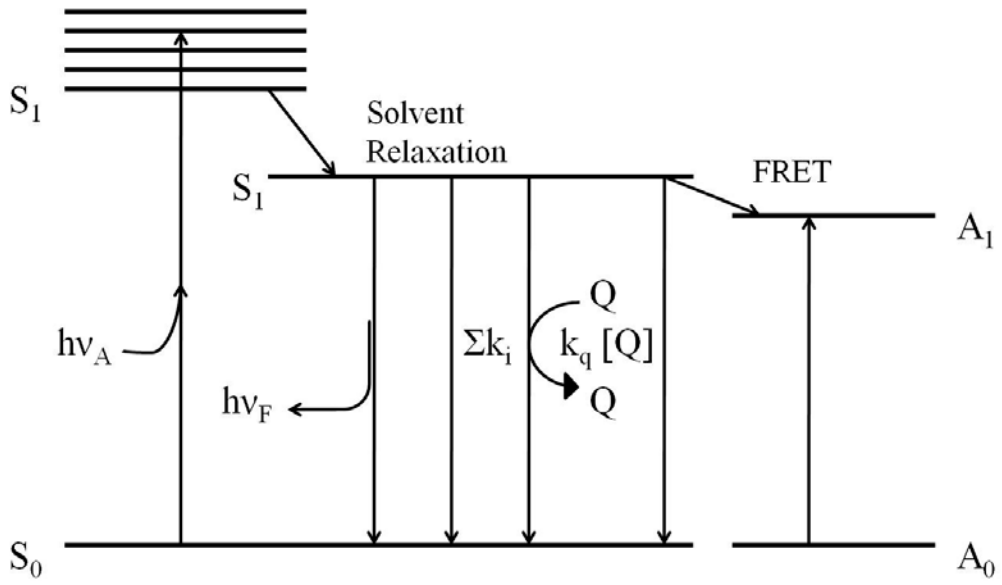

Figure 2.1. Jablonski diagram. Processes that decrease fluorescence intensity (collisional quenching and fluorescence resonance energy transfer) are highlighted. Collisional quenching occurs when a quencher (Q) comes in contact with a fluorophore in the excited state and deactivates it [5]. [Q] is the quencher concentration and k_q is the bimolecular quenching constant. FRET occurs when radiationless energy is transferred from the donor fluorophore to the acceptor. Σk_i represents all other nonradiative paths to the ground state [5].

Quenching is characterized by a decrease in the intensity of fluorescence. Various molecular interactions can cause a decrease in the fluorescence intensity of a compound: excited-state reactions, molecular rearrangements, energy transfer, ground state complex formation and collisional quenching [11]. In collisional quenching, the quencher diffuses to the fluorophore during the lifetime of the excited state and upon contact, causing the fluorophore to return to the ground state (Figure 2.1). The fluorophore does not emit a photon [12]. The Stern-Volmer equation describes the decrease in intensity [5]:

$$\mathbf{F_0/F = 1 + k_q\tau_0[Q]} \qquad \mathbf{(2)}$$

where k_q is the bimolecular quenching constant, τ_0 is the unquenched lifetime, and [Q] is the quencher concentration. If the fluorophore is buried within a protein and the quencher is impermeable to the membrane, collisional quenching cannot occur [5]. Static quenching occurs when the fluorophore and the quencher form a stable nonfluorescent complex. The distinguishing factor between collisional and static quenching is that while both processes cause a decrease in the fluorescence intensity, collisional quenching causes a decrease in fluorescence lifetime. The nonfluorescent complex in static quenching is formed while the fluorophore is in the ground state. Therefore a decrease in the population of fluorophores in the excited state occurs; however, the average lifetime of the fluorophore population is unchanged. Collisional quenching causes a decrease in the lifetime of the fluorophore because the quencher interacts with the fluorophore in the excited state.

It is important to note that the emitted photon is always of lesser energy than the excited photon. In general, the emission of a photon occurs as quickly as the absorption of a photon; however, the lifetime of a photon (or the amount of time the photon remains in the excited state before returning to the ground state) depends on the type of molecule and the solvent. When a molecule is excited, a change in its dipole moment occurs instantly. The change in dipole increases the energy of the system and the solvent molecules surrounding the excited molecule react to this non-equilibrium state by reorienting. Stronger dipole-dipole interactions between the solvent and the excited molecule occur and the energy of the system decreases, known as solvent relaxation. Solvent relaxation occurs more rapidly than fluorescence. The more polar the solvent, the stronger the dipole-dipole interactions which equates to lower energy of the relaxed state. The majority of fluorophores fluoresce in this lower energy state. This is observed as a red-shift of the emission spectrum. The gap between the absorbance maximum and the emission maximum is known as the ‘Stokes Shift’ [13]. However, if an excited molecule is in a more viscous and/or less polar solvent, the dipole-dipole interactions are weaker and there is less energy reduction due to solvent relaxation. More specifically, solvent relaxation effect is slowed down when the viscosity is increased. As a result, photons are emitted on the same time scale as solvent relaxation. The contribution to fluorescence by non-relaxed states leads to a blue shift. In the presence of less polar solvents, the molecule upon excitation travels to higher energy levels and there is less energy reduction due to solvent relaxation. Therefore the ‘Stokes Shift’ is not as great as if the molecule were in a more polar or hydrophilic environment.

2.2.2 Fluorophores

Fluorophores are the molecules or molecular components that experience excitation and emission. Fluorophores are classified as either intrinsic or extrinsic. Intrinsic fluorophores are those that occur naturally in biomolecules. Extrinsic fluorophores are those that are added to a specific system in order to improve the spectral properties of that system. Many fluorophores are extremely sensitive to changes in their microenvironment thus allowing researchers to observe biological processes such as ligand binding, protein unfolding and protein-protein interactions [14-16]. Tryptophan, tyrosine, and phenylalanine are the aromatic amino acids and are natural intrinsic fluorophores. The one most commonly used as a probe is tryptophan. Tryptophan is the dominating intrinsic fluorophore in proteins. Most proteins contain one or a few tryptophan residues. Tryptophan, indole, and their derivatives, have a long wavelength absorption ranging from 240-300 nm [5]. It absorbs light near 280 nm and has a lifetime ranging from one to six nanoseconds. Tryptophan is highly sensitive to the polarity of its environment [17, 18]. As such it is often used to monitor protein conformational changes or binding of ligands, to assess location of tryptophan containing peptides and or regions of proteins in relation to membranes or other proteins, or to analyze tryptophan containing environments [4, 19-22]. As previously mentioned, the exposure of a fluorophore, in this case tryptophan, to a more hydrophobic environment leads to an increase in tryptophan fluorescence and a blue shift [5]. This makes tryptophan a useful probe to study depth of membrane insertion of proteins. The depth of membrane insertion into a membrane correlates with the degree of blue shift [23]. Tryptophan’s quantum yield usually decreases and the spectrum experiences a red shift with increasing polarity

of the surrounding medium. This is caused by a decrease in the energy of the system due to reorientation of the dipoles in the vicinity of the fluorophore [5].

2.2.3 Instrumentation

The essential elements of fluorescence detection systems include an excitation source, wavelength filters to isolate emission photons from excitation photons, and a detector that registers emission photons and produces a recordable output in the form of an electrical signal or a photographic image. The compatibility of these four elements is necessary for optimizing fluorescence detection. Spectrofluorometers and microplate readers measure the average properties of bulk samples, ranging from µL to mL volumes. A spectrofluorometer is extremely flexible, providing continuous ranges of excitation and emission wavelengths. Instruments used to measure fluorescence consist of a light source and wavelength selector for the excitation light, a sample holder, a wavelength selector for the emitted fluorescent light, and a photomultiplier tube to measure the amount of the emitted fluorescent light (Figure 2.2). The wavelength selector can be a filter or monochromator. Xenon lamps are commonly used as the source of exciting light because they have high intensity at all wavelengths ranging upwards from 250 nm. Other light sources include light emitting diodes (LED's) and lasers. There are several components not shown (in Figure 2.2) but are commonly found in a research fluorometer. Shutters are used to eliminate the exciting light or to close off the emission channel. Polarizers are used in both the excitation and emission light paths for measurements of fluorescence anisotropy.

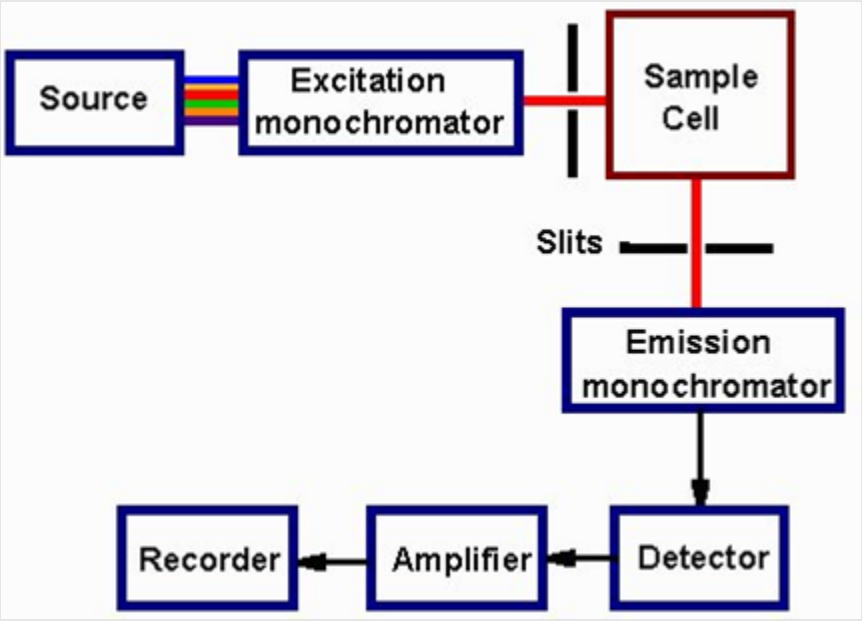

Figure 2.2. Simple schematic of spectrofluorometer. Lamp, LED's, or lasers are generally used as light sources. The excitation and emission monochromators select the wavelength of light that will excite the sample (in the sample cell) and will be measured by the photomultiplier tube, respectively.

2.3 Materials and Methods

2.3.1 Chemicals and reagents.

Test compounds were obtained from Chembridge Corporation (San Diego, CA) and stored as 25 mM stocks in DMSO. All other chemicals, buffers, and salts were purchased from Sigma Aldrich (St. Louis, MO) or Fisher Scientific (Pittsburgh, PA).

2.3.2 Protein expression and purification.

His_{X6}-tagged ERK2 was expressed in BL21 (DE3) *E. coli* as previously described [24, 25]. His_{X6}-tagged p38 was expressed in BL21 (DE3) E. *coli* as well. The cells were grown in LB medium with 100 µg/ml ampicillin and protein expression was induced by isopropyl-B-D-thiogalactoside (IPTG) at a final concentration of 1 mM and incubated for 4 hours. Each step in the protein purification was performed on ice or at 4°C. The cells were harvested by centrifugation and resuspended in lysis buffer (50 mM sodium phosphate, 300 mM NaCl, 10% glycerol, pH 7.8) supplemented with protease inhibitors phenylmethylsulfonylfluoride (PMSF, 1 mM) and benzamidine (10 mM). Lysozyme was added and the mixture sonicated followed by centrifugation at 10,000 rpm for 45 minutes. The cleared lysate was loaded onto a Co^{2+} charged resin and the bound protein washed with 50 mM sodium phosphate, 300 mM NaCl, 10% glycerol, 20 mM imidazole (pH 7.8) and eluted with increasing concentrations of imidazole. The purity of the protein-containing fractions was determined by SDS-PAGE electrophoresis and staining. Fractions containing desired protein were concentrated and dialyzed against 10 mM HEPES, 150 mM NaCl, 10% glycerol, pH 7.8 and protein concentration was determined by UV or Bradford methods.

2.3.3 Substrate phosphorylation assay

Cells were washed with cold phosphate buffered saline (PBS, pH 7.2; Invitrogen) and protein lysates were collected with 2X SDS-PAGE sample buffer (4% SDS, 5.7 M β-mercaptoethanol, 0.2 M Tris pH 6.8, 20% glycerol, 5 mM EDTA) or cold tissue lysis buffer (TLB; 20 mM Tris-HCl pH 7.4, 137 mM NaCl, 2 mM EDTA, 1% Triton X-100, 0.1% SDS, 25 mM β-glycerophosphate, 2 mM sodium pyrophosphate, 10% glycerol, 1 mM sodium orthovanadate, 1 mM phenylmethylsulfonyl fluoride, 1 mM benzamidine). Lysates collected in TLB were centrifuged at 20,000 (X g) to remove insoluble material and then diluted with an equal volume of 2X SDS-sample buffer. Proteins were separated by SDS-PAGE and analyzed by immunoblotting using enhanced chemiluminesence (ECL, GE Healthcare, and United Kingdom). The relative protein levels were determined by densitometry scanning (Alpha Innotech), keeping the pixel intensity within the linear range of detection.

2.3.4 Computer-aided drug design/Computational similarity search.

Low-molecular weight compounds that interact with ERK2, inhibit phosphorylation of ERK substrates, and inhibit cell proliferation were previously identified using computational and cell-based assays [25-27]. A computational search was used to identify additional compounds that share chemical features with two previously identified active compounds, referred to as **17** and **76** [25]. The search based on the chemical similarity using the MAC-BITS fingerprints in conjunction with the Tanimoto Similarity index to search a virtual database of over 1 million commercially available compounds as described [28].

2.3.5 Steady-state measurements and absorption spectroscopy.

Steady-state fluorescence measurements were recorded using a SpectraMax M5 microplate reader (Molecular Devices; Sunnyvale, CA) equipped with a Xenon flash lamp, dual monochromators and SoftMax Pro software and/or a K2 fluorometer (ISS; Champaign, IL) equipped with a xenon lamp, variable slits, and a microprocessor-controlled photomultiplier. The excitation wavelength was 280 nm (no significant difference in data was observed whether excitation was 280 nm or 295 nm) and the emission wavelength was 336 and 342 nm for p38α and ERK2, respectively. The emission spectra of proteins are dependent upon the proteins tertiary structure. Proteins containing multiple tryptophans will likely have varying emission spectra as the emission spectra relates to the micro-environment of the tryptophan [5]. In this case p38 has five tryptophan residues and ERK2 has three tryptophan residues. The emission maximum of p38 tryptophans is blue-shifted in comparison with the emission maximum of ERK tryptophans by 6 nm.

Absorbance spectra of the proteins and optical density of compounds were determined with a Varian Cary Bio 50 UV-visible spectrophotometer (Agilent Technologies; Palo Alto, CA) or the SpectraMax M5 microplate reader. Data were analyzed with SoftMax Pro software, Microsoft Excel, and Microcal Origin 7.0 (Microcal Software; Northhampton, MA). The fluorescence data unless otherwise indicated is reported as the mean and standard error of at least three independent measurements.

2.3.6 Fluorescence quenching.

Fluorescence quenching assays were performed at room temperature in 200 µL volumes in clear Greiner 96-well microplates (Greiner Bio-One, Germany). To screen for binding activity of the compounds, 1 µM ERK2 and/or p38α in 10 mM HEPES, 150 mM NaCl buffer, pH 7.4 was aliquot into each well along with varying concentrations of test compound and/or spectrophotometric grade dimethyl sulfoxide (DMSO) as the control solvent. DMSO concentration was maintained constant at 2.5%. Samples were thoroughly mixed and fluorescence quenching monitored.

Dissociation constants (K_D) were determined by titrating the protein with varying concentrations of the test compounds in each well while maintaining both protein and DMSO concentrations constant. The fluorescence intensity values were plotted as a function of compound concentration. Decreases in fluorescence intensity at 336 nm and 342 nm for p38α and ERK2, respectively, relative to the DMSO-only control were indicative of compound interaction with the MAP kinase protein. The data were fit with a single hyperbola using the following equation:

$$\mathbf{F = 1 - \mathit{f} * x / (\mathit{K_D} + x)} \qquad \mathbf{(3)}$$

where F is the fluorescence intensity normalized to 1 in the absence of ligand, x is the concentration of compound, f is the fraction of binding, and K_D is the dissociation constant.

2.3.7 Inner-filter effect correction.

The inner filter effect is the attenuation in the excitation light when the compound absorbs maximally close to tryptophan's excitation wavelength of the protein being examined and/or the emission light when the compound absorbs at tryptophan's emission wavelength. As a result, an apparent decrease in the emission intensity is observed, which erroneously mimics quenching of tryptophan fluorescence. Moreover, the relationship between absorbance and ligand concentration is directly proportional; therefore, the degree of inner filter effect is dependent upon the concentration of the compounds [5, 29]. To correct for inner filter effect, equation 4 was applied [5].

$$\mathbf{F_{corr} = F_{obs}\ antilog\ ((OD_{ex} + OD_{em}) / 2)} \qquad \mathbf{(4)}$$

where F_{corr} is the corrected fluorescence value, F_{obs} is the measured fluorescence value, OD_{ex} and OD_{em} is the optical density at the excitation and emission wavelength, respectively.

2.4 Results

2.4.1 Inner-filter effect correction

The goal of the current studies was to use fluorescence spectroscopy methods to characterize the binding affinity of these compounds and determine their selectivity for the CD and ED domain of ERK2. The target protein's tryptophan residues are sensitive to changes in the local environment and can therefore be used to monitor structural changes and molecular interactions [2-4, 25, 26]. We evaluated the steady-state fluorescence of ERK2 in the context of test compounds at a single concentration. As shown in Figure 2.3, test compounds caused varying degrees of fluorescence quenching.

The spectral characteristics of compounds were examined to reduce the potential of identifying false positive ERK2 interacting compounds. The inner-filter effect can cause a decrease in the intensity of the excitation at the point of observation or can cause a decrease in the observed fluorescence emission by absorption of the fluorescence [5]. In this case the effect is dependent on the optical density of the sample at the excitation and/or emission wavelength of tryptophan as well as the concentration of the compound. We tested each compound and found one, designated **36.5**, to have the inner filter effect properties. Figure 2.4A shows an overlay of the absorbance profile of **36.5** with the fluorescence emission spectrum of ERK2. It is apparent that the compound absorbs in the range where tryptophan emits. When measuring fluorescence quenching, reabsorption of the emitted light causes a shift in the spectra and/or distortion of the shape of the spectral band (Figure 2.4B). We apply a correction factor (equation 4 in Methods) and the shift in the spectra is no longer present (Figure 2.4C). Thus, this correction is necessary to discriminate between molecular interactions between the compound and the target protein

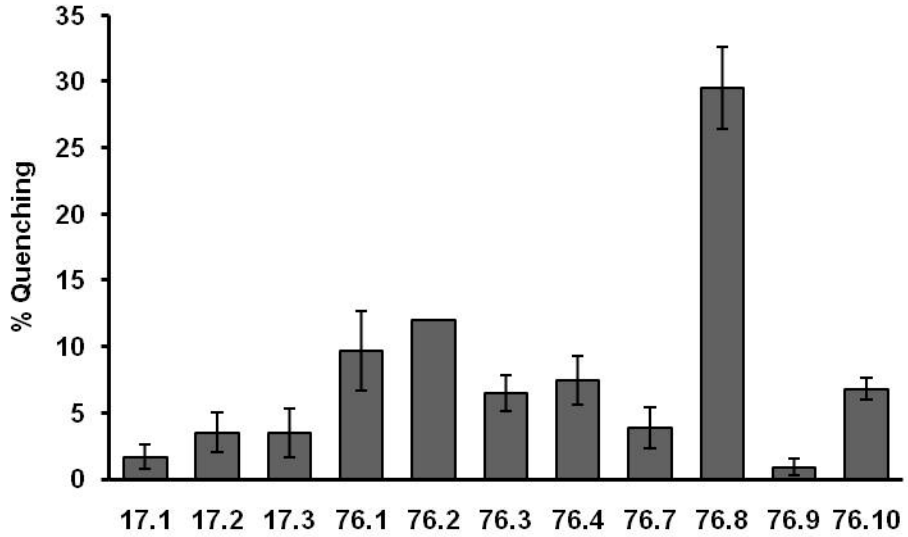

Figure 2.3. Effect of compounds similar to **17** and **76** on ERK2 Fluorescence. Fluorescence quenching of select low molecular weight compounds targeting the region near the CD/ED domain of ERK2 was determined. ERK2 (1 μM) was incubated with 20 μM of the indicated compound. Excitation was 280 nm and emission was observed at 342 nm. Bars represent the mean and standard deviation from 3-4 independent experiments.

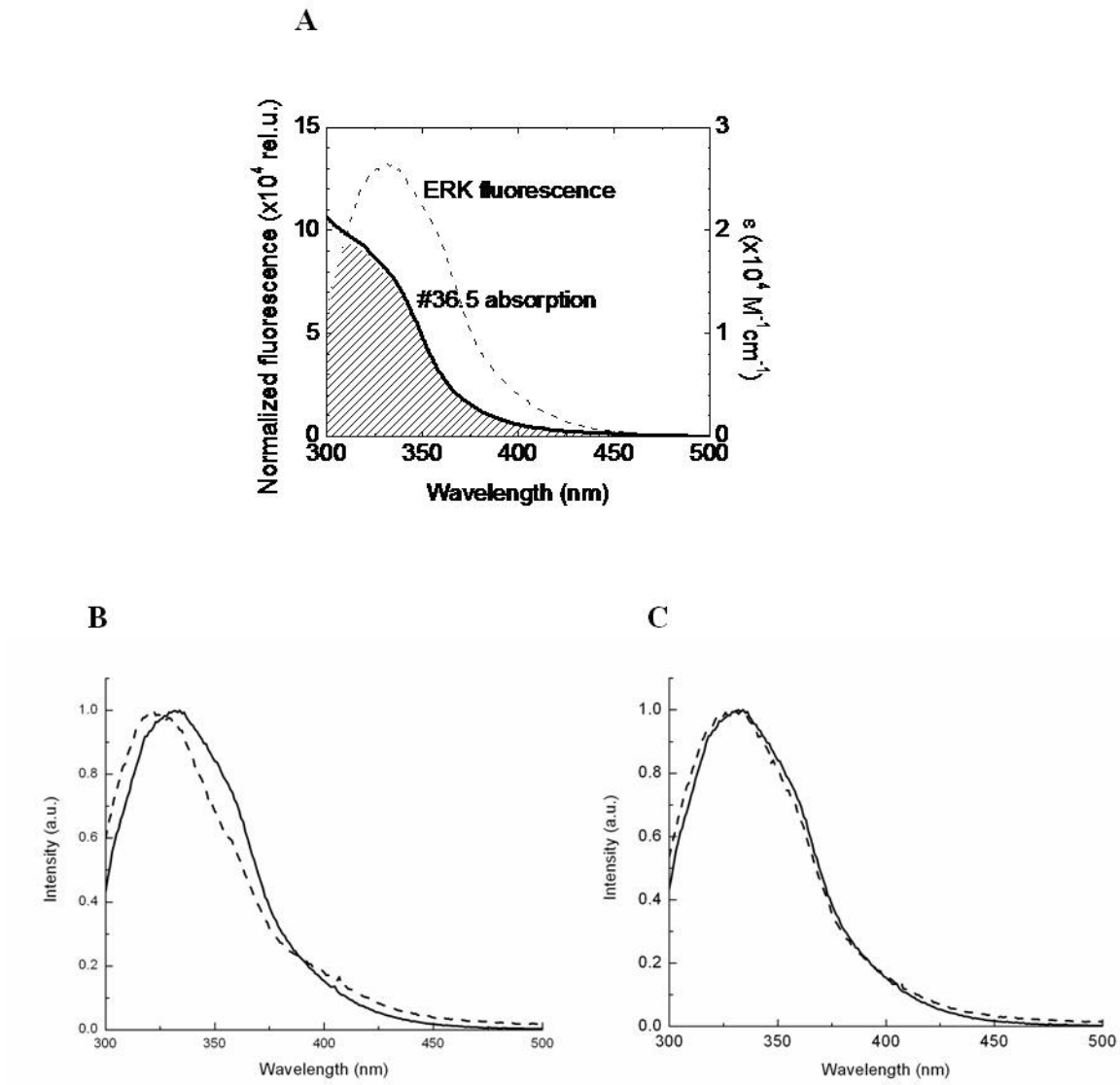

Figure 2.4. Spectral properties of ERK2 and **36.5**. A) ERK2 fluorescence spectrum normalized to the total integrated fluorescence emission is a dashed line (left axis). Absolute absorption spectrum (molar extinction coefficients) of the compound is a solid line (right axes). The spectral overlap is shaded. B) Inner filter effects cause an artificial shift in spectra of ERK2 in the absence of compound (solid line) upon addition of 20 µM **36.5** (dashed line). C) Upon applying a correction factor (equation 4), the distortion in the spectrum disappears. Solid line is no compound. Dashed line is upon addition of 20 µM **36.5**.

and the inherent spectral characteristics of the test compounds, which could result in a false positive.

2.4.2 Selectivity of lead compounds for ERK2 CD/ED domain.

We evaluated the selectivity of lead compounds for the CD and/or ED domain of ERK2. Among the many compounds tested, fluorescence quenching indicated that the parent compound **76** had a binding affinity (K_D) of 5 μM [25]. ERK2 was titrated with compounds showing greatest degree of fluorescence quenching and the K_D values were determined (Table 2.1). The binding of **76.1, 76.2, and 76.8** with ERK2 resulted in K_D values similar to that of lead compound **76** suggesting these alterations did not improve ERK2 binding. However, the K_D value of **76.3** showed a more than 3 fold increase in ERK2 binding affinity as compared to the parent compound. This supports recent studies showing 76.3 is more effective in inhibiting D-domain containing substrates [30].

To determine whether the compounds indeed utilize residues of the CD/ED domain, we tested the compounds against mutants of ERK2: single mutants T157A and D319N and the double mutant T157A/D319N to quantify binding interactions (Table 2.1). D319N is a mutation of the CD domain and T157A is a mutation of the ED domain. As shown by circular dichroism (CD) spectra, the CD/ED mutations did not affect the overall secondary structure of the protein suggesting the mutants are structurally similar to wild-type ERK2 [6]. In addition, the steady state emission spectra of the mutant proteins showed no significant differences as compared to ERK2 wild-type (Figure 2.5).

Table 2.1. Binding affinities of **76** and similar compounds with ERK2. The protein was titrated with compound and the binding affinity or K_D values were obtained by fitting data to single hyperbola. Data shown reflect the mean (μM) ± SEM for three independent experiments.

Inhibitor	*ERK*	*ERKT157A*	*ERKD319N*	*ERKT157A:D319N*
76	5.0 ± 0.30	6.1 ± 0.60	7.0 ± 1.0	6.4 ± 1.0
76.1	4.0 ± 1.0	13 ± 5.0	3.1 ± 0.40	5.0 ± 1.0
76.2	3.3 ± 0.20	2.4 ± 0.40	1.9 ± 0.30	4.0 ± 0.60
76.3	1.5 ± 0.10	8.0 ± 1.0	14 ± 1.0	>20
76.4	2.4 ± 0.90	3.0 ± 1.0	18 ± 2.0	>20
76.8	3.0 ± 1.0	15 ± 4.0	4.0 ± 1.0	10 ± 1.0

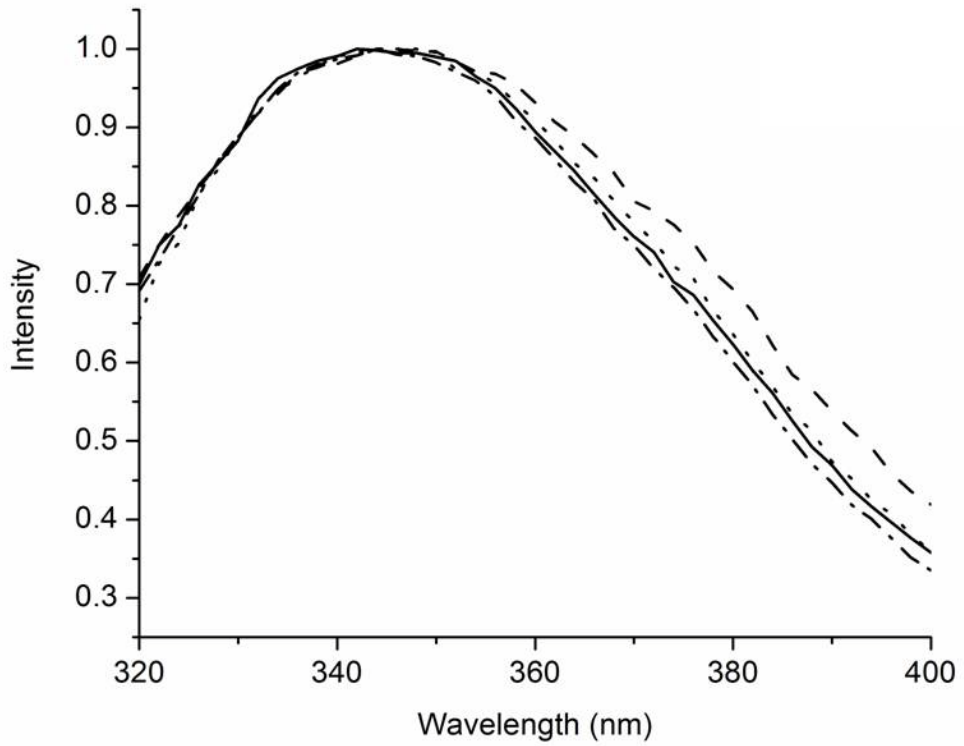

Figure 2.5. Normalized spectra of ERK2 CD/ED domain mutants as compared to wild-type. The solid line (——) represents ERK2 wild-type. The dashed line (- - - -) represents the CD mutant of ERK2 D319N. The dotted line (····) represents spectrum of CD/ED mutant T157A/D319N. The dash–dot (–·–·–) line represents the ED mutant T157A. Excitation wavelength was 280 nm.

As shown in Figure 2.6, there is a decrease in fluorescence quenching of the T157A/D319N mutant of ERK2 as compared to the wild-type in the presence of **76.3** and **76.8**. In the case of **76.3,** binding interactions with both single mutants and the double mutant resulted in decreased binding affinity (Table 2.1). Binding interactions of **76.3** with T157A and D319N produces K_D's of 8.0 ± 1.0 μM and 14.0 ± 1.0 μM, respectively. The binding interaction with the double mutant T157A/D319 yielded a K_D value >20 μM. This suggests that compound **76.3** interacts with both the CD and ED domain, possibly within the groove between the CD and ED domains.

The binding interactions of ERK2 wild-type and the mutant T157A with **76.4** were similar producing K_D's of 2.4 ± 0.9 μM and 3.0 ± 1.0 μM, respectively. However, the D319N mutation resulted in much weaker binding than that of wild-type, yielding a K_D value of 18 ± 2.0 μM. As would be expected, the binding interactions of **76.4** with the double mutant T157A/D319N resulted in much weaker binding affinity as well, a K_D >20 μM. This suggests that the low molecular weight inhibitor **76.4** interacts with the common docking (CD) domain in some capacity.

2.4.3 Selectivity of ERK targeted compounds for structurally similar p38α MAP kinase.

The structurally similar p38α MAP kinase shares an analogous substrate docking site to the CD-ED domain on ERK2 (Figure 2.7). The CD domain of human p38α is characterized by a cluster of acidic residues similar to ERK2: D313, D315, and D316 (Figure 2.8). The CD domain has been shown to facilitate interactions with the p38 activator MKK6, the phosphatase MKP-5, and MNK-1 [31]. The ED domain, unlike

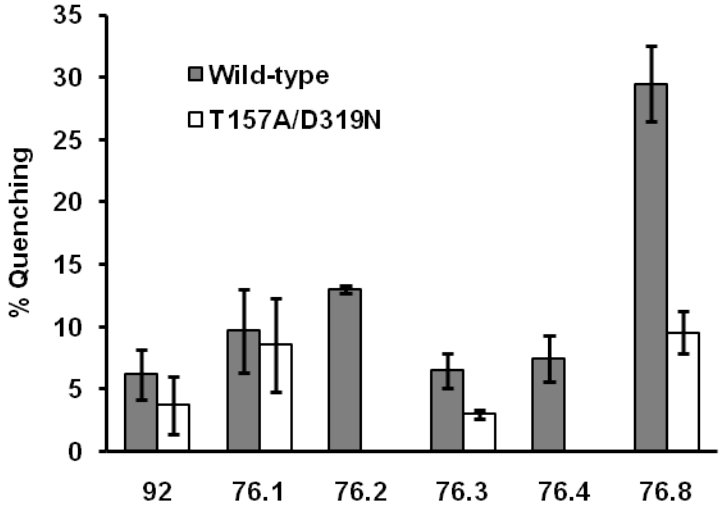

Figure 2.6. Initial screening of compounds for ERK2 wild type and CD/ED domain mutants. ERK2 proteins (1 μM) were incubated with 10 μM of the indicated compound. Excitation was 280 nm and emission was 342 nm. Bars represent the mean and standard deviation from 3-4 independent experiments.

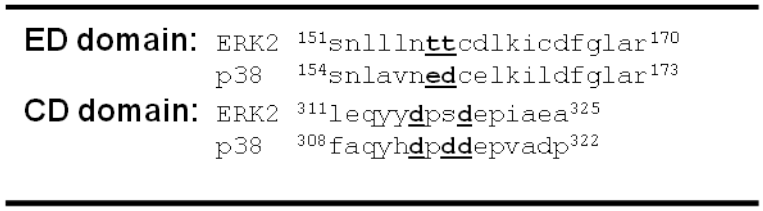

Figure 2.7. CD/ED domain primary sequences of ERK2 and p38α are analogous. The ED domain is named after E160 and D161 of human p38α and corresponds to T157 and T158 of ERK2 of *Rattus norvegicus*. The CD domain contains the acidic residues D316 and D319 (ERK2) and D313, D315 and D316 (p38).

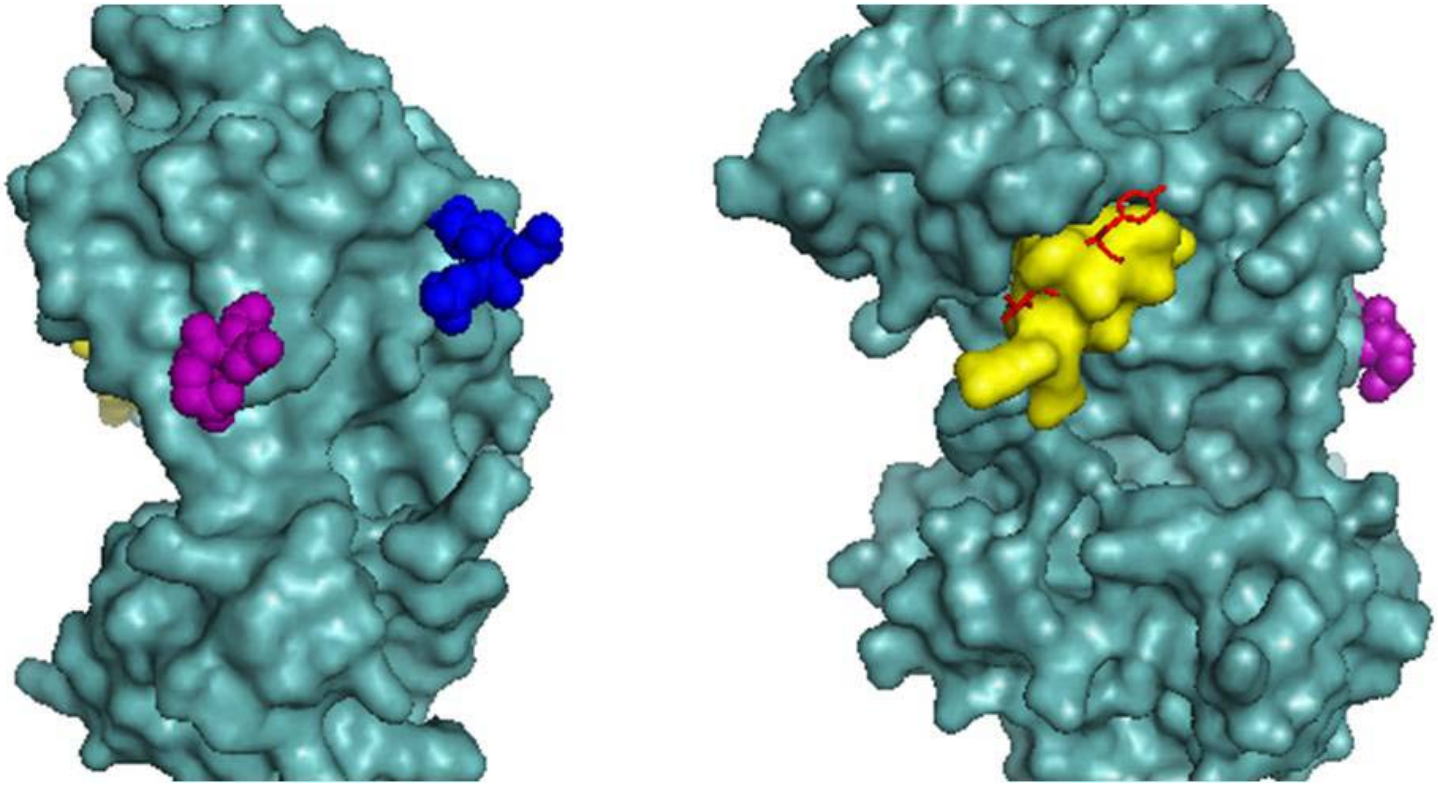

Figure 2.8. p38α docking domains and activation lip. The molecule in panel B is rotated around the vertical axis by 90° relative to the molecule in A. The CD and ED domains are in purple and blue, respectively. The activation lip is in yellow and the phosphorylation site residues (T183 and Y185) are in red. Molecular representations rendered in PyMOL (www.pymol.org).

ERK2, consists of the negatively charged amino acids Glu160 and Asp161, for which this domain is named. Both domains lie opposite to the active center of p38 (Figure 2.8). Test compounds that have been shown to interact with the CD/ED domain of ERK2 were tested against p38 to determine MAP kinase specificity. The selectivity of some of the more active compounds was compared to p38α and data suggests that several compounds showed greater quenching of ERK2. Of the compounds tested, 24%, including **92**, **76.1**, **76.4**, and **76.8,** showed greater quenching of ERK2 compared to p38α (Figure 2.9). Compounds **76.1** and **76.4** showed minimal or no quenching of p38α tryptophan fluorescence (Figure 2.9).

The binding interactions of structurally similar MAP kinases ERK2 and p38α were quantified (Table 2.2). Most of the compounds had similar binding affinities to p38α. K_D values for **76.2** and **76.8** were not statistically different suggesting that the compounds were not selective for ERK2. **76.1** showed a 2-fold increase in binding affinity with p38α as compared to WT. **76.4** interaction with p38α was less than a 2-fold increase in K_D as compared to **76.** Compound **76.3** showed a 3-fold decrease in K_D suggesting there is some selectivity for ERK2.

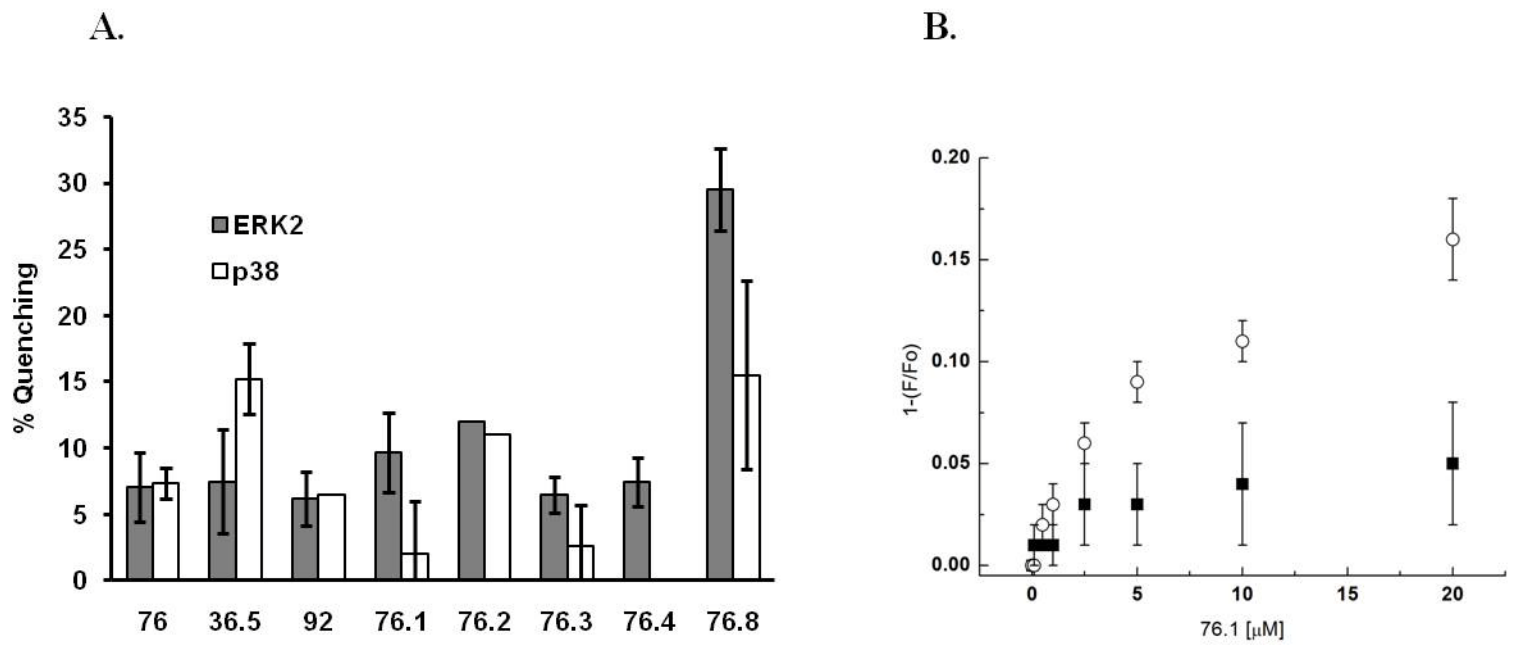

Figure 2.9. Direct interactions of test compounds with structurally similar MAP kinases ERK2 and p38α. **A)** ERK2 and p38 (1 μM) were incubated with 10 μM of the indicated compound. Excitation was 280 nm and emission was 342 nm. Bars represent the mean and standard deviation from 3-4 independent experiments. **B)** Titration of ERK2 and p38 with compound **76.1**. The symbols (open circle – ERK2; filled squares-p38) represent the average fluorescence intensity level (corrected for inner filter effect) at the indicated compound concentration. The bars represent the mean and standard deviation from 3-4 independent experiments. Degree of quenching is significantly less for p38 than for ERK2.

Table 2.2. Binding affinities of **76** and similar compounds with ERK2 and p38α. The protein was titrated with compound and the binding affinity or K_D values were obtained by fitting data to single hyperbola. Data shown reflect the mean (μM) ± SEM for three independent experiments.

Inhibitor	*ERK*	*p38*
76	5.0 ± 0.30	7.0 ± 1.0
76.1	4.0 ± 1.0	9.0 ± 1.0
76.2	3.3 ± 0.20	4.0 ± 1.0
76.3	1.5 ± 0.10	4.5 ± 0.90
76.4	2.4 ± 0.90	4.1 ± 0.20
76.8	3.0 ± 1.0	4.2 ± 1.0

2.5 Discussion

Changes in the fluorescence intensity of tryptophan residues suggest that protein conformation changes occur in the regions surrounding the tryptophan residues. The conformation change is attributed to molecular interactions with the test compound [5, 25, 32, 33]. Thus fluorescence quenching is used as a method to rapidly screen and quantify binding affinity of test compounds with a protein target. An added advantage is that minute amounts of material are required. The use of a fluorescence microplate reader provides the ability to identify hits from high-throughput screening assays. More importantly, extrinsic labeling of fluorophores is not necessary as the natural fluorescence and absorbance of the compound is utilized. However there are limitations when using this technique for the purposes discussed. A limitation of using fluorescence spectroscopy is that it does not provide a definitive description of where on the protein the test compound is binding. Also, it is important to realize that lack of quenching does not exclude compound interaction. Fluorescence quenching of tryptophan fluorescence provides insight as to what happens in the micro-environment of tryptophan. It is possible that conformation changes can occur in a region where tryptophan is not present; therefore, no significant change in tryptophan emission spectrum will be evident.

We tested the fluorescence assay used in these experiments against two alternative methods: isothermal titration calorimetry (ITC) and surface plasmon resonance (SPR). These methods were utilized to validate the binding affinity of compound **2.3.2** (discussed briefly in Chapter 1) to ERK2 [34]. As previously stated, X-ray crystallography demonstrated that **2.3.2** indeed bound to ERK2, though not at the predicted site [34]. The binding affinity as determined by fluorescence titrations was 0.13

μM. Both ITC and SPR yielded submicromolar binding affinities for **2.3.2** in complex with ERK2 of 0.5 and 0.3 μM, respectively [34]. We also used ITC and SPR to validate the binding affinity of the ERK2 inhibitor **3.15** in complex with ERK2, and the K_D's determined were 0.04 and 0.03 μM, respectively for ITC and SPR. The values compared favorable to the binding affinity of 0.018 μM determined via fluorescence. The values obtained indicate that all three methods produce binding affinities within the same order of magnitude for both systems measured. Therefore, we proceeded to determine binding affinities of test compounds using fluorescence spectroscopy as the primary method with the caveat that alternative methods such as ITC, SPR, and X-ray crystallography be used in the future as a means to validate data obtained.

It was also necessary to consider the spectral properties of the compounds being titrated with the protein. An apparent change in the emission spectra of the protein may result if the test compound absorbs in the range where the protein is excited and/or where the protein emits. This effect is known as inner-filter effect. Inner-filter effect may cause a decrease in the intensity of the excitation at the point of observation or can cause a decrease in the observed fluorescence by absorption of the fluorescence [5]. Therefore, optical density of each compound was measured at each concentration (titrated) in the excitation and emission ranges of ERK2/p38α.

In these studies, fluorescence quenching was used to determine selectivity of low molecular weight compounds predicted to interact with specific substrate docking domains of ERK2. To determine the type of quenching (collisional or static), the average lifetime of ERK2 tryptophans was observed in the absence and presence of inhibitor. Both collisional and static quenching cause a decrease in fluorescence intensity;

collisional quenching in addition causes a decrease in the average lifetime of a population of fluorophores, in this case tryptophan. There is an overlap in the emission of ERK2 tryptophans and the absorbance spectrum of **76.3** (though absorbance is not significant at low concentrations), satisfying a pre-requisite for fluorescence resonance energy transfer (FRET). The lifetime of ERK2 in the absence of inhibitor was 4.08 ± 0.01 ns. The addition of 10 μM of **76.3** produced an average lifetime value of 4.00 ± 0.02. As expected, this data suggested that quenching was static and that energy transfer does not occur in this system.

Of the **76** structurally similar compounds screened, data showed that **76.1, 76.2, 76.3, 76.4** and **76.8** interacted directly with the protein based on degree of quenching. Binding interactions were quantified and the compounds with ERK2 wild-type yielded K_D's that were in the lower micromolar range similar to **76**, though the binding affinity of **76.3** to ERK2 wild-type suggests that we are moving in the right direction in terms of selecting compounds that display similar or better activity than the lead compound. To determine whether the compounds interact with CD/ED domain, we tested them against mutants of ERK2. Single mutants are T157A (ED domain) and D319N (CD domain) and the double mutant T157A/D319N. CD spectral analysis showed that the CD/ED mutations did not affect the overall secondary structure of the protein [6]. Also, steady state emission spectra of the mutants suggested no significant differences in the tertiary structure - at least as it relates to the local environment of tryptophan - as compared to ERK2 wild-type. Binding interactions with the double mutant T157A/D319N suggested that **76.3** in fact interacts with the CD/ED domain as predicted. Individual contributions of the CD and ED domain were measured using single mutants D319N and T157A.

There was a marked decrease in binding affinities of both mutants upon titration with **76.3**. However, data suggests that the CD domain contributes more to binding interactions as assessed by its weaker K_D. Of interest is the fact that the sum of the values of each single mutant is greater than 20 μM which suggests that there may be some cross-talk between the two domains. It is likely that the compound binds the hydrophobic groove situated between the CD and ED domains. ERK2 wild-type and T157A with **76.4** produced similar K_D's, however interaction with the D319N mutant resulted in much weaker binding. This suggests that **76.4** interacts with the CD domain in some capacity.

The selectivity of some of the more active compounds for the structurally similar MAPK's was determined as well. Several compounds showed greater degree of quenching of ERK2 than p38α. Three of the compounds showed a two-fold or greater decrease in binding affinity with p38α as compared to ERK2 wild-type. Though not amazingly significant, this suggests that the similarity search produced compounds that show some selectivity for ERK2, which is a great starting point for optimization studies.

2.6 List of References

1. Birdsall, B., et al., *Correction for light absorption in fluorescence studies of protein-ligand interactions.* Anal Biochem, 1983. **132**(2): p. 353-61.
2. Cai, L. and M. Gochin, *A novel fluorescence intensity screening assay identifies new low-molecular-weight inhibitors of the gp41 coiled-coil domain of human immunodeficiency virus type 1.* Antimicrob Agents Chemother, 2007. **51**(7): p. 2388-95.
3. Samworth, C.M., M. Degli Esposti, and G. Lenaz, *Quenching of the intrinsic tryptophan fluorescence of mitochondrial ubiquinol--cytochrome-c reductase by the binding of ubiquinone.* Eur J Biochem, 1988. **171**(1-2): p. 81-6.
4. Tiriveedhi, V. and P. Butko, *A fluorescence spectroscopy study on the interactions of the TAT-PTD peptide with model lipid membranes.* Biochemistry, 2007. **46**(12): p. 3888-95.
5. Lakowicz, J.R., *Principles of Fluorescence Spectroscopy*. 2nd Edition ed. 1999, New York: Springer.
6. Burkhard, K.A., F. Chen, and P. Shapiro, *Quantitative analysis of ERK2 interactions with substrate proteins: roles for kinase docking domains and activity in determining binding affinity.* J Biol Chem, 2011.
7. Sheridan, D.L., et al., *Substrate discrimination among mitogen-activated protein kinases through distinct docking sequence motifs.* J Biol Chem, 2008. **283**(28): p. 19511-20.

8. Zhou, T.J., et al., *Crystal structure of the MAP3K TAO2 kinase domain bound by an inhibitor staurosporine.* Acta Biochim Biophys Sin (Shanghai), 2006. **38**(6): p. 385-92.

9. Tanoue, T., et al., *Identification of a docking groove on ERK and p38 MAP kinases that regulates the specificity of docking interactions.* The EMBO journal, 2001. **20**(3): p. 466-79.

10. Tanoue, T. and E. Nishida, *Molecular recognitions in the MAP kinase cascades.* Cell Signal, 2003. **15**(5): p. 455-62.

11. Hu, Y.J., et al., *Interaction of colchicine with human serum albumin investigated by spectroscopic methods.* Int J Biol Macromol, 2005. **37**(3): p. 122-6.

12. Manceva, S., Pusztai-Carey M, Russo PS, Butko P., *A Detergent-like Mechanism of Action of the Cytolytic Toxin Cyt1A from Bacillus thuringiensis var. israelensis.* Biochemistry, 2005. **44**(2): p. 589-597.

13. Valeur, B., *Molecular Fluorescence: Principles and Applications*. 2002, Weinheim: Wiley-VCH.

14. Kosinski-Collins, M.S. and J. King, *In vitro unfolding, refolding, and polymerization of human gammaD crystallin, a protein involved in cataract formation.* Protein Sci, 2003. **12**(3): p. 480-90.

15. Lasagna, M., et al., *Apohorseradish peroxidase unfolding and refolding: intrinsic tryptophan fluorescence studies.* Biophys J, 1999. **76**(1 Pt 1): p. 443-50.

16. Jameson, D.M., E. Gratton, and J.F. Eccleston, *Intrinsic fluorescence of elongation factor Tu in its complexes with GDP and elongation factor Ts.* Biochemistry, 1987. **26**(13): p. 3894-901.

17. Callis, P.R., *1La and 1Lb transitions of tryptophan: applications of theory and experimental observations to fluorescence of proteins.* Methods Enzymol, 1997. **278**: p. 113-50.

18. Gryczynski, I., et al., *Lifetime distributions and anisotropy decays of indole fluorescence in cyclohexane/ethanol mixtures by frequency-domain fluorometry.* Biophys Chem, 1988. **32**(2-3): p. 173-85.

19. Hasselbacher, C.A., et al., *Environments of the four tryptophans in the extracellular domain of human tissue factor: comparison of results from absorption and fluorescence difference spectra of tryptophan replacement mutants with the crystal structure of the wild-type protein.* Biophys J, 1995. **69**(1): p. 20-9.

20. Butko, P., et al., *Interaction of the delta-endotoxin CytA from Bacillus thuringiensis var. israelensis with lipid membranes.* Biochemistry, 1997. **36**(42): p. 12862-8.

21. Hammarstrom, P., et al., *Structural mapping of an aggregation nucleation site in a molten globule intermediate.* J Biol Chem, 1999. **274**(46): p. 32897-903.

22. Gao, F., et al., *Agonist-mediated conformational changes in acetylcholine-binding protein revealed by simulation and intrinsic tryptophan fluorescence.* J Biol Chem, 2005. **280**(9): p. 8443-51.

23. Ren, J., et al., *Transmembrane orientation of hydrophobic alpha-helices is regulated both by the relationship of helix length to bilayer thickness and by the cholesterol concentration.* Biochemistry, 1997. **36**(33): p. 10213-20.

24. Shapiro, P.S., et al., *Extracellular signal-regulated kinase activates topoisomerase IIalpha through a mechanism independent of phosphorylation.* Mol Cell Biol, 1999. **19**(5): p. 3551-60.

25. Hancock, C.N., et al., *Identification of novel extracellular signal-regulated kinase docking domain inhibitors.* Journal of medicinal chemistry, 2005. **48**(14): p. 4586-95.

26. Chen, F., et al., *Characterization of ATP-independent ERK inhibitors identified through in silico analysis of the active ERK2 structure.* Bioorg Med Chem Lett, 2006. **16**(24): p. 6281-7.

27. Chen, F., et al., *Using Caenorhabditis elegans as a model organism for evaluating extracellular signal-regulated kinase docking domain inhibitors.* J Cell Commun Signal, 2008. **2**(3-4): p. 81-92.

28. Macias AT, et al., *Lead validation and SAR development via chemical similarity searching; application to compounds targeting the pY+3 site of the SH2 domain of p56lck.* . J Chem Inf Model, 2005. **45**: p. 1759-1766.

29. Geoghegan, K.F., *Improved method for converting an unmodified peptide to an energy-transfer substrate for a proteinase.* Bioconjug Chem, 1996. **7**(3): p. 385-91.

30. Boston, S.R., et al., *Characterization of ERK docking domain inhibitors that induce apoptosis by targeting Rsk-1 and caspase-9.* BMC cancer, 2011. **11**: p. 7.

31. Tanoue, T., et al., *A conserved docking motif in MAP kinases common to substrates, activators and regulators.* Nat Cell Biol, 2000. **2**(2): p. 110-6.

32. Sillen, A., et al., *Mechanism of fluorescence and conformational changes of the sarcoplasmic calcium binding protein of the sand worm Nereis diversicolor upon Ca2+ or Mg2+ binding.* Biophys J, 2003. **85**(3): p. 1882-93.

33. Bourbon-Freie, A., et al., *Trp-107 and trp-253 account for the increased steady state fluorescence that accompanies the conformational change in human pancreatic triglyceride lipase induced by tetrahydrolipstatin and bile salt.* J Biol Chem, 2009. **284**(21): p. 14157-64.

34. Zhang, J., et al., *Chemical control of a signaling crossroad: ATP-independent ERK2 inhibitors targeting substrate docking domains.* 2011.

CHAPTER 3: Structure-Activity Relationship (SAR) of Compounds that Target the ERK2 CD Domain.

3.1 Introduction

It has been shown in the previous chapter that structurally similar compounds that have similar biological effects and chemical features may indeed have increased selectivity and potency as compared to the parent compound **76**. In an attempt to further improve the efficacy and selectivity of **76**, a more detailed study of the structure activity relationship has been performed in Dr. Steve Fletcher's laboratory in the Department of Pharmaceutical Sciences. This will lead to a better understanding of the mode of interaction between ERK and the compounds of interest. As previously mentioned, the **76** family of compounds were predicted by CADD to bind a groove between the CD and ED domain. Specifically interactions between the CD domain of ERK2 and the D-domain of substrate proteins include ionic interactions between the basic lysine/arginine residues of the D-domain and the acidic aspartate residues of the CD domain as well as hydrophobic interactions [1-3]. CADD studies also predicted that the phenyl ring of **76** was involved in a cation-pi interaction with R133 of ERK2. The amino group of **76** may be involved in electrostatic interactions, making it a promising target for modifications. Therefore chemical modifications to the amino group of the thiazolidine-2,4,dione core of the parent compound **76** have been introduced via CADD directed medicinal chemistry to create novel low molecular weight compounds with possible increased specificity and potency towards the ERK2 kinase and to better understand which chemical groups are responsible for the compounds' biological effects. Modifications involved functionalizing the amino group of **76** with the addition of secondary and tertiary amines, amides, sulfonamides, and anilines. Fluorescence spectroscopy was used to screen the compounds

against the ERK2 kinase to determine those compounds that caused the greatest degree of quenching of tryptophan fluorescence. Resulting data along with analysis of (cell-based assays/cell proliferation assays) were used to select lead compounds. The K_D values were then determined for lead compounds by titrating ERK2 with the compound of interest. Selectivity for the CD and/or ED domain of ERK2 was determined as well as selectivity for the structurally similar p38α MAP kinase. The chemical structures of the **76** similar compounds are shown in Figure 3.1.

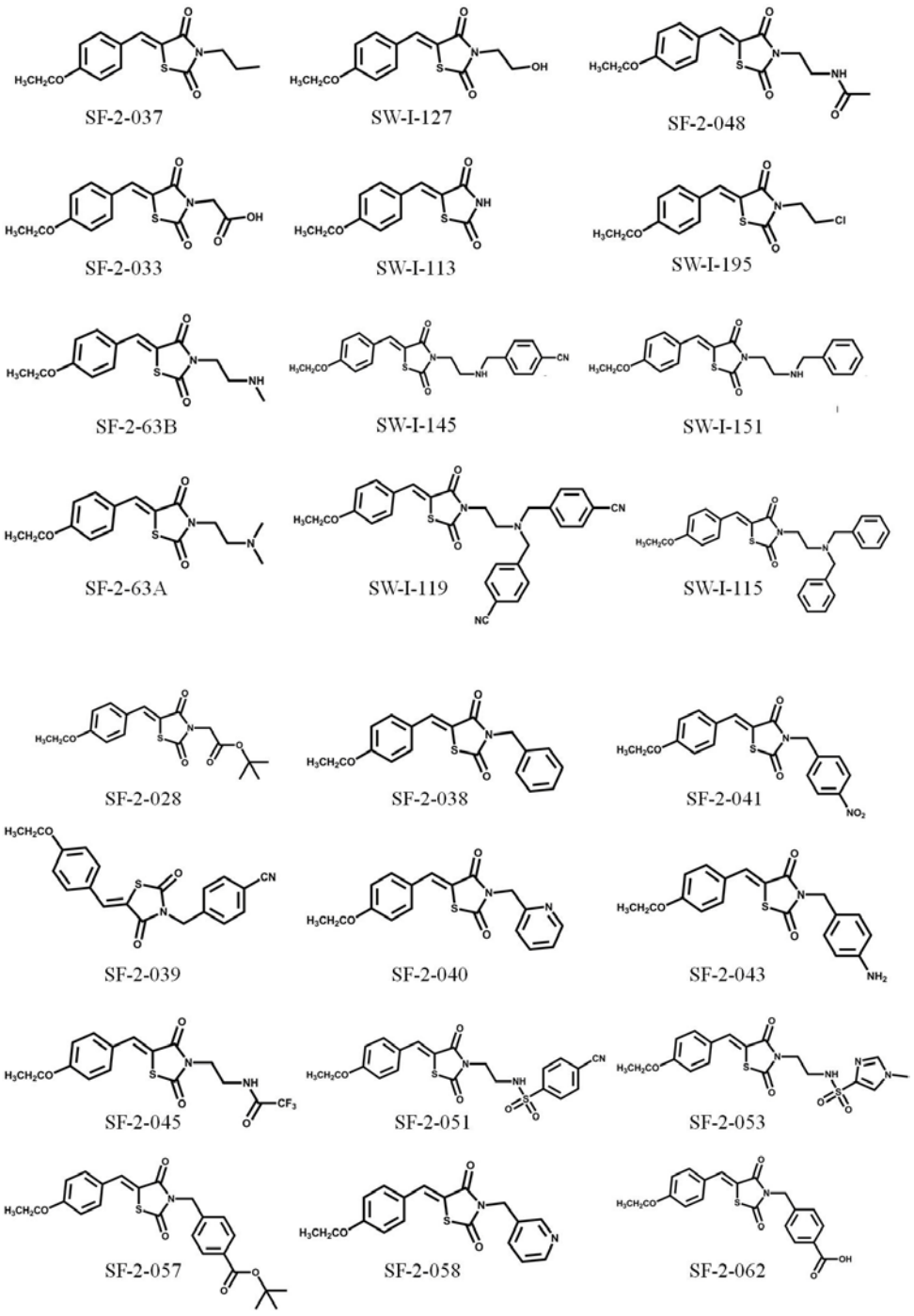

Figure 3.1. Chemical structures of **76** and structurally similar compounds synthesized in Dr. Fletcher's laboratory.

3.2 Methods

3.2.1 Optimization of parent compound 76.

35 novel low molecular weight compounds structurally similar to the parent compound **76** were designed in the laboratory of Dr. Steven Fletcher via CADD directed medicinal chemistry. Briefly, thiazolidin-2,4-dione and 4-ethoxybenzaldehyde underwent a Knoevenagel condensation reaction to introduce the 4-ethoxyphenyl group onto the compound. The primary amino group was functionalized by reductive aminations, acylations, sulfonylations and arylations. The resulting compounds were purified and solubilized in DMSO and stored as 25 mM stock solutions at -20°C.

3.2.2 Cell proliferation assay

Cell proliferation was evaluated by the water soluble tetrazolium-1 (WST-1) assay as previously described [4]. Cells were seeded in 96 well plates and allowed to adhere overnight. The cells were treated with 50 μM test compounds for 48 hours. WST-1 reagent was added and the absorbance read at 450 nm with background readings taken at 650 nm. The background was subtracted and the values were normalized to the control (DMSO only) cells.

3.2.3 Fluorescence quenching.

Fluorescence quenching assays were performed at room temperature in 200 μL volumes in clear Greiner 96-well microplates (Greiner Bio-One, Germany). To screen for binding activity of the compounds, 1 μM ERK2 and/or p38α in 10 mM HEPES, 150 mM NaCl buffer, pH 7.4 was aliquot into each well along with varying concentrations of test

compound and/or spectrophotometric grade dimethyl sulfoxide (DMSO) as the control solvent. DMSO concentration was maintained constant at 2.5%. Samples were thoroughly mixed and fluorescence quenching monitored.

Dissociation constants (K_D) were determined by titrating the protein with varying concentrations of the test compounds in each well while maintaining both protein and DMSO concentrations constant. The fluorescence intensity values were plotted as a function of compound concentration. Decreases in fluorescence intensity at 336 nm and 342 nm for p38α and ERK2, respectively, relative to the DMSO-only control were indicative of compound interaction with the MAP kinase protein. The data were fit with a single hyperbola using equation 1:

$$\mathbf{F = 1 - f_{*}x / (K_D + x)} \qquad \mathbf{(1)}$$

where F is the fluorescence intensity normalized to 1 in the absence of ligand, x is the concentration of compound, f is the fraction of binding, and K_D is the dissociation constant.

3.3 Results

3.3.1 Rationale for compound design

To assess the importance of the primary amino group, we initially focused on replacing/functionalizing the amino group of **76** to alter its chemical properties (i.e. polarity, basicity, hydrophobicity). Using chemical synthesis to add new groups and/or remove groups to modify the biological activity and potency of the compounds presented a more direct approach to understanding SAR of these compounds. The first set of compounds produced assessed the importance of the amino group and contained modifications that varied the polarity and basicity of the linkage (Figure 3.1). **SF-2-048** is non basic. The amine group of **SW-I-195** and **SF-2-037** was replaced with a chorine and methyl group, respectively making both compounds non basic and non polar. Replacing the amine group with a hydroxyl group rendered **SF-I-127** non basic and polar. A carboxyl group replaced the amine group in **SF-2-033** rendering it polar and acidic. The ethylamine group of compound **SW-I-113** was completely removed to test the importance of the entire moiety to the activity of the compound. Some modifications were amino group isosteres (**SW-I-127** and **SF-2-037**). The second group of compounds was designed to assess the need of a primary group. The primary amino group was converted to secondary (**SF-2-063B** and **SW-I-119**) and tertiary (**SF-2-63A** and **SW-I-145**) amines. Several other compounds with varying functionalities were created as well (Figure 3.1).

3.3.2 Initial screening of compounds structurally similar to 76.

An initial screening of the compounds was performed to determine which compounds directly interacted with ERK2. Quenching of tryptophan fluorescence of ERK2 in the presence of 10 μM of test compound was evaluated (Figure 3.2). The extent of fluorescence quenching varied among the compounds tested. **SF-2-062** and **SW-I-151** quenched protein fluorescence 24% and 15%, respectively. The compounds **SW-I-113** and **SW-I-195** quenched tryptophan fluorescence 13 and 12%, respectively. Both **SW-I-127** and **SF-2-043** caused a 10% decrease in tryptophan fluorescence upon interaction with ERK2. The fact that ERK2 fluorescence was altered upon interaction of the test compounds suggested that the compounds directly interacted with ERK2.

3.3.3 Inhibition of A375 and HeLa cell proliferation by compounds structurally similar to 76.

Two cell lines were used in this study: A375 melanoma cells and HeLa cells. A375 cells harbor a mutation at residue 600 of B-Raf in which valine is replaced by glutamic acid (V600E). This mutation leads to elevated RAF signaling in these cells [7, 8]. Thus A375 cells exhibit constitutive activation of the ERK signaling pathway in vivo [7, 9]. B-Raf mutations have been identified in a variety of cancers including 70% of known melanoma cases, 50% of papillary thyroid cancers, and 10% of colorectal cancers [7, 10-12]. The HeLa cell line was derived from cervical cancer cells and is commonly used in cancer research. The effects of the 76 similar compounds on inhibition of cell proliferation were next examined (Figure 3.3). This work was done by Sarice Boston and Ramin Samadani in our laboratory. Some compounds that inhibited cell proliferation also

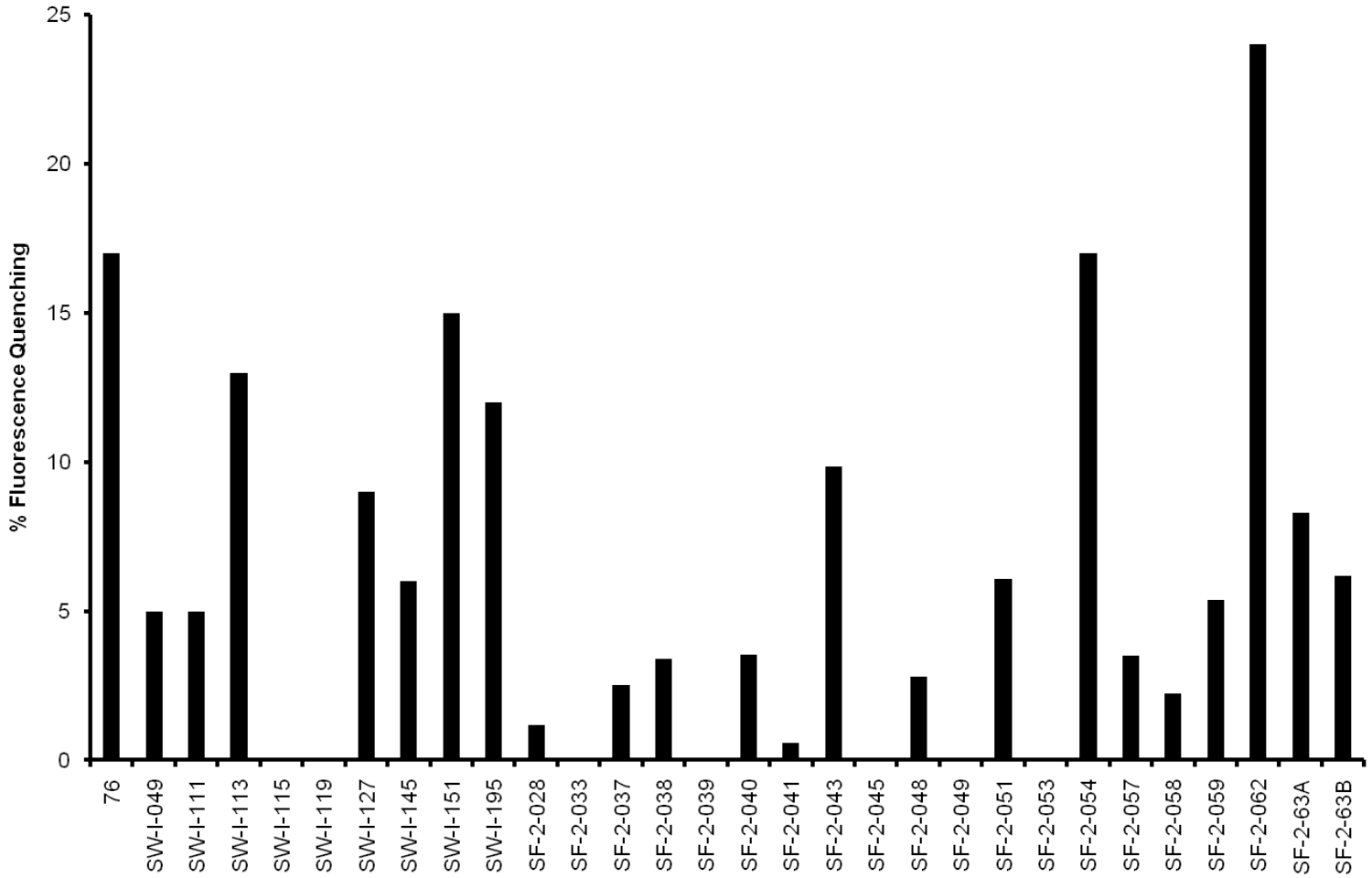

Figure 3.2. Initial screening of compounds similar to **76** on ERK2 fluorescence. ERK2 (1 µM) was incubated with 10 µM of the indicated compound. Excitation was 280 nm and emission was 342 nm.

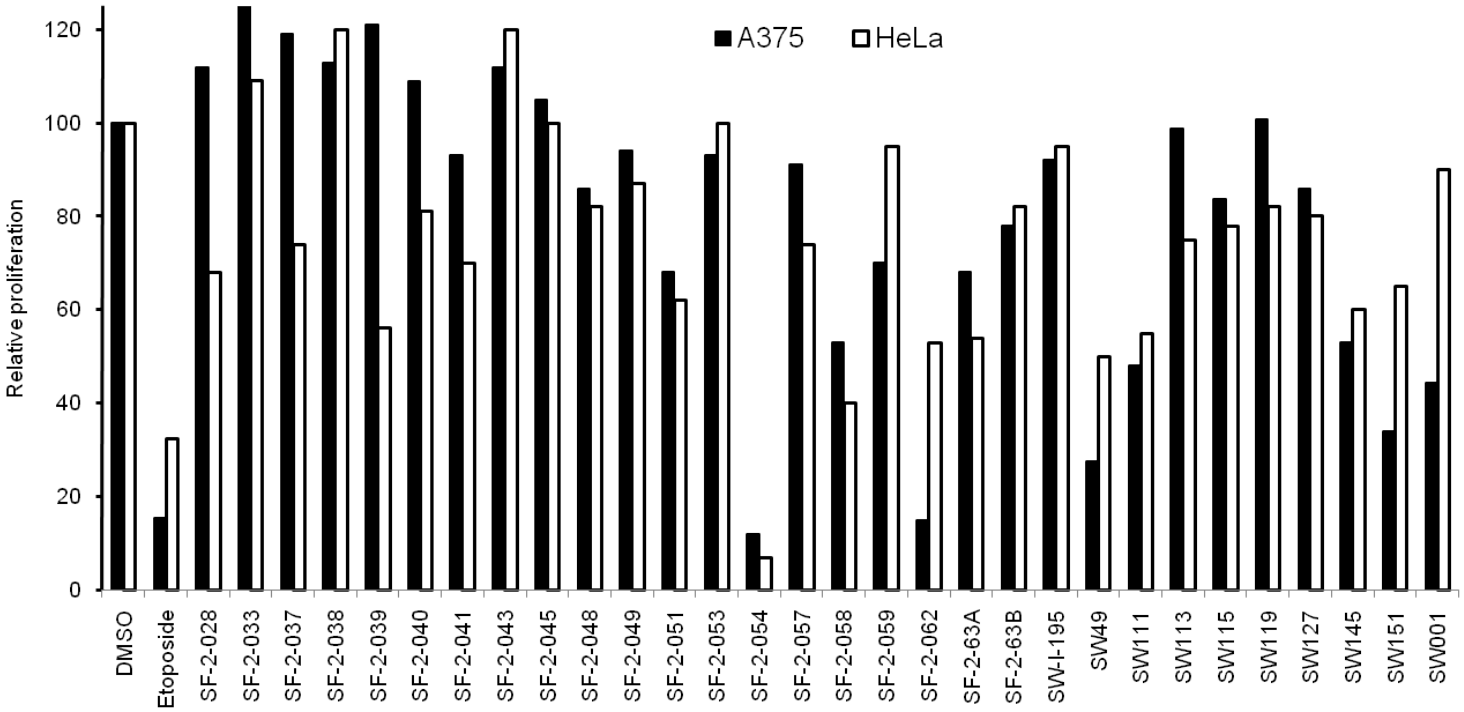

Figure 3.3. Inhibition of cell proliferation with **76** structurally similar compounds. The water soluble tetrazolium salt-1 (WST-1) assay was used to evaluate cell proliferation of A375 (B-Raf mutation) or HeLa cells. DMSO is vehicle control and etoposide is positive control. The cells (5000 cells/well) were seeded in 96 well plates, allowed to adhere overnight followed by incubation in the absence or presence of 50 µM test compound or etoposide for 48 hours. Values were normalized to the control (DMSO only) cells.

interacted directly with ERK2 as shown in the fluorescence quenching assays previously mentioned (Figure 3.2). Compounds **SW-I-49**, **SW-I-111**, **SW-I-145**, **SW-I-151**, and **SF-2-058** inhibit cell proliferation of A375 cells similar to compound **76** (Figure 3.3). All five of these compounds – though some to a lesser degree - caused a decrease in fluorescence quenching upon interaction. Though **SW-I-113**, **SW-I-127**, **SW-I-195**, and **SF-2-043** were shown to interact directly with ERK2, the compounds did not inhibit cell proliferation of A375 cells, nor did they significantly affect proliferation of HeLa cells.

SF-2-049 is a neutral compound and was shown to both quench tryptophan fluorescence of ERK2 and inhibit cell proliferation. We decided to make simple analogues of **SF-2-049**; however, harsh reaction conditions were needed to produce the anilines and ultimately led to decomposition of the compounds. To change the reactivity of **SF-2-049**, Dr. Fletcher introduced a triazine ring with chlorines attached (**SF-2-054**) as shown in Figure 3.1. Even though the analogues created from the intermediate were insoluble, the intermediate compound was assayed for bioactivity.

SF-2-054 produced an extent of quenching value of 17%. Interestingly, **SF-2-054** and **SF-2-062** inhibited A375 cell proliferation similar to the positive control, etoposide. At 50 μM dose, **SF-2-054** was more potent in inhibiting cell proliferation of HeLa cells than etoposide. In the case of A375 melanoma cells, a 50 μM dose of **SF-2-054** and **SF-2-062** inhibited cell growth by 88% and 85%, respectively. A dose response curve was generated for both compounds with A375 cells and the IC_{50} values were 4.2 and 21 μM for **SF-2-054** and **SF-2-062**, respectively (data not shown). Both **SF-2-054** and **SF-2-062** were more potent in inhibiting cell proliferation of A375 cells as compared to compound **76**, which was shown to inhibit A375 melanoma cells with an IC_{50} of 27 μM. Compound

7**6** was previously reported to inhibit HeLa cell proliferation with an IC_{50} of approximately 15-20 μM [13]. **SF-2-054** inhibited cell growth of HeLa cells similar to **76** with an IC_{50} 16 μM. Thus data suggests modifications made to the compounds enhance biological effects of **76**. Moreover, **SF-2-054** was more potent at inhibiting cell proliferation of A375 melanoma cells at 50 μM dose as compared to HeLa cells. This is significant in that A375 cells, as previously mentioned, contain the B-Raf V600E mutation which constitutively activates the MEK-ERK pathway. It is thought that aberrant ERK activity is the key to continued cell proliferation of the A375 melanoma cell line [14]. It has been shown that BAD, a substrate of ERK, experiences elevated phosphorylation at residue S134 primarily through over-stimulation of the Raf-MEK-ERK pathway which affects the efficiency of apoptosis and proliferation [8]. In that over-stimulation of the ERK pathway is the driving force of cell proliferation in A375 cells, greater inhibition of A375 cell growth by **SF-2-054** compared to HeLa cells not only suggested that the compound directly interacted with the ERK pathway and inhibited one or more of ERK's substrates responsible for cell proliferation, but also that **SF-2-054** and **SF-2-062** could be effective at inhibiting cancer cells displaying elevated ERK activity.

3.3.4 Quantification of interactions between compounds structurally similar to 76 with ERK2.

Compounds resulting in the most dramatic changes in fluorescence quenching tested were used in titration assays. ERK2 was titrated with 0-20 μM of the test compounds and – taking into account the spectral properties of the compounds - the decrease in the protein's fluorescence was used to quantify the binding affinities. In a

separate assay each compound's spectral properties in relation to ERK2 tryptophans' excitation and emission wavelengths were characterized and the need for inner filter effect corrections was determined. It is important to note that correction for inner filter effect for compounds with sufficiently low absorbance (<0.2) at the endpoint of the titration is not necessary [15] and may not have been applied. As previously mentioned, the binding interactions of the parent compound **76** with wild-type ERK2 showed a K_D of 5.0 μM.

The binding interactions of **SF-2-062** and **SF-2-054** showed more than a 3 and 25 fold increase, respectively, as compared to **76** in binding affinity to ERK2. This supports the previously mentioned studies showing that both compounds are more effective inhibitors of A375 cell proliferation (Figure 3.3). **SW-I-151** was shown to directly interact with ERK2 in the above quenching assay and the binding affinity was 1.1 ± 0.2 μM.

3.3.5 Selectivity of compounds structurally similar to 76 for ERK2 CD/ED domain.

Mutations in the CD/ED domain of ERK2 (T157A/D319N) decreased the binding affinity of **SF-2-062** about 5 fold as compared to ERK2 wild-type (Table 3.1). The binding affinity of **SF-2-054** with ERK2 mutant T157A/D319N decreased 10 fold. The individual contributions of the CD and ED domain were examined by observing the interactions between single mutants D319N (CD domain) and T157A (ED domain) and the compounds. The binding interactions of **SF-2-062** with ERK2 mutants T157A and D319N were 10.2 ± 1.3 μM and 3.7 ± 0.2 μM, respectively. The binding interactions of **SF-2-054** with the single mutants T157A and D319N were 6.0 ± 1.5 μM and 0.4 ± 0.1

Table 3.1. Selectivity of **76** and similar compounds to ERK2 CD/ED domain. ERK2 was titrated with 0-20 µM of the test compounds and the decrease in the protein's fluorescence was used to quantify the binding affinities. The fluorescence intensity values were plotted as a function of compound concentration. The data points were fit with a single hyperbola using equation 1. Data shown reflect the mean (µM) ± SEM for three independent experiments. ND = not determined.

Compound	ERK2WT	T157A	D319N	T157A/D319N
76 (parent)	5.0 ± 0.30	6.1 ± 0.60	7.0 ± 1.0	6.4 ± 1.0
SW-I-151	1.1 ± 0.20	ND	ND	ND
SF-2-054	0.17 ± 0.020	6.0 ± 1.5	0.40 ± 0.10	1.7 ± 0.20
SF-2-062	1.3 ± 0.40	10 ± 1.3	3.7 ± 0.20	6.8 ± 1.6

μM, respectively. This suggests that though both the CD and ED domain may facilitate binding of the compounds, the ED domain may contribute more to the interactions of **SF-2-062** and **SF-2-054** than the CD domain. The interactions of the ED domain (glutamate and aspartate) with p38 substrates include electrostatic interactions in that both amino acids carry a negative charge at physiologic pH. In the case of ERK2 however, threonine is a polar amino acid that does not carry a net charge at physiologic pH. Circular dichroism analysis of the single mutants suggested that the overall structure is similar to that of ERK2 wild-type [16]. The weaker binding interaction may be attributed to a localized structural change in the mutated region that disrupts binding similar to the effects of mutated amino acid residues on c-Fos binding to ERK2[16].

3.3.6 Selectivity of ERK-targeted compounds for structurally similar MAPK protein p38α.

Given the effects of the lead compounds **SF-2-054**, **SF-2-062**, and **SW-I-151** on cell proliferation and the fact that the compounds interacted directly with ERK2, the next question to address was whether the compounds could discriminate between structurally similar MAPK proteins. As previously mentioned, p38α shares an analogous substrate docking site to the CD-ED domain of ERK2. Both domains are located opposite the activation loop. Key differences within the ED domains of ERK2 and p38α do exist, however, and this domain is thought to regulate binding specificity [17].

Compound **76** has shown selectivity for inhibiting phosphorylation of ERK substrates. Phosphorylation of the ERK substrate p90RSK-1 in response to EGF stimulation was inhibited ~50% in the presence of **76** [13]. Also phosphorylation of the

transcription factor Elk-1, another known substrate of ERK, was also inhibited in the presence of increasing concentrations of **76** [13]. However, our lab showed that the compound had no effect on the ERK-mediated phosphorylation of the proapoptotic substrate Bim (unpublished data). Though **76** has been shown to directly interact with ERK2 (fluorescence quenching data) and is somewhat selective for inhibiting the phosphorylation of some ERK substrates, the compound does interact with p38 and has been shown to effect p38 substrate phosphorylation. The K_D values of **76** with ERK2 and p38α were not significantly different (5.0 μM and 7.0 μM, respectively). The activating transcription factor 2 (ATF2) is a substrate of p38. Upon stimulation by anisomycin, phosphorylation of ATF2 was inhibited ~40% in the presence of **76** (unpublished data).

In an effort to improve selectivity, binding interactions of selected structurally similar compounds with MAPK proteins were quantified. Selectivity of three of the more active compounds was compared to p38α MAP kinase (Table 3.2). The binding interaction of **SW-151** with p38α was identical to ERK2 wild-type (K_D's 1.1 ± 0.2 μM for ERK2 and 1.3 ± 0.3 μM for p38α) (Table 3.2), suggesting that this compound also did not preferentially interact with ERK2. In contrast, compound **SF-2-062** affinity to p38α resulted in a K_D value that was more than 3 fold higher as compared to ERK2 wild-type. In addition, the binding affinity of **SF-2-054** with p38α was 12.0 ± 2.0 μM, more than a 70 fold increase in K_D as compared to ERK2 wild-type. Thus, chemical modifications in **SF-2-054** can indeed support discrimination between the structurally similar kinases ERK2 and p38α.

Table 3.2. Selectivity of lead compounds similar to **76** for MAP kinases ERK2 and p38α. ERK2 and/or p38α was titrated with 0-20 μM of the test compounds and the decrease in fluorescence intensity at 336 nm and 342 nm for p38α and ERK2, respectively, relative to the DMSO-only control was used to quantify binding interaction. Data were fit with a single hyperbola (equation 1). The data shown reflect the mean (μM) ± SEM for three independent experiments.

Compound	ERK2WT	p38
76 (parent)	5.0 ± 0.30	6.1 ± 0.60
SW-I-151	1.1 ± 0.20	1.3 ± 0.30
SF-2-054	0.17 ± 0.020	12 ± 2.0
SF-2-062	1.3 ± 0.40	4.2 ± 0.30

3.3.7 Neutral compound analogues of SW-1-049 and SW-1-111

It was predicted that the chlorines attached to the triazoline ring may contribute to the increased reactivity of compound **SF-2-054**. As a control, Dr. Fletcher synthesized a structurally similar compound that lacked the reactive chlorine (**SS-1-019**). **SW-I-111** was originally used as a precursor to synthesize lead compound **76**, but the compound was shown to have bioactivity. It was shown to both quench tryptophan fluorescence of ERK2 and inhibit cell proliferation. Modifications were made to the carbamate group of **SW-I-111** to investigate altering hydrophobicity. As a result, a less hydrophobic compound (**SF-2-094**) was created while the addition of a fluorene group (**SF-2-095**) increased the hydrophobicity of the lead compound. Two additional novel low molecular weight compounds were synthesized and the chemical structures of all compounds designed are shown in Figure 3.4. An initial screening of the compounds was performed to determine which compounds directly interact with ERK2. Quenching of tryptophan fluorescence of ERK2 in the presence of 10 μM of test compound was evaluated (Figure 3.5). The extent of quenching for all compounds was ~10% or greater. **SS-1-019** caused the greatest decrease in fluorescence intensity of ERK2 tryptophans (>25% decrease) upon addition. **SF-2-095** and **SF-2-096** quenched ERK protein fluorescence ~20%. **SF-2-094** and **SF-2-052** quenched ERK protein fluorescence 13% and 9%, respectively. All five compounds were subjected to titration assays to quantify the binding interactions with ERK2 wild-type. Compound concentration ranged from 0-20 μM. The binding interaction of **SF-2-052** and **SF-2-094** (0.18 ± 0.06 μM and 0.27 ± 0.10 μM, respectively) were identical as compared to the parent compound **SF-2-054**. Though the difference in

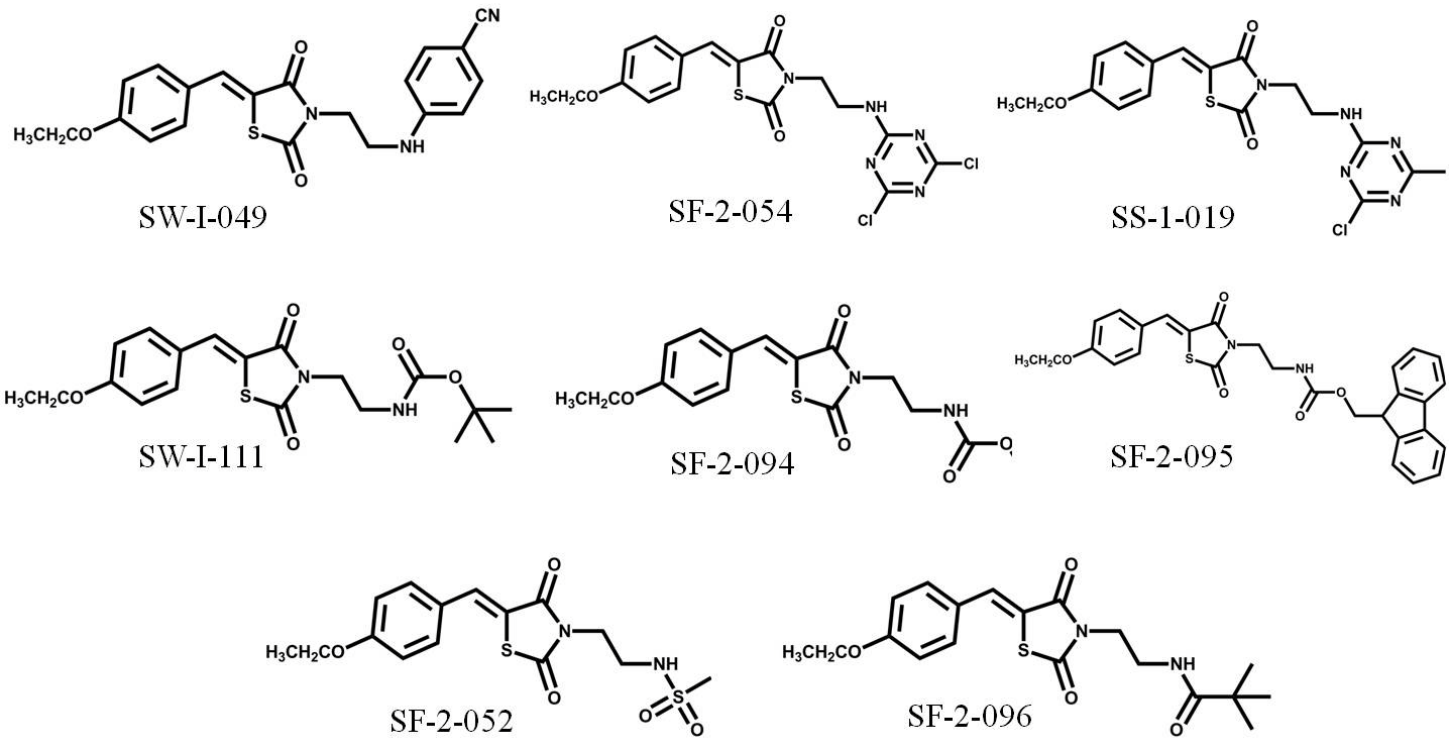

Figure 3.4. Chemical structures of neutral compound analogues. Compounds similar to **SW-I-049** and **SW-I-111** were synthesized in Dr. Fletcher's laboratory.

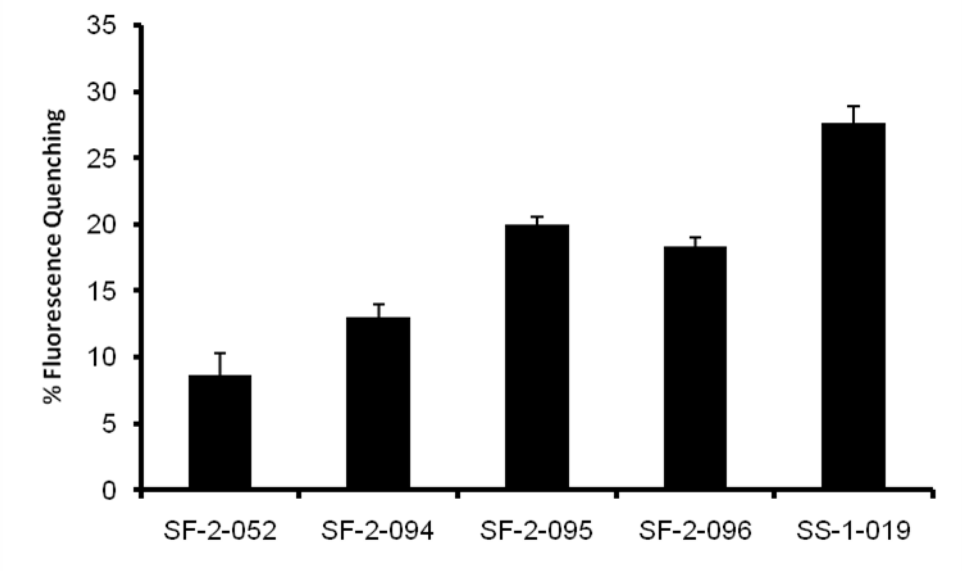

Figure 3.5. Direct interactions of neutral compounds with ERK2. ERK2 (1 µM) was incubated with 10µM of the indicated compound. Excitation was 280 nm and emission was 342 nm. Bars represent the mean and standard deviation from 3 independent experiments.

the binding affinity of **SF-2-095** (K_D of 0.07 ± 0.02 μM) to the parent compound is relatively small (slightly more than 2 fold increase in binding affinity), the values are statistically different. Compound **SF-2-095** has a fluorene group attached. Fluorene is hydrophobic and has been shown to increase potency of pharmacological agents [18, 19]. This may explain the stronger binding affinity as compared to the parent compound. The two compounds that displayed the most dramatic decrease in fluorescence in the initial screening - **SF-2-096** and **SS-1-019** - showed weaker binding interactions as compared to ERK2 wild-type (K_D's 4.5 μM and 9.3 μM, respectively). Extent of quenching in this case relates to changes in the microenvironment of tryptophans of ERK2 caused by changes in protein conformation. Changes in conformation are a direct result of the compound binding to the protein. It is possible that a compound can interact with the protein and not cause a major change in protein conformation in the tryptophan containing region. As is the case with **SF-2-052**, the extent of quenching as compared to the other four compounds was the lowest percentage; however, the binding interaction of **SF-2-052** with ERK2 wild-type was one of the strongest, comparable to the parent compound.

3.3.8 Inhibition of A375 and HeLa cell proliferation by neutral compound analogues.

The structurally similar compounds were evaluated for the ability to inhibit cell growth in A375 melanoma cells and HeLa cells (Figure 3.6). This work was done by Ramin Samadani in our laboratory. Data showed that **SF-2-052** and **SS-1-019** did not

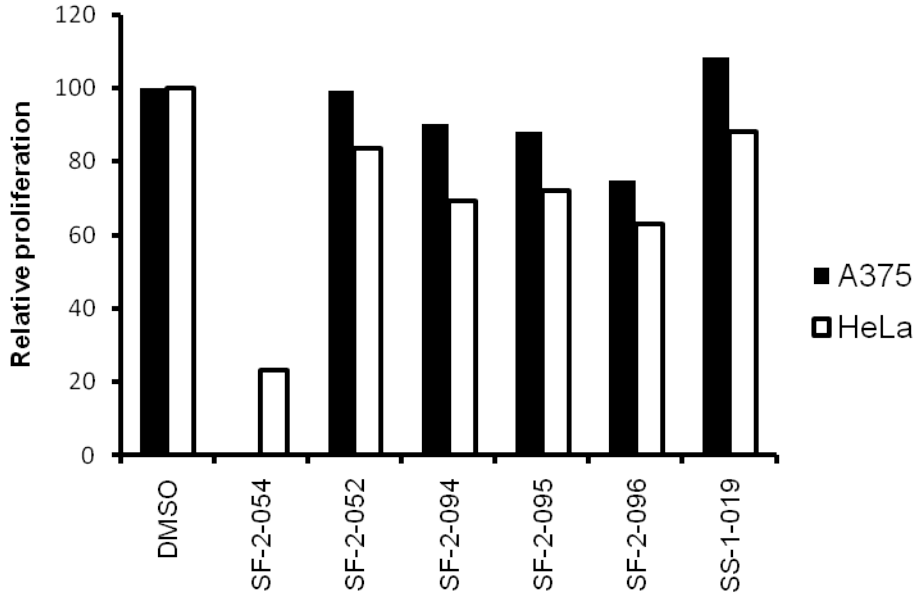

Figure 3.6. Inhibition of cell proliferation. The water soluble tetrazolium salt-1 (WST-1) assay was used to evaluate cell proliferation A375 (B-Raf mutation) or HeLa cells. DMSO is vehicle control and etoposide is positive control. The cells (5000 cells/well) were seeded in 96 well plates, allowed to adhere overnight followed by incubation in the absence or presence of 50 µM test compound or chemotherapeutic agent for 48 hours. Upon addition of WST-1 reagent, absorbance was read at 450 nm with background readings taken at 650 nm. After background subtraction, values were normalized to the control (DMSO only) cells.

inhibit cell proliferation of A375 cells. **SF-2-094** and **SF-2-095** inhibited cell growth of A375 cells 10-12%. **SF-2-096** inhibited cell growth 25%. All five compounds exhibited a decrease ~20-40% in inhibition of HeLa cell growth as compared to **SF-2-054** (Figure 3.6).

3.3.9 Selectivity of neutral compound analogues for the CD/ED domain of ERK2.

Compound **SF-2-052** has a lower binding affinity with the ERK2 CD/ED domain mutant T157A/D319N than that of wild-type ERK2 (Table 3.3). The K_D of the compound with the double mutant is 1.6 ± 0.12 μM. With an increase in K_D ~10 fold, this suggests that the compound interacts with the CD and/or ED domain. The binding interaction of the single mutants D319N and T157A with **SF-2-052** was quantified to determine the contributions of the CD and ED domain. The binding affinity of **SF-2-052** with D319N and T157A was 1.1 ± 0.05 μM and 0.5 ± 0.04 μM, respectively. The binding affinity of **SF-2-052** with the ED domain mutant D319N decreased ~6 fold. Though the binding interaction with the CD domain mutant T157A is close in value to that of ERK2 wild-type, the difference in K_D's is statistically significant, suggesting that this compound also interacts with both the CD and ED domains. It is possible that the compound interacts with the groove located centrally between the two domains. It is interesting to note that the sum of the K_D's for the CD and ED domain mutants with **SF-2-052** is equal to the K_D of the T157A/D319N mutant with the same compound. With the binding interaction of the compound with the mutants in the low micro molar range, it is likely that this compound interacts with another site on the protein in addition to the CD/ED domain.

Table 3.3. Binding interactions of **SF-2-054** and neutral compound analogues with ERK2 CD/ED domain. ERK2 was titrated with 0-20 μM of the test compounds and the decrease in the protein's fluorescence was used to quantify the binding affinities. The fluorescence intensity values were plotted as a function of compound concentration. The data points were fit with a single hyperbola using equation 1. Data shown reflect the mean (μM) ± SEM for three independent experiments. ND = not determined.

Compound	ERK2WT	T157A	D319N	T157A/D319N
SF-2-054	0.17 ± 0.020	6.0 ± 1.5	7.0 ± 1.0	1.7 ± 0.20
SF-2-052	0.18 ± 0.060	0.50 ± 0.040	1.1 ± 0.050	1.6 ± 0.12
SF-2-094	0.27 ± 0.10	ND	ND	0.22 ± 0.060
SF-2-095	0.070 ± 0.020	ND	ND	0.040 ± 0.0030
SF-2-096	4.5 ± 1.6	ND	ND	ND
SS-1-019	9.3 ± 2.4	ND	ND	9.4 ± 0.80

The binding constants for **SF-2-094, SF-2-095,** and **SS-1-019** with T157A/D319N mutant of ERK2 showed little difference compared to the binding affinity of ERK2 wild-type suggesting that these compounds may bind to other sites on the protein. It is also likely that these compounds may not require T157 and/or D319 to bind effectively to ERK2. A single amino acid change within either domain simply may not have an effect on the overall interaction. It can only be concluded that the interaction of the three compounds do not initiate a conformational change of ERK2 in the region where the tryptophans reside.

3.3.10 Selectivity of compounds for p38α MAP kinase.

The two compounds with similar binding affinities as **SF-2-054** discussed above showed selectivity for ERK2 when compared to the structurally similar p38α MAP kinase, though the decrease in binding affinities were not as significant as that of **SF-2-054** (Table 3.4). Both **SF-2-052** and **SF-2-094** showed a slightly more than 5 fold increase in binding interaction with p38α as compared to ERK2 wild-type. Compounds **SF-2-096** and **SS-1-019** showed similar binding affinities with p38α as compared to ERK2 wild-type.

Table 3.4. Binding interactions of **SF-2-054** and neutral compound analogues with p38α as compared to ERK2. ERK2 and/or p38α was titrated with 0-20 μM of the test compounds and the decrease in fluorescence intensity at 336 nm and 342 nm for p38α and ERK2, respectively, relative to the DMSO-only control was used to quantify binding interaction. Data were fit with a single hyperbola (equation 1). The data shown reflect the mean (μM) ± SEM for three independent experiments.

Compound	ERK2WT	p38
SF-2-054	0.17 ± 0.020	12 ± 2.0
SF-2-052	0.18 ± 0.060	1.0 ± 0.50
SF-2-094	0.27 ± 0.10	1.5 ± 0.20
SF-2-095	0.070 ± 0.020	0.24 ± 0.010
SF-2-096	4.5 ± 1.6	4.0 ± 0.40
SS-1-019	9.3 ± 2.4	8.3 ± 1.4

3.4 Discussion

Fluorescence spectroscopy was used to characterize the binding of structurally similar compounds to ERK2 and related MAP kinase proteins. It has been shown that chemical modifications to the parent compound **76** produced novel low molecular weight compounds which exhibit increased potency and selectivity as compared to the parent compound. We wanted to investigate the importance of the primary amino group to the activity of **76** and similar compounds. The first set of compounds was designed to assess the importance of the amino group: **SF-2-048**, **SW-I-195**, **SW-I-127**, **SF-2-037**, **SF-2-033**, and **SW-I-113**. It was observed that changing the basicity of the ethylamine moiety reduced the bioactivity of the compounds as measured by a reduction in the inhibitory effects of the compounds on cell proliferation. When the primary amine was converted to secondary and tertiary amines, a decrease in binding and inhibition of cell proliferation was observed. This suggested that the primary amino group is important to the bioactivity of the compounds. Replacing the ethylamine moiety of **76** with a propyl group (compound **SF-2-037**) significantly decreased direct interaction with ERK2 (as defined by change in the microenvironment of the tryptophan residues due to protein conformational change). However, replacement of the amine group with a chloride in **SW-I-195** led to improved binding over **SF-2-037**, though slightly less than **76**. In compound **SW-I-127**, the amine group was replaced with a hydroxyl which led to binding somewhat similar to **SW-I-195**. In several compounds, the amine functionality was replaced with an aromatic group: **SF-2-038**, **SF-2-041**, **SF-2-039**, **SF-2-057**, **SF-2-040**, **SF-2-058**, and **SF-2-059**. Binding interactions of these compounds with ERK2 was significantly reduced with the exception of the para-cyano group of **SF-2-039** which

completely abolished binding of the compound to ERK2. Direct substitution of the ethylene moiety with a primary aromatic amine in **SW-2-043** led to improved binding over the previously discussed compounds.

It was found that **SF-2-054** and **SF-2-062** caused the greatest decrease in fluorescence quenching in the presence of 10 μM of test compound (Figure 3.2). The ethylamine moiety of **76** was replaced with benzoic acid in **SF-2-062** which, unlike the other aromatic additions discussed above, led to improved binding over **76**. In cell proliferation assays, **SF-2-062** significantly inhibited cell growth of A375 cells. However, the IC_{50} of **SF-2-062** with A375 cells was determined to be 21 μM, similar to the value reported for **76**. The binding interaction of **SF-2-062** was quantified following titration of ERK2 wild-type, and a steady state binding affinity was determined. Though there was a decrease in the K_D, the value was in the same order of magnitude as that of **76**. Though maybe not significant, it suggests that modifications are being made that lead in the right direction: increasing potency and bioactivity of the test compounds.

The basicity of **76** was maintained in the design of **SW-I-151**, only the primary amine was changed to a secondary amine which appears to improve binding as compared to ERK2 wild-type. Maintaining the secondary amine, the addition of a dichlorotriazine ring (**SF-2-054**) substantially improved the binding affinity as compared to the parent compound **76** with a 25 fold increase. A dose response curve was generated for **SF-2-054** with A375 cells and the IC_{50} values were 4.2 μM as compared to the value previously determined for **76** (27 μM) [13]. Though the maximum effect of **SF-2-054** on HeLa cells was similar to that of A375 cells, the potency of the compound against HeLa cells was similar to that of **76** (IC_{50} value of 16 μM) [13]. Over stimulation of the B-Raf containing

A375 cells (which exhibit constitutive activation of the MEK-ERK pathway) is thought to be the reason for continued cell proliferation of the A375 cell line [14]. The fact that **SF-2-054** inhibits A375 cell growth to a greater extent as compared to HeLa cells (in terms of IC_{50} values or potency of the drug) suggests that the compound may inhibit one or more of ERK's substrates responsible for cell proliferation. An increase in the K_D upon interaction with the T157A/D319N mutant suggested that this compound interacts with the CD/ED domain to some extent. The ED domain of ERK2 may contribute more to the binding interactions of **SF-2-054**. It is possible that there is communication between the CD and ED domains that would account for the decrease in binding affinity of **SF-2-054** and **SF-2-062** with the double mutant T157A/D319N. The CD mutation does not significantly affect the binding affinity of **SF-2-054** or **SF-2-062** with ERK2, whereas the ED mutation significantly decreases the binding affinity of **SF-2-054**, and to a lesser degree **SF-2-062**, with ERK2. Because the CD mutation does not significantly affect the binding affinity of either compound with ERK2, it is possible that cooperativity between the two sites exist. The binding of ligand to the ED domain could possibly increase the affinity of the CD domain for the ligand, maybe due to slight protein conformation changes in that region that could make the ligand more accessible.

Selectivity studies of **SF-2-054** for the structurally similar MAP kinase p38α showed that the compound is indeed selective for ERK. Binding affinity to p38α was decreased ~70 fold. These findings greatly support the fact that the chemically modified compound **SF-2-054** can indeed discriminate between the structurally similar kinases ERK2 and p38α. It is possible that the chlorines attached to the triazine group of **SF-2-054** causes the increased reactivity of the compound to the protein. To test this, a control

was designed in which the reactive chlorine was removed. Interestingly, removal of one chlorine atom (**SS-1-019**) abolished inhibition of cell growth in both A375 and HeLa cells and decreased the binding affinity ~9 fold and ~2 fold as compared to **SW-I-151** and **76**, respectively. It is important to note that **SF-2-054** still exhibits great selectivity and a significant increase in potency despite the increased reactivity due to the reactive chlorine.

Modifications to the active lead compounds **SW-I-151**, **SF-2-054**, and **SF-2-062** markedly improved potency and selectivity of these compounds for the MAP kinase ERK2. The latter two compounds were shown to interact with the CD/ED domain with the ED domain contributing more to the interaction. Data suggested that mutations in the ED domain of ERK2 yielded weaker binding interactions to compounds **SF-2-062** and **SF-2-054**. The common thread is that neither p38 nor the ED mutant of ERK2 contains threonine in the equivalent position to T157 of ERK2. This suggests that threonine is necessary somehow to this interaction. Threonine is neutral and does not participate in electrostatic interactions. Nevertheless, the amino acid has a hydroxyl group on the side chain that allows it to participate in hydrogen bonding. It is plausible that the effects on binding interactions between the compound and the protein are due to structural changes in ERK2 that occur in the absence of threonine. In the case of the ERK2 single mutant T157A, it is possible that threonine forms hydrogen bonds intramolecularly and the replacement of threonine with alanine results in a localized change in the structure of ERK2 (in the mutated region). This is plausible in that the overall secondary structure of the T157A ERK2 mutant was not significantly different in comparison with ERK2 wild-type [16].

It is important to note that fluorescence quenching in this context provides information of changes in the microenvironment of tryptophan resulting from protein conformational changes. It is possible that a compound can directly interact with ERK2 and not initiate a conformational change in the region where tryptophans reside. Therefore it is beneficial to analyze the data in conjunction with other assays (discussed further in Chapter 5).

3.5 List of References

1. Chen, Z., et al., *MAP kinases.* Chem Rev, 2001. **101**(8): p. 2449-76.
2. Tanoue, T., et al., *Identification of a docking groove on ERK and p38 MAP kinases that regulates the specificity of docking interactions.* The EMBO journal, 2001. **20**(3): p. 466-79.
3. Rubinfeld, H., T. Hanoch, and R. Seger, *Identification of a cytoplasmic-retention sequence in ERK2.* The Journal of biological chemistry, 1999. **274**(43): p. 30349-52.
4. Boston, S.R., et al., *Characterization of ERK docking domain inhibitors that induce apoptosis by targeting Rsk-1 and caspase-9.* BMC cancer, 2011. **11**: p. 7.
5. Hamm, H.E., et al., *Trp fluorescence reveals an activation-dependent cation-pi interaction in the Switch II region of Galphai proteins.* Protein science : a publication of the Protein Society, 2009. **18**(11): p. 2326-35.
6. Pan, J.Y., J.C. Sanford, and M. Wessling-Resnick, *Effect of guanine nucleotide binding on the intrinsic tryptophan fluorescence properties of Rab5.* The Journal of biological chemistry, 1995. **270**(41): p. 24204-8.
7. Davies, H., et al., *Mutations of the BRAF gene in human cancer.* Nature, 2002. **417**(6892): p. 949-54.
8. Polzien, L., et al., *BAD Contributes to RAF-mediated Proliferation and Cooperates with B-RAF-V600E in Cancer Signaling.* The Journal of biological chemistry, 2011. **286**(20): p. 17934-44.
9. Wan, P.T., et al., *Mechanism of activation of the RAF-ERK signaling pathway by oncogenic mutations of B-RAF.* Cell, 2004. **116**(6): p. 855-67.

10. Roberts, P.J. and C.J. Der, *Targeting the Raf-MEK-ERK mitogen-activated protein kinase cascade for the treatment of cancer.* Oncogene, 2007. **26**(22): p. 3291-310.

11. Cagnol, S. and J.C. Chambard, *ERK and cell death: mechanisms of ERK-induced cell death--apoptosis, autophagy and senescence.* The FEBS journal, 2010. **277**(1): p. 2-21.

12. Cohen, Y., et al., *BRAF mutation in papillary thyroid carcinoma.* Journal of the National Cancer Institute, 2003. **95**(8): p. 625-7.

13. Hancock, C.N., et al., *Identification of novel extracellular signal-regulated kinase docking domain inhibitors.* Journal of medicinal chemistry, 2005. **48**(14): p. 4586-95.

14. Karasarides, M., et al., *B-RAF is a therapeutic target in melanoma.* Oncogene, 2004. **23**(37): p. 6292-8.

15. Birdsall, B., et al., *Correction for light absorption in fluorescence studies of protein-ligand interactions.* Anal Biochem, 1983. **132**(2): p. 353-61.

16. Burkhard, K.A., F. Chen, and P. Shapiro, *Quantitative analysis of ERK2 interactions with substrate proteins: roles for kinase docking domains and activity in determining binding affinity.* J Biol Chem, 2011.

17. Tanoue, T. and E. Nishida, *Molecular recognitions in the MAP kinase cascades.* Cell Signal, 2003. **15**(5): p. 455-62.

18. Dunlop, J., et al., *Characterization of novel aryl-ether, biaryl, and fluorene aspartic acid and diaminopropionic acid analogs as potent inhibitors of the high-affinity glutamate transporter EAAT2.* Mol Pharmacol, 2005. **68**(4): p. 974-82.

19. Hicks, L.D., et al., *Improved, selective, human intestinal carboxylesterase inhibitors designed to modulate 7-ethyl-10-[4-(1-piperidino)-1-piperidino]carbonyloxycamptothecin (Irinotecan; CPT-11) toxicity.* J Med Chem, 2009. **52**(12): p. 3742-52.

20. Burkhard, K., et al., *Development of extracellular signal-regulated kinase inhibitors.* Curr Top Med Chem, 2009. **9**(8): p. 678-89.

CHAPTER 4: Lipid-Induced Conformation Changes in Cytolytic Toxins from *Bacillus thuringiensis*

4.1 Introduction

4.1.1 Significance of Research

Bioinsecticides are beneficial in several capacities. A very important characteristic of bioinsecticides is their high selectivity. They have the ability to infect and control a very narrow range of target pests [1, 2]. More importantly, bioinsecticides can replace the many chemical pesticides that are known to have toxic effects beyond their target pests. *Bacillus thuringiensis* (Bt) is a bacterium known for its use as an environmentally safe insecticide [3]. *Bacillus thuringiensis* var. *israelensis* is of particular importance to our lab. In a time where insect resistance to pesticides, whether chemical or bacterium based, is increasingly prevalent, the ability of this subspecies to stop or delay target pests from acquiring resistance is very significant. Bt produces two types of toxins that work independently or synergistically to kill susceptible insects: Cry (crystal) and Cyt (cytolytic) [4, 5]. While the action of Cry proteins, specific against moths and beetles, has been well established, the mechanism of action of Cyt proteins remains elusive. It is known that Cyt1A interacts with phospholipids as shown by studies with multilamellar liposomes [6, 7] and planar lipid bilayers [8]. Non-specific protein-lipid interactions mediate Cyt1A activity. It has been hypothesized that Cyt1A acts in one of two ways: by forming cation selective channels in the cell membrane or by forming aggregates on the membrane surface thus introducing faults through which cellular contents leak out. However, the molecular mechanism of the protein-lipid interaction is unknown.

Thomas and Ellar proposed that Cyt1A forms pores in the lipid membrane causing the cell to swell and eventually lyse [9]. We hypothesize that Cyt1A damages the lipid membrane in a detergent-like manner. Several lines of experimental evidence suggest that instead of inserting in the lipid bilayer and forming a pore, Cyt1A binds to the membrane surface thereby disrupting packing of the lipid membrane and introducing faults which allow cellular contents to leak through [10]. While the membrane is broken up into protein-lipid complexes, which eventually results in the cell disintegration, the toxin is essentially denatured at the lipid-water interface in the molten-globule state. This state is very dynamic and lacks long-range order, which explains why attempts to crystallize the toxin in the presence of lipid have been unsuccessful. In the absence of X-ray crystal structures of the protein in complex with the lipid membrane, less direct methods, such as fluorescence spectroscopy and computer simulations must be employed to gain information on protein conformation and its changes.

In vivo, Cyt toxins are specific against members of the order Diptera. However, Cyt toxins display broad cytolytic activity *in vitro* against various insect and mammalian cells. Studies have shown that Cyt1A adds the important trait of making it difficult for insects (mosquitoes) to develop resistance against certain Bti strains [11]. A potentially important strategy for delaying resistance to insecticidal toxins is to incorporate mixtures of protein toxins that interact synergistically and act at more than one target. Thus, it is vital to elucidate the molecular details of the mechanism of action of Cyt1A. Careful analysis and synthesis of the data obtained from our research will provide information on the conformation of the lipid-bound toxin and thereby prove/disprove one of the competing hypotheses on the mode of action of Cyt1A. Furthermore, this knowledge

would spark further research into the application of Cyt toxins in biomedical applications. In one study, a Cyt1A-insulin conjugate was produced that displayed specificity for target cells over-expressing insulin receptors, but exhibited a lower activity level and response rate in comparison to free Cyt1A [12]. More promising results were shown by Cohen et. al in targeting murine myeloma cells. Activated Cyt1A was conjugated to a myelin basic protein peptide via genetic modification and data showed an increase in toxicity of Cyt1A in comparison to Cyt1A linked to peptides by chemical conjugation [13]. This suggests that understanding what portion of the Cyt1A molecule interacts with the membrane could provide information as to the best location to attach the protein toxin to the targeting carrier molecule. Most cytotoxic agents currently used in cancer chemotherapy require repeated applications and cellular internalization, both of which may induce resistance over time. Cyt1A is a membrane-acting toxin as opposed to receptor-mediated; thus it is not likely to induce development of resistant cell lines, and it could broaden the spectrum of cellular mechanisms that may be targeted by anti-cancer drugs [13]. Thus, knowledge of Cyt1A mediated action would spark further research into the application of Cyt toxins in both environmental and biomedical applications.

4.1.2 History of *Bacillus thuringiensis*

Bacillus thuringiensis (Bt) is a spore-forming bacterium commonly used in insecticide preparations. The interest in using Bt as a pesticide stems from its target specificity. Pesticides have a broad spectrum of activity often targeting not only the insect of interest but also predators and parasites of the target pest. In contrast to broad-spectrum chemical pesticides, bioinsecticides are highly selective having the ability to

infect and control a very narrow range of pest species [1, 2]. Bioinsecticides are naturally occurring organisms that produce chemicals which are able to affect the growth, development, and immune system of insect pests. More importantly, bioinsecticides significantly reduce harm done to the environment and non-target organisms as well as adverse impacts on food safety. Because of its nontoxicity to humans and animals in vivo, Bt based pesticides are recommended for use on food crops. The activity of Bt against insects is caused by the toxins produced by Bt during spore formation. Bt is not active against adult insects because it is a stomach poison insecticide. It is active only during the larval or feeding stage of insect development. When Bt is ingested by the target insect, the crystalline bodies dissolve in the insect's intestine and damage the intestinal cells. As a result, the insect no longer digests food normally and eventually stops feeding on host plants. The insect dies within a few hours to a few weeks of application of Bt.

There are more than seventy Bt subspecies that have been identified. A broad range of insects are susceptible to the toxic effects of Bt subspecies in some way [14]. Bt subspecies include Bt aizawai (Bta) which affects wax moth larvae in honeycombs, Bt kurstaki (Btk) which affects various types of lepidopterous insects, including the gypsy moth and the cabbage looper [15, 16], Bt morrisoni (Btm) is toxic to the Colorado potato beetle [17], and Bt israelensis (Bti) is toxic against mosquito and blackfly larvae. A common characteristic of all subspecies is crystal formation [18].

The protein inclusions that are produced during sporulation are termed α-exotoxins, β-exotoxins, and δ-endotoxins [19]. The α-exotoxins are soluble toxic proteins isolated from *Bacillus cereus* and several other Bt culture supernatants. It is heat-labile

and at high concentrations, is active against mice and many lepidopteran insects [20]. The β-exotoxins are produced during the vegetative growth phase by some Bt subspecies (thuringiensis, gallarial, and darmstadiensis). β-exotoxin is a nucleotide analog that is heat stable and has differing chemical structures between strains [20]. The presence of β-exotoxins in Bt based pesticides in not permitted in most countries including the USA because of its mechanism of action: it is an inhibitor of DNA-dependent RNA polymerase and acts competitively with ATP in various biological processes [21]. The δ-endotoxin family of proteins is produced by the Bt subspecies in parasporal inclusion bodies during the sporulation phase of the bacterial growth cycle (Figure 4.1) [4]. These proteins account for 20 to 30% of the total dry weight of sporulated cultures [22, 23]. The δ-endotoxins kill predators that feed on the Bt spores, giving Bt a survival advantage over other spore-forming bacteria. Thus, it is probable that δ-endotoxins are formed during the starvation period of the bacterial growth.

4.1.3 Composition of δ-endotoxins

The δ-endotoxin group is a heterogeneous family of proteins, each with characteristic specificity. This has been shown by using a variety of bioanalytical qualitative techniques [24]. The Bt toxins have been divided into two groups: the insect specific Cry (crystal) proteins and the generally cytolytic Cyt proteins. The δ-endotoxin composition of the crystalline bodies determines the specificity and toxicity of Bt [25]. Based on their evolutionary divergence as estimated by phylogenetic algorithms, the Bt proteins are classified into 24 sets (Cyt1, Cyt2, and Cry1 through 22) [15]. Cry proteins

are used most often in commercial insecticide preparation and have been studied extensively. The Cry toxins generally target the orders Lepidoptera and Coleoptera. The mechanism of action of Cry toxins is well understood. A susceptible insect ingests

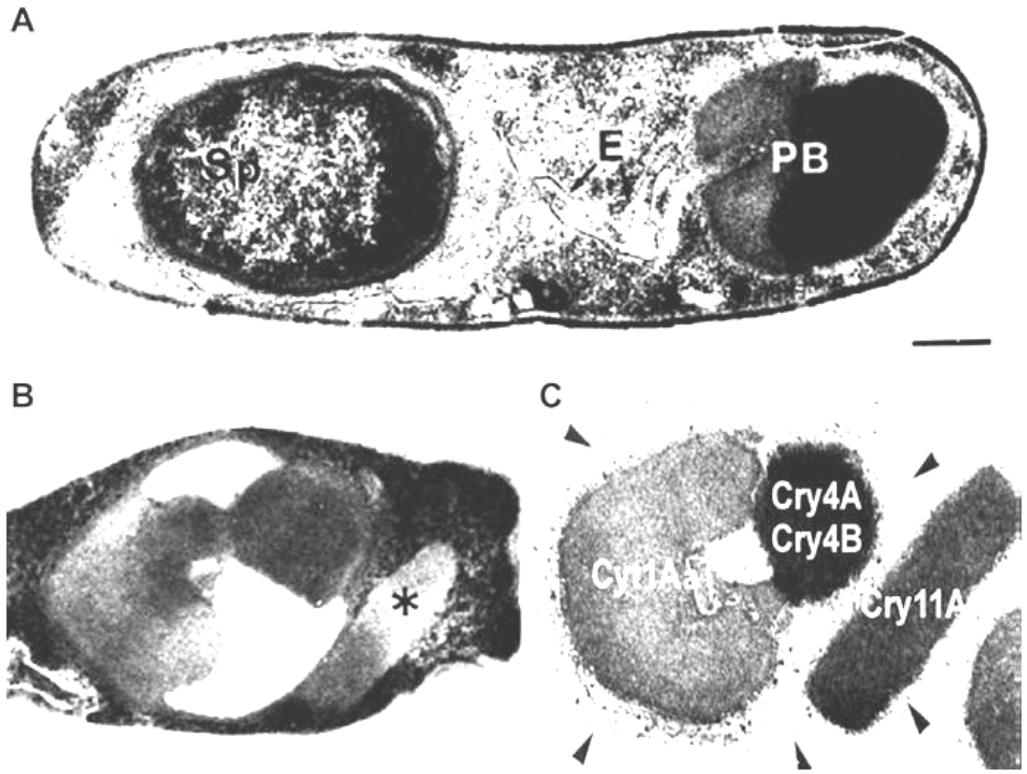

Figure 4.1. Sporulating cell of *Bacillus thuringiensis* var. *israelensis*. **a** Sporulating cell illustrating the developing spore (*Sp*) and parasporal body (*PB*). The parasporal body, composed primarily of Cry4A, Cry4B, Cry11A, and Cyt1A proteins, is assembled outside the exosporium membrane (*E*). **b** Portion of sporulating cell just prior to lysis. The Cry11A crystal (*asterisk*) lies adjacent to the Cyt1A and Cry4A and Cry4B inclusions. **c** Purified parasporal body showing the components of the parasporal body. In this subspecies, the individual protein inclusions are enveloped in a multilamellar fibrous matrix (*arrowheads*) of unknown composition, which also surrounds the crystals holding them together. A typical mature parasporal body of this subspecies measures 500–700 nm in diameter. *Bar* in **a** 100 nm. This figure was reprinted from Federici et. al. 2006.

crystals carrying one or more Cry proteins which are dissolved by the digestive midgut juices [26]. After dissolution, midgut proteases cleave peptides from both the N- and C-termini, activating the toxin [5, 27]. The molecules bind to specific receptors and insert into the microvillar membrane and oligomerize [26, 28, 29]. The formation of cation-selective channels causes an influx of cations such as potassium which leads to a simultaneous influx of water. The cell swells and undergoes lysis leaving the host paralyzed [5, 30]. Paralysis is thought to be caused by the release of alkaline midgut juice into the body cavity which raises the blood pH and disrupts nerve conductance [5]. Death ensues within a day or two of ingesting the toxin. In addition, X-ray crystallography has provided the structures of Cry1A [31] and Cry3A [32]. Although the three dimensional structure of Cyt2A has also been determined by X-ray crystallography [33], the mechanism of action of Cyt proteins in general remains elusive.

Bt strains that are active against mosquitoes, such as *Bacillus thuringiensis* var. *israelensis* (Bti), are the only subspecies known to produce Cyt proteins. The four major endotoxins produced by Bti are Cry4A (128kDa), Cry4B (134kDa), Cry11A (72kDa) and Cyt1A (27kDa) (Figure 4.1) [34]. The proteins produced by this subspecies are contained in separate multilamellar fibrous envelopes of unknown composition. Additional layers of these same fibrous materials hold them together within a spherical parasporal body. The parasporal body is about 500-700 nm in diameter at maturity. The high toxicity of Bti is attributed to synergistic interactions that occur between Cyt1A and Cry proteins. The role of each individual toxin as it relates to the activity of Bti as a whole is unclear. Cry11A is the most toxic of the four, whereas Cyt1A is less toxic. However, synergistic interactions between Cyt1A and Cry proteins attributes to Bti exhibiting the most potent

bacteria-derived mosquito larvicidal activity known thus far [35]. Moreover, Cyt1A has been shown to delay evolutionary resistance [11]. Cyt proteins have amino acid sequences very different from those of Cry proteins. In vivo, Cyt proteins are toxic to mosquitoes and black flies [36], but in vitro they exhibit broad cytolytic activity against various insect and mammalian cells such as erythrocytes, lymphocytes and fibroblasts [30, 37]. Although the members of the Cry family and the Cyt family of δ-endotoxins show no amino acid sequence homology, there exists homology in the amino acid sequences of all the Cyt proteins. Thus it is believed that the structures and functions of Cyt proteins are closely related. Given the similarity within the Cyt family of δ-endotoxins, we represent the Cyt1A protein as a model for the entire family of Cyt proteins.

4.1.4 Structure of Cyt1A

The predicted structure of Cyt1A is shown below in Figure 4.2. The three-dimensional structure of Cyt2Aa1 determined by Li et al [32]. was used as a basis for prediction since it is believed that the structures and functions of Cyt proteins are closely related. Cyt1A and Cyt2Aa1 share 70% functional homology and 39% identity [38]. Cyt1A consists of two outer alpha helix hairpins represented by letters A-B and C-D flanking (on the outer edge of) mixed β-sheet strands numbered 1-7. The amino acid sequence alignment of Cyt toxins revealed four conserved blocks of similarity: α-helix A, the short β-strand 4 and the loop connecting it to α-helix D, β-strands 5 and 6, and α-helix E and the loop connecting it to β-strand 7. The blocks are important for proper folding

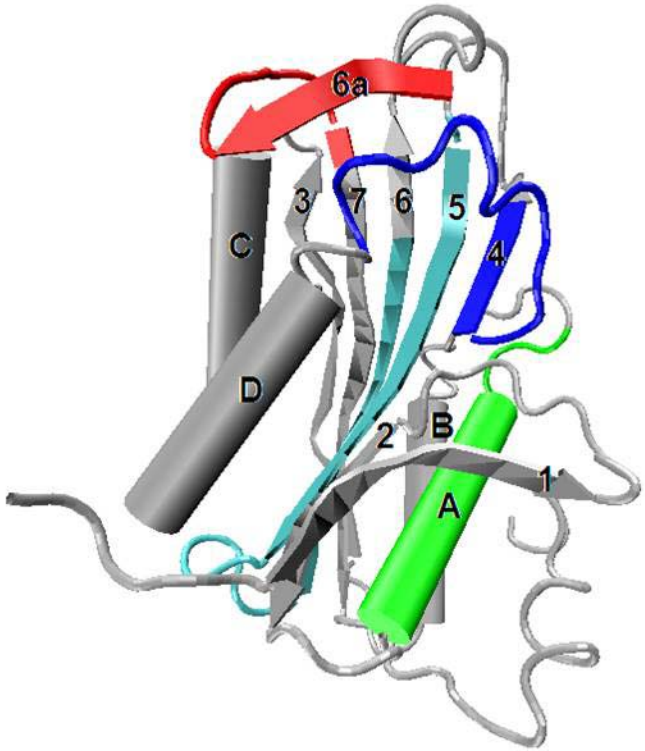

Figure 4.2. Amino acid sequence alignment of Cyt protein from different Bt subspecies. The amino acid sequence alignment reveals four highly conserved blocks of similarity [39]. The four conserved blocks are colored green (α-helix A), blue (the short β-strand 4 and the loop connecting it to α-helix D), cyan (β-strands 5 and 6), and red (α-helix E, previously thought to be β-strand 6a, and the loop connecting it to β-strand 7). The structure of Cyt1A was produced by SpdbViewer [40] and reprinted from Li et. al. 2009.

and stability of the molecule in solution [39]. Ward et. al performed systematic mutagenesis of Cyt1Aa1 [41]. Several amino acids, mostly charged, were replaced with alanine. Lipid-binding assays and in vivo toxicity assays revealed that some mutations were benign, but some affected toxicity to various degrees. The dysfunctional mutations are marked in red and the benign mutations are marked in blue (Figure 4.3). Of the 11 dysfunctional mutations identified, 7 were found in the loops located at the top half of the molecule. Five of the 17 benign mutations were found in the same region of the molecule. This suggests that these loops are the portion of the protein most responsible for toxicity and lipid binding.

It is important to note that several of the dysfunctional mutations are located in regions that are conserved among Cyt toxins. It might be tentatively assumed that the mutated residues are important for electrostatic interactions with the lipid head groups. However, it is equally possible that the mutated residues do not directly bind to the lipid, but rather provide stability to the native, active conformation of the toxin.

4.1.5 Proposed models of Cyt1A action

Cyt1A is of interest for several reasons. Studies have shown that Cyt1A adds the important trait of making it difficult for insects (mosquitoes) to develop resistance against certain Bti strains [11]. Wirth et al. found that Cyt1A working synergistically with *B. sphaericus* delayed evolution of resistance in mosquitoes of the genus *Culex* [42]. Thus Cyt1A has the potential to significantly advance the production of environmentally safe pesticides. The key to such vital developments of the toxin is to understand the molecular

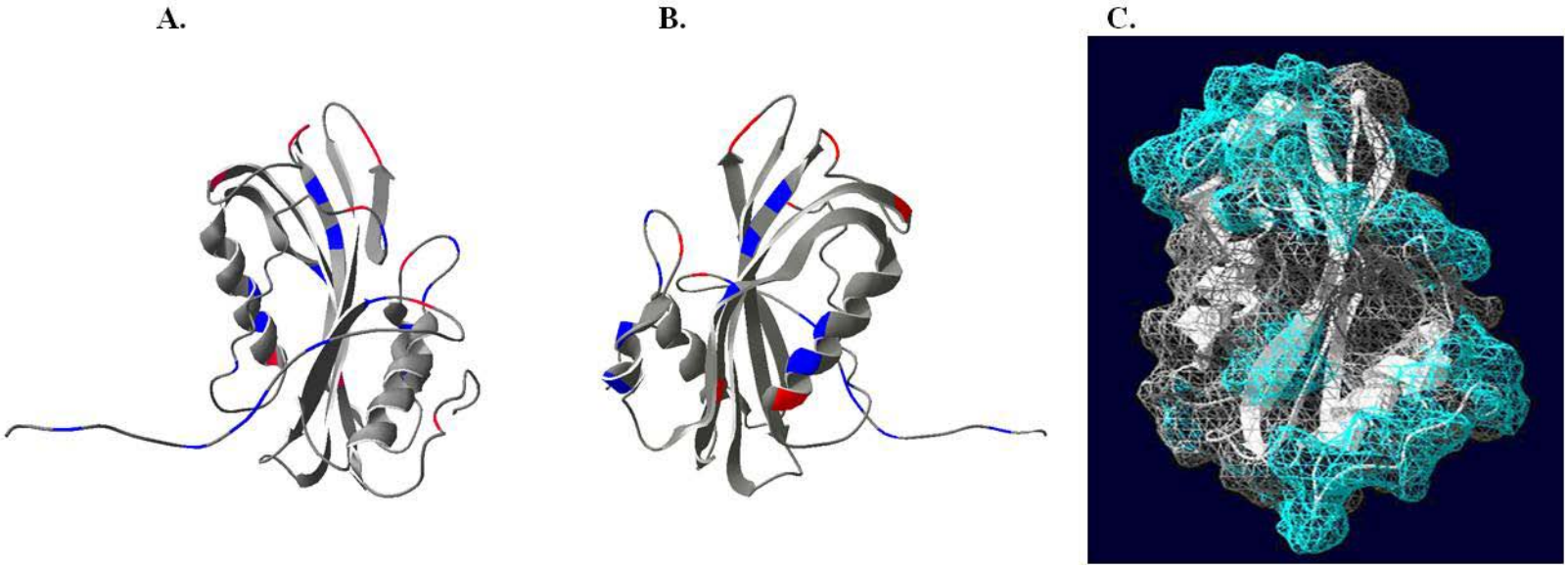

Figure 4.3. Systematic mutagenesis of Cyt1A and suggested regions of toxicity and lipid binding [39]. The predicted structure of Cyt1A includes dysfunctional mutation (red) and benign mutation (blue). (A) represents the front view, and (B) represents the back view. Seven dysfunctional mutations are in the loops at the top half of the molecule. Suggests this region is responsible for toxicity and lipid binding. Mutations were from the work of Ward et al [41].

details of the mechanism by which Cyt1A acts. There are currently two models that attempt to explain how Cyt1A acts.

4.1.5.1 Colloid-osmotic lysis mechanism of Cyt1A-mediated cell damage

According to the pore model of Cyt1A-mediated cell damage, the toxin conformation as it interacts with the lipid membrane is comparable to an umbrella. β-strands of a defined number of Cyt1A molecules insert into the lipid membrane forming well-defined pores, or cation-selective channels, while the alpha helices splay on the membrane surface. The cation concentration equilibrates across the cell membrane resulting in osmotic movement of water. The cell swells and eventually ruptures. This hypothesis has received support from many authors [30]. However, significant observations challenging this model were introduced [10].

4.1.5.2 Evidence against the Colloid-Osmotic Lysis Mechanism

Fluorescent studies in which tryptophan fluorescence of Cyt1A was measured in the absence and presence of lipid were done. Observations included a lack of a blue shift, lack of quenching by lipidic quenchers, and a decreased quantum yield in the presence of lipid, all of which suggest that the tryptophan containing region of Cyt1A (β-strand 4 and the flanking areas) does not insert into the lipid bilayer [43]. In correlation, Du et al. found that when Cyt1A was combined with vesicle containing proteases, proteolysis of Cyt1A did not occur [44]. Both studies suggest that Cyt1A did not penetrate the interior surface of the membrane. A transmembrane pore, by definition, must contain at least one

part of the molecule that reaches across the lipid bilayer to the other side of the membrane [45].

In addition to the above observation, Butko et al. provided other data challenging the pore model hypothesis. The first set of data showed that Cyt1A-induced leakage from vesicles exhibited kinetics independent of the size of the leaking molecule between 0.6 and 10 kDa [43]. The second set of data showed the rate of exchange of the amide II proton/deuteron upon hydration of lyophilized Cyt1A in D_2O increased in the presence of lipid [45]. This signifies that when Cyt1A is bound to lipid, all the amide protons are exposed to the solvent, indicating that no significant portion of the toxin inserts in the lipid bilayer. Therefore we hypothesize that Cyt1A does not insert in the lipid bilayer but rather is mostly (or entirely) spread out on the membrane surface [10]. Evidence provided by Butko et al. further supports the above hypothesis. Differential scanning calorimetry showed that Cyt1A in the presence of lipid did not undergo any measurable cooperative thermal transition. Simultaneously, circular dichroism spectra revealed that upon binding to the membrane, the secondary structure of Cyt1A displayed no significant changes [45]. Consequently, the tertiary structure only is loosened upon lipid binding; a major portion of the secondary structure is maintained, likely in a form similar to the so-called molten globule state [45].

An important factor in the pore hypothesis is the aggregation of Cyt1A on the membrane. The formation of a transmembrane pore often involves the assembly of several toxin molecules to create the lining of the pore. This observation has been noted in the study of anthrax toxin [46, 47] and aerolysin [48, 49]. Chow et al. provided the first evidence of Cyt1A aggregating on the lipid membrane. While studying the binding of

^{125}I-labeled Cyt1A to red blood cells and cells of *Aedes albopictus* and *Choristoneuara fumiferana* [50], Chow et al. observed protein aggregates with a molecular weight of 400 kDa inside the insect cells. Although the size of the aggregates were not altered due to increasing toxin concentration, a threshold concentration was necessary for aggregation to occur. Current evidence of Cyt1A aggregating on the lipid membrane was provided by Manceva et al., who investigated whether Cyt1A self-assembled into well-defined pores or nonspecific protein-lipid aggregates [51] using gel electrophoresis. If self-assembly occurs, well-defined protein-lined pores would be formed containing a stoichiometric number of protein units, which is observed with α-hemolysin [52]. Alternatively, the Cyt1A in the gel would display a laddering pattern with bands corresponding to monomers, dimers, etc., to unresolvable polymers of high molecular mass if Cyt1A aggregates on the lipid membrane. Manceva et al. observed in the presence of lipid, a laddering pattern of Cyt1A bands with molecular masses ranging from 48kDa to infinity, indicating that Cyt1A-lipid aggregates are formed [51].

Previous studies showed that Cyt1A fluorescence intensity experienced a 50% decrease in the presence of lipid [45]. To determine whether the decrease was caused by collisional quenching, due to increased exposure of the two Trp residues to polar solvent molecules in the solution, or by static quenching, caused by the close proximity of opposing Trp residues in Cyt1A aggregates in the membrane, Manceva et al. investigated the change in fluorescence lifetime of Cyt1A in the absence and presence of lipid. The investigations revealed that the addition of lipid to Cyt1A caused no change in the fluorescence lifetime of Cyt1A [51]. These findings in addition to the observations and challenges previously stated [10, 43-45] strongly support the notion that upon binding to

the lipid membrane, Cyt1A aggregates into aggregates of indeterminate sizes on the membrane surface.

Based on the findings discussed, an alternative hypothesis has been developed which suggests that instead of forming pores, Cyt1A forms aggregates of indeterminate sizes, presumably on the surface of the membrane, which leads to a detergent-like mechanism of cell damage according to the following description:

> Cyt1A diffuses in the extra-cellular phase. In response to a decrease in local pH caused by the negative charge on the membrane surface, Cyt1A undergoes a change in conformation. The conformation change causes an increase in the toxin's hydrophobicity and ultimately its affinity to the lipid. Cyt1A aggregates on the lipid membrane in a "carpet-like manner" and disturbs the lipid packing. Introduced faults allow intracellular molecules to leak through resulting in cell death (Figure 4.4).

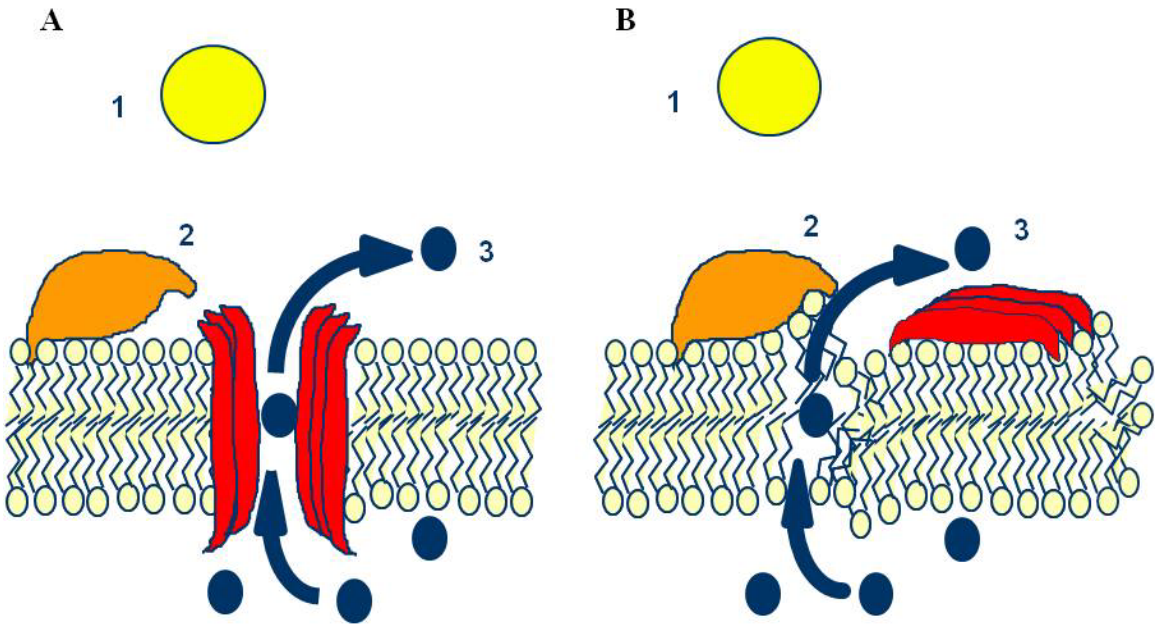

Figure 4.4. Proposed models of Cyt1A action. (A) The pore-forming model states that 1) the protein inserts into the lipid bilayer, 2) well-defined protein-lined pores are formed and lipids are well-organized, and 3) the cation concentration equilibrates across the cell membrane causing osmotic movement of water and ultimately the cell swells and ruptures. (B) The detergent-like model suggests that 1) protein aggregates on the membrane surface, 2) packing faults are introduced and the lipids become more disordered, leading to 3) the membrane breaking up into protein/lipid complexes. Figure from Butko 2003.

4.2 Materials and methods

Sheep red blood cells (10% in phosphate buffered saline, PBS, pH 7.4) were obtained from Sigma. The fluorescence probe 5-((((2-iodoacetyl)amino)ethyl)amino) naphthalene-1-sulfonic acid (1,5-IAEDANS) was from Molecular Probes (Eugene, OR) and N, N-dimethylformamide from Fisher Scientific (Pittsburgh, PA). All buffers and salts were from Sigma-Aldrich (St. Louis, MO), VWR (Atlanta, GA), or Fisher Scientific (Pittsburgh, PA).

4.2.1 Protein Expression

Cyt toxins Bt 4Q7 containing pSFCyt1-1 and W161F were grown in 2-L flasks containing 400 ml nutrient broth/glucose (NBG) broth [53] with the selective antibiotic erythromycin (25 µg/ml) at 30°C, 200 rpm for 5 days. The cells auto-lysed and the spores were collected according to the following procedure. The media containing the cells were centrifuged at 3,000 x g for 10 min. The supernatant was discarded, the pellet was washed with sterile H_2O and then centrifuged at 3,000 x g for 10 min. The wash steps were repeated until the supernatant was clear.

Sodium dodecyl sulfate polyacrylamide gel electrophoresis (SDS-PAGE) was used to determine the presence of Cyt1A protein and to give an approximation of the amount produced by each strain [54]. Cyt1A crystals were solubilized in protein loading buffer and boiled for 5 minutes. A 12% separating gel was used.

4.2.2 Purification of Cyt1A

Cyt1A was purified in the laboratory of Dr. Marianne Pusztai-Carey (Case Western Reserve University, Cleveland, OH). The bacteria are lysed and parasporal

crystals are separated and solubilized in 10 mM dithiothreitol (DTT), 50 mM Na_2CO_3/HCl, pH 9.5 buffer. Purification of the Cyt1A protoxin is performed using high performance liquid chromatography (HPLC) on a mono-Q ion-exchange column (Pharmacia LKB, Uppsala, Sweden) with the elution buffer NH_4HCO_3, pH 8.5 and a linear gradient from 10 mM to 800 mM. The 27 kDa protoxin is converted to Cyt1A by tryptic digestion. Cyt1A is then purified by HPLC on a Protein Pack SP SPW column (Millipore, Milford, MA) with the same elution gradient. Sodium dodecyl sulfate polyacrylamide gel electrophoresis (SDS PAGE) is used routinely to monitor the purity of the preparation. Once purified, the toxin is lyophilized and stored at -20°C [55].

4.2.3 Preparation of small unilamellar vesicles (SUV's)

To prepare a 13 mM lipid stock, phosphatidyl choline (PC) was dissolved in choloroform and dried under a slow stream of nitrogen gas. The vial was carefully rotated to form a thin film on the sides of the vial. The film was then hydrated in 0.5 mL of 10 mM 4-(2-hydroxyethyl)-1-piperazineethanesulfonic acid (HEPES), 100 mM NaCl, pH 7.4. The lipid suspension was sonicated for 30 minutes at 4°C using a Sonic Dismembrator-Model 300 from Fisher Scientific (Pittsburgh, PA) [43].

4.2.4 Absorption spectroscopy

Absorbance spectra of the proteins and optical density of compounds were determined with the JASCO V-530 UV spectrophotometer (Easton, MD) and/or the Varian Cary Bio 50 UV-visible spectrophotometer (Agilent Technologies; Palo Alto,

CA) Data were analyzed with Microsoft Excel and Microcal Origin 7.0 (Microcal Software; Northhampton, MA).

4.2.5 Determination of Cyt1A concentration

Cyt1A was dissolved in 0.1 M NH_4HCO_3, pH 8.5. According to the Lambert-Beer's law absorbance of the protein solutions in the range of 0.2 – 1.0 is a linear function of the concentration. The concentration was determined using Lambert-Beer's law:

$$A_{280} = C \bullet \varepsilon \bullet l \qquad (1)$$

where A_{280} is the absorbance at 280 nm, C is the concentration of the solution in M, ε is the molar extinction coefficient (20,500 M^{-1} cm^{-1}), and l is the length of the light path.

4.2.6 Labeling of Cyt1A with 1,5 IAEDANS

Cyt1A was fluorescently labeled by a straightforward procedure with several modifications [56]. Cyt1A was dissolved in 0.1 M NH_4HCO_3, pH 8.5 to give a concentration of 0.2 mM. 1,5-IAEDANS was dissolved in N,N-dimethylformamide (DMF), pH > 6 to give a concentration of 226 mM. A 50-fold molar excess of IAEDANS and 1 mM EDTA were added, and the solution was incubated for 2 h at 37 °C, after which the free probe was separated from the conjugate by size exclusion chromatography on a PD-10 column (GE Healthcare, Piscataway, NJ) or by filtration through Microcon 10 filters. Using the PD-10 columns, the column was equilibrated with 25 ml of 0.1 M

NH_4HCO_3, pH 8.5, and the labeled protein was eluted with the same buffer and collected in three fractions. With the Microcon 10 filters, the labeled Cyt1A was centrifuged at 14,000 x g for 30 minutes, followed by three 20 min washes with 0.1M NH_4HCO_3, pH 8.5. The protein was recovered in buffer.

Stoichiometry of labeling was determined by absorption spectroscopy on a Jasco V-530 UV-Vis spectrophotometer with the values of molar extinction coefficients 5700 $M^{-1}cm^{-1}$ and 20,500 $M^{-1}cm^{-1}$ for IAEDANS [57] and Cyt1A, respectively, at the wavelengths of their respective absorption maxima, 336 and 280 nm. The labeled protein was kept in the dark as much as possible to prevent photodegradation of the probe.

4.2.7 Hemoglobin release assay

Activity of the labeled protein was determined using a hemoglobin release assay as previously described [58] using unlabeled protein as a reference. 1% RBC suspension in PBS and $NaHCO_3$ was treated with 50 nmol and 100 nmol of unlabeled cyt1A and 50 nmol and 100 nmol of the protein-dye conjugate and incubated for 20 min at room temperature. The samples were centrifuged at 6,000 x g for 5 min to remove any intact cells and cell debris. The hemoglobin-containing supernatant was transferred to microplates and the amount of released hemoglobin was quantified at 540 nm using the EL 800 Universal Microplate Reader from Bio-Tek Instruments. 1% RBC suspension left untreated was used as a blank representing 0% hemoglobin release. 1% RBC suspension in Triton X-100 served as a control to exhibit 100% hemoglobin release. Percentage of hemoglobin release from the treated samples was calculated.

4.2.8 Mosquito-larvicidal assay

Mosquito-larvicidal assays were carried out as described [59]. Briefly, assays were performed in duplicate using 3rd instar Aedes aegypti larvae supplied by the Institute of Molecular Biology and Genetics, Mahidol University. The toxin inclusions were diluted in water as two-fold serial dilutions from 512 to 0.125 µg/ml. 1 mL of diluted inclusions was added to 1 ml of water in each well of a 24-well tissue culture plate with well diameter of 1.5 cm. 10 larvae were placed in each well. Protein inclusions from acrystalliferous Bti strain Bt4Q7 were used as a negative control. After 24 hour incubation at 30°C, mortality was recorded.

4.2.9 Steady-state and lifetime measurements

For FRET, steady-state fluorescence spectra were recorded with an ISS K2 spectrofluorometer (Champaign, IL). Spectra of labeled and unlabeled Cyt1A in NH_4HCO_3, pH 8.5, at a final concentration of 0.5 µM in a 3mm x 3mm quartz cell were collected. Fluorescence of IAEDANS was corrected for the non-negligible direct excitation of IAEDANS by the tryptophan-exciting light (280 nm) with the help of a factor found from the comparison of free IAEDANS fluorescence excited at 280 nm and 336 nm. FRET efficiency (E) was calculated as

$$E = A_A(\lambda_D) / A_D(\lambda_D) [(I_{AD}(\lambda_D) / I_A(\lambda_D)) - 1] \quad (2)$$

where λ_D is the wavelength of the absorption maximum of the donor, $A_A(\lambda_D)$ and $A_D(\lambda_D)$ are the acceptor and donor absorbances, respectively, at λ_D, and $I_{AD}(\lambda_D)$ and $I_A(\lambda_D)$ are

the intensities of the acceptor emission at λ_D in the presence and absence of the donor, respectively [60, 61]. Fluorescence lifetime of IAEDANS-labeled Cyt1A was determined using the PicoQuant Fluotime 200 time-resolved spectrometer (Berlin, Germany) with a pulsed 285 nm LED, having a resolving power of 100 ps. The sample in a 3mm x 3mm quartz cell contained 4 μM labeled Cyt1A. It was excited at 285 nm and the emission was measured at 344 nm through a 320 nm long pass filter. FRET efficiency was calculated as

$$E = 1 - (\tau_{DA}/\tau_D) \quad (3)$$

where τ_{DA} is the lifetime of the donor in the presence of acceptor and τ_D is the lifetime of the donor in the absence of the acceptor [60, 61]. The distance between the fluorescence donor (tryptophan) and acceptor (IAEDANS) was calculated from the experimentally determined efficiency (E) as

$$R = R_0 [(1 - E) / E)]^{1/6} \quad (4)$$

where R_0 is the Forster radius, the distance at which E=1/2. The value of R_0 was taken as 21.7 Å and the orientation factor k^2 was implicitly assumed to be 2/3 [60, 61].

4.2.10 Computer simulations

Cyt1A has 249 residues with 3846 atoms and a molecular weight of 27332.1 Da. Dr. Xiaochun Li generated the solution conformation of Cyt1A by homology modeling based on the experimentally determined structure of the related Cyt2Aa1 [33, 62]. The

Cyt1A conformation was generated and analyzed with Visual Molecular Dynamics (VMD) [63]. The model was refined by energy minimization and several short-term (sub-nanosecond) molecular dynamics simulations were carried out. Since the N-terminal portion of the toxin is cleaved in proteolytic activation of Cyt1A (either in the insect's gut or in the laboratory), the first 19 residues were not included in the molecular dynamics simulations [39].

4.3 Results

4.3.1 Labeling of Cyt1A

Thiol-reactive probes can be used to determine distances within the protein or between the protein and ligand using FRET and follow changes in protein conformation using environment-sensitive probes [57]. A significant property of Cyt1A is that it contains a single cysteine residue. We used the fluorescent probe 1,5 IAEDANS, a thiol reactive probe, to label Cyt1A. Labeling efficiency was determined and the toxin/dye molar ratio was 1:1.4. Activity of the labeled toxin was assessed in a red-blood-cell hemolysis assay. The activity of the labeled toxin was comparable to native Cyt1A (data not shown).

4.3.2 Validation of the model

The best way to validate a computer model of a macromolecule is to compare it with the experimentally determined structure. Up to date, the only known structure of a Cyt toxin remains that of the toxin Cyt2A, obtained by Li et al. [33]. However, that structure was the point of departure in creating our model. A suitable alternative is to measure an intramolecular distance (or even better — a set of distances) between specific points in the protein and compare the experimental data with the model. Fortuitously, Cyt1A contains a single cysteine residue, C190, which is readily amenable to fluorescence labeling, and two tryptophans, only 2 amino acids apart, on the short strand β4. Labeling the cysteine with the fluorescence probe IAEDANS, which can act as a fluorescence energy acceptor for tryptophan, enabled us to estimate the distance between the cysteine and the tryptophans by FRET. Figure 4.5 shows the fluorescence spectrum of

the IAEDANS-labeled Cyt1A excited at 280 nm. The fluorescence of IAEDANS, clearly visible at 473 nm, demonstrates energy transfer between the tryptophan donors and IAEDANS acceptor. Efficiency of the energy transfer, determined from the decrease of fluorescence lifetime of tryptophan in the labeled toxin (Figure 4.6), was used to calculate the distance between the donors and the acceptor. The wild-type unlabeled Cyt1A molecule exhibited two fluorescence lifetimes of tryptophan, with the amplitude-weighted average of 4.4 ± 0.1 ns. The decay (the red line in Figure 4.6) was well approximated by a two-exponential model with the lifetimes 2.3 and 5.3 ns and respective relative amplitudes of 0.31 and 0.69. The goodness of fit (χ^2=1.05) did not improve significantly with the addition of a third component. When IAEDANS was covalently linked to C190, a third lifetime component was needed to obtain a good fit (the green line in Figure 4.6), with the lifetimes 0.7, 2.3, and 5.2 ns and amplitudes 0.39, 0.45, and 0.16, respectively. The main point is that the amplitude-weighted average lifetime value decreased to 2.1 ± 0.1 ns, which signifies a 52% efficiency of FRET. Further evaluation of these data is complicated by the fact that the single FRET acceptor–IAEDANS–accepts energy from two donors in the molecule of Cyt1A —W158 and W161. The classical mathematical formalism of FRET was developed for the case of single donor–acceptor pairs [60, 61]. The problem of immobilized (i.e., non-diffusible) multiple donors/ acceptors in complex geometries is encountered quite often in practice, but it has received little attention of theorists. Only recently numerical methods and computer simulations started to be employed in addressing the issue [64]. While efficiency of energy transfer is more-or-less directly measured in the experiment, the

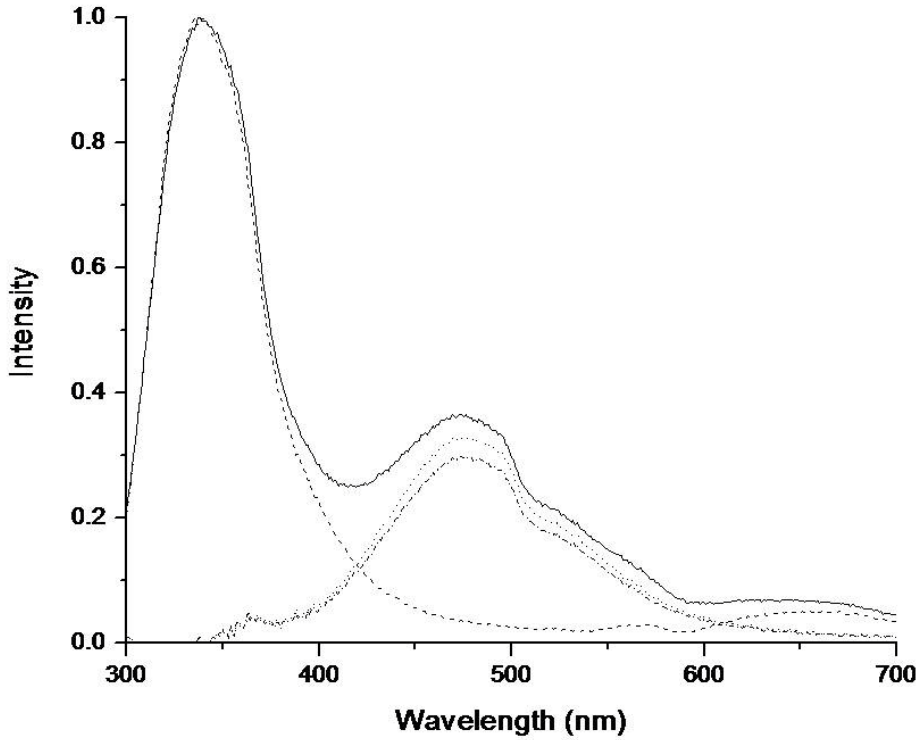

Figure 4.5: FRET from tryptophan to IAEDANS in Cyt1A. The solid line (—) represents IAEDANS-labeled Cyt1A excited at 280 nm. The dashed line (- - -) represents native Cyt1A excited at 280 nm. The dotted line (···) represents spectrum of IAEDANS fluorescence after subtracting the tryptophan fluorescence (solid line). The dash-dot (-·-·-) line represents fluorescence of IAEDANS due to energy transfer; it was obtained by subtracting direct excitation of IAEDANS with the 280-nm light from the dotted-line spectrum [39].

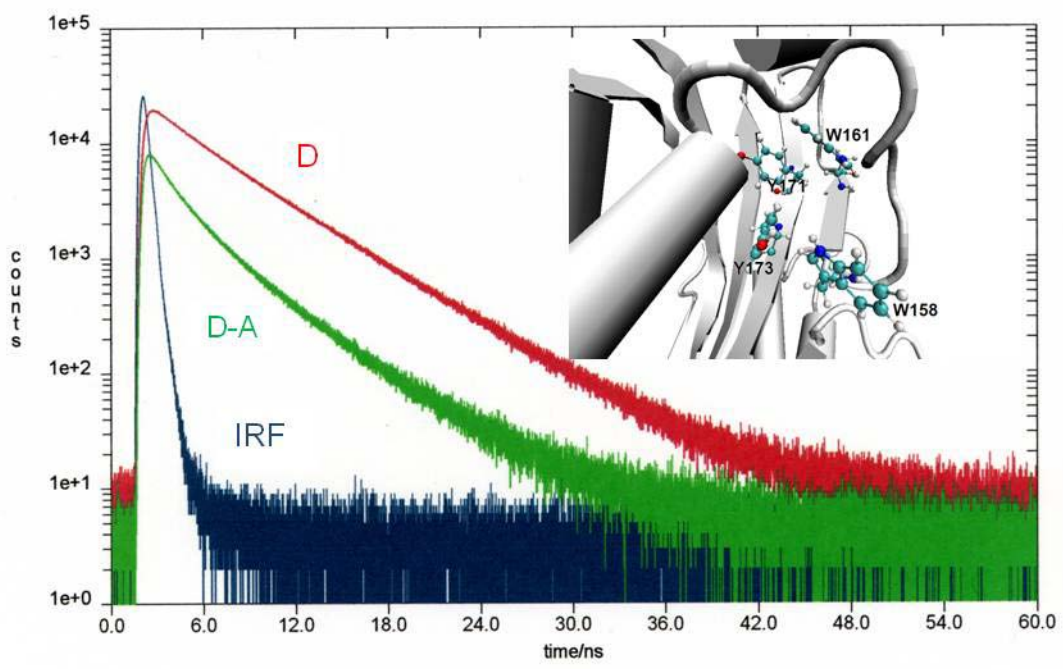

Figure 4.6. Fluorescence intensity decays of tryptophan emission from labeled/unlabeled Cyt1A. Intensity decays for Cyt1A in the absence (red, D) and presence of IAEDANS acceptor (green, D-A), which was covalently linked to cysteine 190, are denoted. The excitation flash is labeled IRF [39].

donor/acceptor distance is calculated from the FRET data and its interpretation is contingent on factors such as the number of donors/acceptors and their mutual distances and orientations. Of course, one can always calculate a distance from any set of FRET data, but, as in our case, the problem is what distance is actually calculated: Is it the distance from the cysteine to the nearest tryptophan or to the center of gravity of the two tryptophans or to some weighted average of the tryptophans' positions? The simplest of all the simplifying assumptions is that the measured FRET efficiency can be subject to the classical formalism to calculate the distance between the acceptor and the midpoint between the two donor tryptophans, which is equivalent to saying that each of the two tryptophans contributes the same energy to the acceptor. This approach is simple, but unlikely to be true in general. Since efficiency of FRET is a steep function of distance, efficiency of transfer from the more distant donor might be significantly lower than that from the nearer one, assuming the same rotational mobility of the two. Hence another simplifying assumption is possible, namely, that all energy is only transferred from the nearest donor, as the more distant donors would contribute progressively smaller fractions of energy. This also may not always be true, since transfer efficiency depends not only on distance, but also on the mutual orientation of the donor and acceptor. When the lifetime data were treated with the classical formalism for FRET (which in our case means the assumption of equal energy transfer from the two tryptophans and essentially treating the latter as a single energy donor located midway between W158 and 161), an efficiency of 0.52 implied the distance 2.2 ± 0.1 nm (the error was calculated from the experimental uncertainty in lifetime determination). This was compared with the following distances extracted from the model: 1.80 nm for C190-W158, 2.54 nm for

C190-W161, and the average ± range 2.2 ± 0.4 nm. Bearing in mind the above-mentioned interpretation difficulties, the average distance in the computer model, 2.2 nm, matches the value extracted from the experimental data.

4.3.3 Site-directed mutagenesis

E. coli was used for cloning because it has a higher copy number than the host bacterium *Bacillus thuringiensis* (Bt). Mutagenic primers were developed to create C190A and subsequent primers to place cysteine in various positions within the toxin: V129C, A182C, K225C, and S232C (Table 4.1).

The rationale for mutant design was as follows. FRET studies using the single tryptophan mutant W161F will provide a defined distance between the W158 and the fluorescently labeled acceptor. The cysteine free mutant W161F:C190A (hereafter referred to as C190A) will serve as a template to create mutants with cysteine judiciously placed within the molecule. According to the pore model, β5, β6 and β7 span the lipid bilayer. The portion containing A182 was suggested to be in the inner monolayer. Energy transfer between Trp located on β4 (on the outer surface of the membrane) and the fluorescently labeled W161F:C190A:A182C (hereafter referred to as A182C) mutant will be measured and the distance will be calculated. S232 was presumed to be in the outer lipid membrane. Quenching studies and FRET with W161F:C190A:S232C (hereafter referred to as S232C) would be performed to determine location relative to the membrane. V129 is located on the loop region between αC and αD. Upon interaction with the lipid membrane, the alpha helices are thought to spread out as the beta strands span the bilayer, similar to an umbrella opening. Therefore lipid-induced conformation

Table 4.1. Mutagenic primers for site-directed mutagenesis. Primers were designed based on Cyt1Aa1 sequence. Mutation sequences are underlined. Silent mutations are denoted with a lower case alphabet. Restriction sites were highlighted in bold print.

Primer	Sequence (5'→3')	Restriction Enzyme
C190A	GGC GTT ATG TAT GC**G** **GTA CCA** GTT GGT TTT	Kpn I
V129C	ACT GTA TTA GGA **TGC** **GCA** TTA AGT GGA TCT	Fsp I
A182C	GCA ATC CAA AAT TGT CAA **ACc** **GGT** GGC GTT	Age I
K225C	TC CAA TCT TTG TGC TT**T** **GCg** **CA**A CCA TTA G	Fsp I
S232C	CA CAA CCA TTA GT**g** **TGC** **TC**A AGT CAG TAT C	Bsp1286I

change of the protein should cause a decrease in energy transfer between the fluorescently labeled mutant W161F:C190A:V129C (hereafter referred to as V129C) and the tryptophan donor. W161F:C190A:K225C (hereafter referred to as K225C) will be fluorescently labeled and FRET will be measured to compare with distance values extracted from the computer model of Cyt1A between K225 and the W158.

The single-tryptophan mutant, W161F, was successfully produced and was confirmed by restriction endonuclease digestion and DNA sequencing. This mutant was used to create a cysteine-free mutant (C190A) in which C190 was replaced by alanine. Restriction endonuclease digestion and DNA sequencing confirmed that the cysteine-free mutant was successfully produced as well. The C190A mutant was used as a template to produce four cysteine mutants. Agarose gel analysis of the PCR product confirmed that for each of the cysteine mutants, a band of the expected size existed. Digesting the product with Dpn I determined that the bands shown were indeed PCR products and not template DNA. The PCR products were transformed into *E. coli* strain *DH5α* and the transformants were screened for triple mutants by restriction endonuclease digestion. Restriction analysis and DNA sequencing analysis confirmed the mutations were successful. The recombinant plasmids were transformed into expression vector Bt4Q7 (Figure 4.7A and 4.7B). The transformation for K225C was unsuccessful (data not shown). SDS-PAGE and Western blot analysis (Figure 4.7C) confirm that mutants W161F, C190A, and A182C are expressing Cyt1A. Further studies are necessary to determine whether transformation of V129C and S232C was unsuccessful or if the Bt4Q7 containing the mutants simply do not express the toxin.

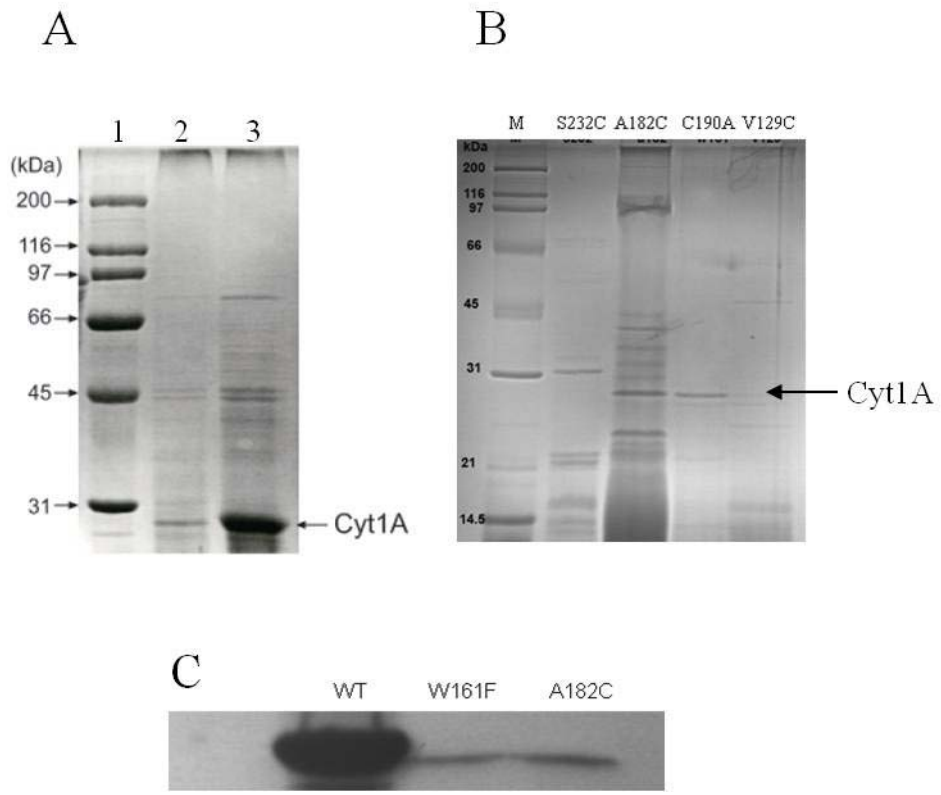

Figure 4.7. SDS-PAGE and Western analysis of mutant protein expression. **A)** The acrystalliferous strain contained plasmid pHT3101 + Cry1ACP + p20 with either the W161F mutant (lane 2) or the native Cyt1A (lane 3). Lane 1 is molecular mass markers. **B)** SDS-PAGE analysis of Cyt1A triple mutant protein expression. The acrystalliferous strain contained plasmid pHT3101 + Cry1ACP + p20 with either the S232C, A182C, C190A, or V129C mutant. A 27kDa band corresponding to Cyt1A is present in A182C and C190A. **C)** Western blot analysis confirming Cyt1A expression by transformed Bt as detected by an anit-Cyt1A serum.

4.4 Discussion

In order to validate the molecular dynamics model of the solution structure of the toxin Cyt1A, we used resonance energy transfer to measure the distance between the cysteine C190 and the two tryptophans, W158 and W161. With some caveats, the experimental value agreed well with the predicted one. The agreement between the theoretical and experimental values also supported the notion that the two tryptophans likely donate energy to the IAEDANS acceptor in equal, or sufficiently similar, proportions. Had that not been the case, the experimental value would be closer to either of the two values of the distance between C190 and the respective tryptophan (1.80 nm or 2.54 nm).

Even though both experimental and theoretical values favorably compared, it is fraught with uncertainty due to the presence of multiple fluorescence energy donors. The value obtained from the computer model assumes that both tryptophans transfer energy to IAEDANS in similar proportions. Therefore a single-tryptophan mutant (W161F) of the toxin was created and was used as a template for subsequent cysteine mutations. W161F mutant toxin expressed a lower yield of protein as compared to the wild-type. However, preliminary bioassay studies on mosquito larvae *in vivo* were performed and data show that the W161F mutant toxin was as active as the wild-type. Future experiments with the single-tryptophan mutant will allow for a less ambiguous and more precise determination of the cysteine-tryptophan distance in the molecule in solution.

4.5 List of References

1. Tabashnik, B.E., *Evolution of resistance to Bacillus thuringiensis.* Annu Rev. Entomol, 1994. **39**: p. 47-79.
2. Burges, H.D., ed. *Microbial control of pests and plant diseases*. 1981, Academic Press: New York.
3. Paris, M., J.P. David, and L. Despres, *Fitness costs of resistance to Bti toxins in the dengue vector Aedes aegypti.* Ecotoxicology. **20**(6): p. 1184-94.
4. Hofte, H. and H.R. Whiteley, *Insecticidal crystal proteins of Bacillus thuringiensis.* Microbiol Rev, 1989. **53**(2): p. 242-55.
5. Federici, B.A., Hyun-Woo Park, Yuko Sakano, *Insecticidal Protein Crystals of Bacillus thuringiensis*, in *Microbiology Monographs*. 2006, Springer Berlin/Heidelberg. p. 195-236.
6. Haider, M.Z. and D.J. Ellar, *Mechanism of action of Bacillus thuringiensis insecticidal delta-endotoxin: interaction with phospholipid vesicles.* Biochim Biophys Acta, 1989. **978**(2): p. 216-22.
7. Drobniewski, F.A. and D.J. Ellar, *Toxin-membrane interactions of Bacillus thuringiensis d-endotoxin.* Biochem Soc. Trans., 1988. **16**: p. 38-40.
8. Knowles, B.H., et al., *A cytolytic delta-endotoxin from Bacillus thuringiensis var. israelensis forms cation-selective channels in planar lipid bilayers.* FEBS Lett, 1989. **244**(2): p. 259-62.

9. Knowles, B.H., and D. J. Ellar *Colloid-osmotic lysis is a general feature of the mechanism of action of Bacillus thuringiensis delta-endotoxins with different insect specificity.* Biochim. Biophys. Acta, 1987. **924**: p. 509-518.

10. Butko, P., *Cytolytic toxin Cyt1A and its mechanism of membrane damage: data and hypotheses.* Appl Environ Microbiol, 2003. **69**(5): p. 2415-22.

11. Federici, B.A., et al., *Recombinant bacteria for mosquito control.* J Exp Biol, 2003. **206**(Pt 21): p. 3877-85.

12. Al-yahyaee, S.A. and D.J. Ellar, *Cell targeting of a pore-forming toxin, CytA delta-endotoxin from Bacillus thuringiensis subspecies israelensis, by conjugating CytA with anti-Thy 1 monoclonal antibodies and insulin.* Bioconjug Chem, 1996. **7**(4): p. 451-60.

13. Cohen, S., et al., *Specific targeting to murine myeloma cells of Cyt1Aa toxin from Bacillus thuringiensis subspecies israelensis.* J Biol Chem, 2007. **282**(39): p. 28301-8.

14. Aronson, A.I.Y.S., *Why Bacillus thuringiensis insecticidal toxins are so effective: unique features of their mode of action.* FEMS Microbiol Lett, 2001. **195**: p. 1-8.

15. Crickmore, N., et al., *Revision of the nomenclature for the Bacillus thuringiensis pesticidal crystal proteins.* Microbiol Mol Biol Rev, 1998. **62**(3): p. 807-13.

16. Chaufaux, J., Marchal, N. Gilois, I. Jehanno, and C. Buisson, *Investigation of natural strains of Bacillus thuringiensis in different biotopes throughout the world.* Can. J. Microbiol., 1997. **43**: p. 337-343.

17. Federici, B.A., *Cyt1Aa protein of Bacillus thuringiensis is toxic to the Cottonwood Leaf Beetle, Chrysomela scripta, and suppresses high levels of resistance to Cry3Aa.* Appl Environ Microbiol, 1998. **64**(11): p. 4368-4371.

18. Shao, Z., *Effects of the 20-Kilodalton Helper Protein on Cry1Ac Production and Spore Formation in Bacillus thuringiensis.* Appl Environ Microbiol, 2001. **67**(12): p. 5362-5369.

19. Gingrich, R.E., N. Allan, and D.E. Hopkins, *Bacillus thuringiensis: laboratory tests against four species of biting lice (Mallophaga: Trichodectidae).* J Invertebr Pathol, 1974. **23**(2): p. 232-6.

20. Krieg, A.F., *Concerning alpha-endotoxin produced by vegetative cells of Bacillus thuringiensis and Bacillus cereus.* J. Invertebrate Pathol., 1971. **17**: p. 134-135.

21. Sebesra, K.a.H.S., *The specificity of inhibition of DNA-dependent RNA polymerase Bacillus thuringiensis exotoxin.* FEBS Lett, 1970. **8**: p. 233-235.

22. Bulla, L.A., Jr., et al., *Purification and characterization of the entomocidal protoxin of Bacillus thuringiensis.* J Biol Chem, 1981. **256**(6): p. 3000-4.

23. Aronson, A.I., W. Beckman, and P. Dunn, *Bacillus thuringiensis and related insect pathogens.* Microbiol Rev, 1986. **50**(1): p. 1-24.

24. Yamamoto, T. and R.E. McLaughlin, *Isolation of a protein from the parasporal crystal of Bacillus thuringiensis var. Kurstaki toxic to the mosquito larva, Aedes taeniorhynchus.* Biochem Biophys Res Commun, 1981. **103**(2): p. 414-21.

25. Knowles, B.H. and D.J. Ellar, *Differential specificity of two insecticidal toxins from Bacillus thuringiensis var. aizawai.* Mol Microbiol, 1988. **2**(1): p. 153-7.

26. Hoffman, D., P. Luthy, R. Hutter, and V. Pliska, *Binding of the d-endotoxin of Bacillus thuringiensis to brush-border membrane vesicles of the cabbage butterfly (Pieris brassiacae).* Eur J Biochem, 1988. **173**: p. 85-91.

27. Toho, A.a.K.A., *Dissolution and degradation of Bacillus thuringiensis d-endotoxins by gut juice protease of the silkworm Bombyx mori.* Appl Environ Microbiol, 1983. **45**: p. 576-580.

28. Van Rie, J., et al., *Specificity of Bacillus thuringiensis delta-endotoxins. Importance of specific receptors on the brush border membrane of the mid-gut of target insects.* Eur J Biochem, 1989. **186**(1-2): p. 239-47.

29. Van Rie, J., et al., *Receptors on the brush border membrane of the insect midgut as determinants of the specificity of Bacillus thuringiensis d-endotoxins.* Appl Environ Microbiol, 1990. **56**(5): p. 1378-1385.

30. Knowles, B.H.a.D.J.E., *Colloid-osmotic lysis is general feature of the mechanism of action of Bacillus thuringiensis delta-endotoxins with different insect specificity.* Biochim Biophys Acta, 1987. **924**: p. 509-518.

31. Grochulski, P., et al., *Bacillus thuringiensis CryIA(a) insecticidal toxin: crystal structure and channel formation.* J Mol Biol, 1995. **254**(3): p. 447-64.

32. Li, J.D., J. Carroll, and D.J. Ellar, *Crystal structure of insecticidal delta-endotoxin from Bacillus thuringiensis at 2.5 A resolution.* Nature, 1991. **353**(6347): p. 815-21.

33. Li, J., P.A. Koni, and D.J. Ellar, *Structure of the mosquitocidal delta-endotoxin CytB from Bacillus thuringiensis sp. kyushuensis and implications for membrane pore formation.* J Mol Biol, 1996. **257**(1): p. 129-52.

34. Ibarra, J.E. and B.A. Federici, *Isolation of a relatively nontoxic 65-kilodalton protein inclusion from the parasporal body of Bacillus thuringiensis subsp. israelensis.* J Bacteriol, 1986. **165**(2): p. 527-33.

35. Cohen, S., et al., *High-resolution crystal structure of activated Cyt2Ba monomer from Bacillus thuringiensis subsp. israelensis.* J Mol Biol, 2008. **380**(5): p. 820-7.

36. Goldberg, L.J., and Margalit, J., *A bacterial spore demonstrating rapid larvicidal activity against Anopheles sergantii, Uranotaenia ungguiculata, Culex univitattus, Aedes aegypti, and Culex pipines.* Mosquito News, 1977. **37**: p. 355-358.

37. Thomas, W.E. and D.J. Ellar, *Bacillus thuringiensis var israelensis crystal delta-endotoxin: effects on insect and mammalian cells in vitro and in vivo.* J Cell Sci, 1983. **60**: p. 181-97.

38. Koni, P.A. and D.J. Ellar, *Cloning and characterization of a novel Bacillus thuringiensis cytolytic delta-endotoxin.* J Mol Biol, 1993. **229**(2): p. 319-27.

39. Li, X., Nevels, K. J., Gryczynski, Z., Gryczynski, I., Pusztai-Carey, M., Xie, D., and Butko, P., *A Molecular Dynamics Model of the Bt Toxin Cyt1A And Its Validation by Resonance Energy Transfer.* Biophysical Chemistry, 2009. **(under revision)**.

40. Guex, N. and M.C. Peitsch, *SWISS-MODEL and the Swiss-PdbViewer: an environment for comparative protein modeling.* Electrophoresis, 1997. **18**(15): p. 2714-23.

41. Ward, E.S., D.J. Ellar, and C.N. Chilcott, *Single amino acid changes in the Bacillus thuringiensis var. israelensis delta-endotoxin affect the toxicity and expression of the protein.* J Mol Biol, 1988. **202**(3): p. 527-35.

42. Wirth, M.C., et al., *Evolution of resistance toward Bacillus sphaericus or a mixture of B. sphaericus+Cyt1A from Bacillus thuringiensis, in the mosquito, Culex quinquefasciatus (Diptera: Culicidae).* J Invertebr Pathol, 2005. **88**(2): p. 154-62.

43. Butko, P., et al., *Membrane permeabilization induced by cytolytic delta-endotoxin CytA from Bacillus thuringiensis var. israelensis.* Biochemistry, 1996. **35**(35): p. 11355-60.

44. Du, J., et al., *Biochemical characterization of Bacillus thuringiensis cytolytic toxins in association with a phospholipid bilayer.* Biochem J, 1999. **338 (Pt 1)**: p. 185-93.

45. Butko, P., et al., *Interaction of the delta-endotoxin CytA from Bacillus thuringiensis var. israelensis with lipid membranes.* Biochemistry, 1997. **36**(42): p. 12862-8.

46. Collier, R.J. and J.A. Young, *Anthrax toxin.* Annu Rev Cell Dev Biol, 2003. **19**: p. 45-70.

47. Sellman, B.R., S. Nassi, and R.J. Collier, *Point mutations in anthrax protective antigen that block translocation.* J Biol Chem, 2001. **276**(11): p. 8371-6.

48. Ptitsyn, O.B., et al., *Evidence for a molten globule state as a general intermediate in protein folding.* FEBS Lett, 1990. **262**(1): p. 20-4.

49. van der Goot, F.G., et al., *The cytolytic toxin aerolysin: from the soluble form to the transmembrane channel.* Toxicology, 1994. **87**(1-3): p. 19-28.

50. Chow, E., G.J. Singh, and S.S. Gill, *Binding and aggregation of the 25-kilodalton toxin of Bacillus thuringiensis subsp. israelensis to cell membranes and alteration by monoclonal antibodies and amino acid modifiers.* Appl Environ Microbiol, 1989. **55**(11): p. 2779-88.

51. Manceva, S., Pusztai-Carey M, Russo PS, Butko P., *A Detergent-like Mechanism of Action of the Cytolytic Toxin Cyt1A from Bacillus thuringiensis var. israelensis.* Biochemistry, 2005. **44**(2): p. 589-597.

52. Walker, B., et al., *Assembly of the oligomeric membrane pore formed by Staphylococcal alpha-hemolysin examined by truncation mutagenesis.* J Biol Chem, 1992. **267**(30): p. 21782-6.

53. Park, H., et al., *Differential enhancement of Cry2A versus Cry11A yields in Bacillus thuringiensis by use of the cry3A STAB mRNA sequence.* FEMS Microbiol Lett, 1999. **181**(2): p. 319-27.

54. Park, H.W., et al., *Recombinant larvicidal bacteria with markedly improved efficacy against culex vectors of west nile virus.* Am J Trop Med Hyg, 2005. **72**(6): p. 732-8.

55. Chilcott, C.N. and D.J. Ellar, *Comparative toxicity of Bacillus thuringiensis var. israelensis crystal proteins in vivo and in vitro.* J Gen Microbiol, 1988. **134**(9): p. 2551-8.

56. Schneider, J.M., C.I. Barrett, and S.S. York, *lac Repressor cysteine-140 reacts selectively with a fluorescent probe bound to the core-headpiece interface.* Biochemistry, 1984. **23**(10): p. 2221-6.

57. Haugland, R.P., *Handbook of fluorescent probes and research products*, ed. J. Gregory. 2002.

58. Sellman, B.R., B.L. Kagan, and R.K. Tweten, *Generation of a membrane-bound, oligomerized pre-pore complex is necessary for pore formation by Clostridium septicum alpha toxin.* Mol Microbiol, 1997. **23**(3): p. 551-8.

59. Promdonkoy, B., et al., *Amino acid substitutions in alphaA and alphaC of Cyt2Aa2 alter hemolytic activity and mosquito-larvicidal specificity.* J Biotechnol, 2008. **133**(3): p. 287-93.

60. Van Der Meer, B.W., G. Coker, and S.Y. Simon Chen, *Resonance Energy Transfer: Theory and Data*. 1994: VCH Publishers, INC.

61. Lakowicz, J.R., *Principles of Fluorescence Spectroscopy*. 2nd Edition ed. 1999, New York: Springer.

62. Xie, J., P. Butko, and D. Xie, *Molecular dynamics simulations of the cytolytic toxin Cyt1A in solution.* IEEE Trans Nanobioscience, 2005. **4**(3): p. 235-40.

63. Humphrey, W., A. Dalke, and K. Schulten, *VMD: visual molecular dynamics.* J Mol Graph, 1996. **14**(1): p. 33-8, 27-8.

64. Corry, B., D. Jayatilaka, and P. Rigby, *A flexible approach to the calculation of resonance energy transfer efficiency between multiple donors and acceptors in complex geometries.* Biophys J, 2005. **89**(6): p. 3822-36.

CHAPTER 5: Future Studies

5.1 Future Studies: Evaluating Small Molecules Targeting MAP Kinases and Their Regulation of Protein Substrate Interactions

Fluorescence spectroscopy was used to characterize the binding of test compounds to ERK2 utilizing the naturally occurring tryptophan residues as monitors of protein conformational change. Upon titrating ERK2 protein with the test compound, binding affinity was quantified by plotting quenching of Trp fluorescence as a function of increasing concentrations of test compound. Situations in which test compounds absorb and/or fluoresce at the excitation and emission wavelength range of the protein can complicate data interpretation. Significant absorption by the test compounds in the protein's excitation and emission wavelength range erroneously mimicked Trp fluorescence quenching. The apparent decrease was often accompanied by a shift in the Trp emission peak. In Chapter 2, it was shown that applying a correction factor eliminated the shift and the apparent fluorescence decrease. Yet those compounds that strongly absorb at relatively lower concentrations of test compounds put a limit on the titration range, possibly resulting in inaccurate binding affinities. Likewise, auto-fluorescing compounds that directly bind to ERK2 can also mimic quenching of Trp fluorescence. Though fluorescence spectroscopy is a convenient technique, it is not without its limitations. For future studies, I suggest complementing the data previously discussed with alternative techniques such as isothermal titration calorimetry (ITC).

ITC directly measures the heat absorbed or released during a binding event and provides data such as the binding constants in addition to the binding enthalpy (ΔH) and the binding stoichiometry of the compounds with - in this case - ERK2 [1]. Additional information such as the entropy of binding (ΔS) and the number of binding sites can be

determined. When measuring binding interactions with fluorescence spectroscopy as previously mentioned, the spectral properties of the compounds being tested must be considered. Binding interactions measured by ITC are not influenced by the absorbance and/or fluorescence that some test compounds display. ITC has the added advantage over fluorescence techniques of allowing poorly quenching and/or nonquenching test compounds that display activity in biological assays to be studied. A limitation of this technique is that systems with extremely tight binding affinities may not be measured accurately. Also, ITC requires high protein and ligand concentrations, which may be a limiting factor for compounds that are purchased.

In Chapters 2 and 3, test compounds that were active against ERK2 were tested for selectivity against structurally similar kinases, specifically p38α. p38α shares similar activation loop sequences as well as similarities in the CD and ED docking domain as compared to ERK2. Though a number of active compounds observed in this study show selectivity for ERK2, it is necessary to test these compounds against other members of the MAP kinase family. A high-throughput fluorescence screening assay has been developed and will be used to verify that the active compounds do not bind to other structurally similar kinases (such as JNK). In addition it will be necessary to perform substrate phosphorylation assays with substrates specific for the structurally similar kinases being tested. The most time consuming would likely be protein expression and purification of both the MAP kinases and the substrates being tested. Possible limitations would be acquiring antibodies specific for the various substrates being tested for Western analysis.

Our lab has used cell proliferation assays to identify test compounds that have biological activity. Substrate phosphorylation assays have been used to identify compounds that interfere with phosphorylation of ERK substrates. Fluorescence based assays have been used to quantify the binding interactions of active test compounds. The next logical step would be to observe in real time the ability of the test compounds to selectively disrupt ERK2 protein-substrate interactions. Our lab has already investigated and quantified ERK2 interactions with known ERK2 substrates using surface plasmon resonance (SPR) [2]. In addition, individual contributions of the two known docking sites of the substrates being studied were measured [2]. Using the binding affinities attained from these studies as a reference, SPR can be used to measure the binding interactions of ERK2 protein with its substrates in the presence of test compounds. Changes in binding affinities of the system in the presence/absence of test compound will suggest selective inhibition.

Further validation of binding of test compounds to ERK2 will be gained by obtaining the X-ray crystal structure of active compounds discovered in these studies to support CADD based predictions of binding sites of test compounds and to direct compound optimization. It is suggested that **SF-2-054** be subjected to further modifications to better understand which chemical groups are responsible for the compounds' biological effects and to improve its selectivity for substrates of ERK involved in cell survival. Eventually, **SF-2-054** should be tested for inhibitory effects on tumor growth in animal models. The ultimate goal will be for the active compounds to be taken into clinical trials.

5.2 Future Studies: Lipid-Induced Conformation Changes of the Cytolytic Toxin Cyt2Aa2

As discussed in Chapter 4, the X-ray structure of one member of the Cyt family - Cyt2Aa2, hereafter referred to as Cyt2A - was solved by Li et.al. and is shown to consist of a single domain resembling a three layered core comprising two α-helix hairpins wrapped around a core of mixed β-sheets [3]. This structure was used as a basis to predict the structure of Cyt1A since it is believed that the structures and mechanism of action of Cyt proteins are similar due to their homologous amino acid sequences. A common characteristic of all Cyt toxins is that they can interact with membranes composed of synthetic lipids suggesting that no protein receptor is necessary [4, 5]. Presently the molecular details of Cyt toxin's mechanism of action are not clearly defined, though two models currently exist: the pore forming model as proposed by Promdonkoy and Ellar [6] and the detergent-like model as proposed by Butko [7].

The overall goal of our study with Cyt toxins was to determine the molecular details of the mechanism of action of Cyt toxins. Previous experiments were performed using Cyt1A as the model toxin. Currently active Cyt1A toxin cannot be produced for various reasons; therefore I propose that studies may be continued utilizing Cyt2A. The directives set forth in this proposal will be aimed at characterizing the conformation change that Cyt2A undergoes as it interacts with the lipid membrane.

To characterize the lipid-induced conformation change that Cyt2A undergoes, we propose the following experiments. First, the lifetime of both Cyt2Awild-type and W157F in the absence of lipid and in the presence of lipid will be measured. It is necessary to take into consideration scattering by the lipid vesicles. The Trp mutant will

make the study less ambiguous. Moreover, the two remaining Trp in the mutant are not as close in proximity (Trp 132 in αD, Trp 154 in β4).

Sangcharoen et. al state that a stable intermediate state similar to molten-globule like state has been identified [8]. Surface accessibility of aggregates in the molten-globule-like state has been studied by monitoring excimer fluorescence [9]. Time-resolved FRET has also been used to study unfolding reactions (native to molten-globule state) via changes in distance between the donor-acceptor pair Trp-IAEDANS labeled Cys [10]. It is suggested that the average Trp lifetime of Cyt2A (both wild-type and W157F mutant) at each conformation state of the unfolding pathway of Cyt2A as defined by Sangcharoen et. al be determined [8]. Granted the molten-globule state does not have a defined tertiary structure; it would be interesting to compare the lifetime value calculated in the molten-globule state with the calculated lifetime of Cyt2A in the presence of lipid. If the values are in agreement, it may be possible to study conformation change of Cyt proteins using artificial conditions to minimize complications caused by presence of lipid.

FRET can be used to calculate the intramolecular distance changes between fluorescently labeled mutant cysteine residues and Trp in the presence of lipid-induced and/or chemically-induced conformation change. According to the pore model, β5, β6, and β7 of Cyt2A span the lipid bilayer. Several cysteine mutants located within these regions will be created and subsequently labeled with IAEDANS. E178 is located in the β5-β6 loop region. In the presence of lipid, this portion is suggested to be in the aqueous phase of the inner bilayer. Energy transfer between Trp residues (on the outer surface of the membrane) and the fluorescently labeled E178C will be measured and the distance

calculated. A decrease in energy transfer translates into an increase in distance between the labeled region and Trp. Having two Trp residues introduces the question of what distance is being measured? If the β strands do span the bilayer, however, an average distance of ≥ 4 nm will tell us that the Trp (thought to be on the outer surface of the bilayer) and E178C (thought to be on the inner surface of the bilayer) are on opposite sides of the bilayer. L172 and L187 are located on β5 and β6 strands, respectively. Both residues will be replaced by cysteine and fluorescently labeled. FRET will be used to measure distance changes that occur upon conformation change. If the residues are located within the bilayer, we expect to see a marked decrease in energy transfer upon interaction with lipid (in conjunction with quenching of the fluorescently labeled cysteines by acrylamide and/or iodide quenchers). V125 is located in the αC/αD loop region. Of interest is the fact that this residue is very close in proximity to W134. Therefore we will assume that W134 primarily donates energy to fluorescently labeled V125C and W154 contribution is negligible. Because V125C is located in the loop region of αC/αD and the Trp donor is located in αD, lipid-induced conformation change of the protein should not cause a significant change in distance between the donor/acceptor pair. FRET data in conjunction with fluorescence quenching of the labeled cysteine mutants will provide information as to the location of the selected regions of the toxin in relation to the lipid membrane. As a side note, data from this experiment will provide information about energy transfer with multiple donors.

It is well known that Cyt toxins bind to the lipid membrane to initiate their toxic effects [6, 7]. How the toxin arranges itself with the lipid membrane is unkown. In order to characterize the interaction of Cyt2A with the lipid bilayer, the exposure of judiciously

selected regions of Cyt2A to the membrane phase will be probed. Intermolecular distances (by FRET) between Cyt2A and the lipid membrane will be determined by taking fluorescence measurements between the toxin and various lipid membrane probes. Single-cysteine mutants of Cyt2A discussed previously will be labeled with a fluorophore (IAEDANS and/or Acrylodan). Labeled lipids (DPH, TMA-DPH, and/or rhodamine DHPE, for ex.) will serve as the acceptor. Either Trp or fluorescently labeled cysteine will serve as the donor. A mixture of labeled and unlabeled Cyt2A mutants will be exposed to increasing concentration of fluorescently labeled lipid vesicles. FRET will be used to estimate average intermolecular distances between the donor-acceptor pair. The values will aid in determining the extent of Cyt2A insertion into the lipid bilayer. Changes in fluorescence anisotropy will be used to assess interaction of Cyt2A with either DPH or TMA-DPH labeled lipids. As previously mentioned, Cyt2A mutants L172C and L187C are located on β5 and β6 strands. DPH associates inside the lipid bilayer whereas TMA-DPH is anchored on the membrane surface. Comparing data from FRET experiments between L172C/L187C and both DPH and TMA-DPH will provide insight on the depth of insertion of β5 and β6 strands. Likewise, FRET experiments using V125 C (located in the loop region between αC and αD) and DPH/TMA-DPH or rhodamine DHPE will provide insight on the location of the alpha helix hairpin which is said to flay the lipid membrane surface like an umbrella being opened.

5.3 List of References

1. Burkhard, K., et al., *Development of extracellular signal-regulated kinase inhibitors.* Curr Top Med Chem, 2009. **9**(8): p. 678-89.
2. Burkhard, K.A., F. Chen, and P. Shapiro, *Quantitative analysis of ERK2 interactions with substrate proteins: roles for kinase docking domains and activity in determining binding affinity.* J Biol Chem, 2011.
3. Li, J., P.A. Koni, and D.J. Ellar, *Structure of the mosquitocidal delta-endotoxin CytB from Bacillus thuringiensis sp. kyushuensis and implications for membrane pore formation.* J Mol Biol, 1996. **257**(1): p. 129-52.
4. Haider, M.Z. and D.J. Ellar, *Mechanism of action of Bacillus thuringiensis insecticidal delta-endotoxin: interaction with phospholipid vesicles.* Biochim Biophys Acta, 1989. **978**(2): p. 216-22.
5. Thomas, W.E. and D.J. Ellar, *Mechanism of action of Bacillus thuringiensis var israelensis insecticidal delta-endotoxin.* FEBS Lett, 1983. **154**(2): p. 362-8.
6. Promdonkoy, B. and D.J. Ellar, *Investigation of the pore-forming mechanism of a cytolytic delta-endotoxin from Bacillus thuringiensis.* Biochem J, 2003. **374**(Pt 1): p. 255-9.
7. Butko, P., *Cytolytic toxin Cyt1A and its mechanism of membrane damage: data and hypotheses.* Appl Environ Microbiol, 2003. **69**(5): p. 2415-22.
8. Sangcharoen, A., et al., *Investigation of the unfolding pathway of Bacillus thuringiensis Cyt2Aa2 toxin reveals an unfolding intermediate.* J Biotechnol, 2009. **141**(3-4): p. 137-41.
9. Hammarstrom, P., et al., *Structural mapping of an aggregation nucleation site in a molten globule intermediate.* J Biol Chem, 1999. **274**(46): p. 32897-903.

10. Lakshmikanth, G.S., et al., *Structure is lost incrementally during the unfolding of barstar*. Nat Struct Biol, 2001. **8**(9): p. 799-804.

VI. BIBLIOGRAPHY

Adjei, A. A., R. B. Cohen, et al. (2008). "Phase I pharmacokinetic and pharmacodynamic study of the oral, small-molecule mitogen-activated protein kinase kinase 1/2 inhibitor AZD6244 (ARRY-142886) in patients with advanced cancers." J Clin Oncol **26**(13): 2139-46.

Ahn, N. G. (2009). "PORE-ing over ERK substrates." Nat Struct Mol Biol **16**(10): 1004-5.

Akella, R., T. M. Moon, et al. (2008). "Unique MAP Kinase binding sites." Biochim Biophys Acta **1784**(1): 48-55.

Al-yahyaee, S. A. and D. J. Ellar (1996). "Cell targeting of a pore-forming toxin, CytA delta-endotoxin from Bacillus thuringiensis subspecies israelensis, by conjugating CytA with anti-Thy 1 monoclonal antibodies and insulin." Bioconjug Chem **7**(4): 451-60.

Anjum, R. and J. Blenis (2008). "The RSK family of kinases: emerging roles in cellular signalling." Nat Rev Mol Cell Biol **9**(10): 747-58.

Aronson, A. I., W. Beckman, et al. (1986). "Bacillus thuringiensis and related insect pathogens." Microbiol Rev **50**(1): 1-24.

Aronson, A. I. Y. S. (2001). "Why *Bacillus thuringiensis* insecticidal toxins are so effective: unique features of their mode of action." FEMS Microbiol Lett **195**: 1-8.

Bardwell, A. J., M. Abdollahi, et al. (2003). "Docking sites on mitogen-activated protein kinase (MAPK) kinases, MAPK phosphatases and the Elk-1 transcription factor

compete for MAPK binding and are crucial for enzymic activity." Biochem J **370**(Pt 3): 1077-85.

Birdsall, B., R. W. King, et al. (1983). "Correction for light absorption in fluorescence studies of protein-ligand interactions." Anal Biochem **132**(2): 353-61.

Boston, S. R., R. Deshmukh, et al. (2011). "Characterization of ERK docking domain inhibitors that induce apoptosis by targeting Rsk-1 and caspase-9." BMC cancer **11**: 7.

Boulton, T. G., G. D. Yancopoulos, et al. (1990). "An insulin-stimulated protein kinase similar to yeast kinases involved in cell cycle control." Science **249**(4964): 64-7.

Bourbon-Freie, A., R. E. Dub, et al. (2009). "Trp-107 and trp-253 account for the increased steady state fluorescence that accompanies the conformational change in human pancreatic triglyceride lipase induced by tetrahydrolipstatin and bile salt." J Biol Chem **284**(21): 14157-64.

Bulla, L. A., Jr., K. J. Kramer, et al. (1981). "Purification and characterization of the entomocidal protoxin of Bacillus thuringiensis." J Biol Chem **256**(6): 3000-4.

Burges, H. D., Ed. (1981). Microbial control of pests and plant diseases. New York, Academic Press.

Burkhard, K., S. Smith, et al. (2009). "Development of extracellular signal-regulated kinase inhibitors." Curr Top Med Chem **9**(8): 678-89.

Burkhard, K. A., F. Chen, et al. (2011). "Quantitative analysis of ERK2 interactions with substrate proteins: roles for kinase docking domains and activity in determining binding affinity." J Biol Chem.

Butko, P. (2003). "Cytolytic toxin Cyt1A and its mechanism of membrane damage: data and hypotheses." Appl Environ Microbiol **69**(5): 2415-22.

Butko, P., F. Huang, et al. (1996). "Membrane permeabilization induced by cytolytic delta-endotoxin CytA from Bacillus thuringiensis var. israelensis." Biochemistry **35**(35): 11355-60.

Butko, P., F. Huang, et al. (1997). "Interaction of the delta-endotoxin CytA from Bacillus thuringiensis var. israelensis with lipid membranes." Biochemistry **36**(42): 12862-8.

Cagnol, S. and J. C. Chambard (2010). "ERK and cell death: mechanisms of ERK-induced cell death--apoptosis, autophagy and senescence." The FEBS journal **277**(1): 2-21.

Cai, L. and M. Gochin (2007). "A novel fluorescence intensity screening assay identifies new low-molecular-weight inhibitors of the gp41 coiled-coil domain of human immunodeficiency virus type 1." Antimicrob Agents Chemother **51**(7): 2388-95.

Callis, P. R. (1997). "1La and 1Lb transitions of tryptophan: applications of theory and experimental observations to fluorescence of proteins." Methods Enzymol **278**: 113-50.

Camps, M., A. Nichols, et al. (2000). "Dual specificity phosphatases: a gene family for control of MAP kinase function." Faseb J **14**(1): 6-16.

Camps, M., A. Nichols, et al. (1998). "Catalytic activation of the phosphatase MKP-3 by ERK2 mitogen-activated protein kinase." Science **280**(5367): 1262-5.

Canagarajah, B. J., A. Khokhlatchev, et al. (1997). "Activation mechanism of the MAP kinase ERK2 by dual phosphorylation." Cell **90**(5): 859-69.

Chan, S. H., E. Y. Sun, et al. "Extracellular signal-regulated kinase 1/2 plays a pro-life role in experimental brain stem death via MAPK signal-interacting kinase at rostral ventrolateral medulla." J Biomed Sci **17**: 17.

Chaufaux, J., Marchal, N. Gilois, I. Jehanno, and C. Buisson (1997). "Investigation of natural strains of Bacillus thuringiensis in different biotopes throughout the world." Can. J. Microbiol. **43**: 337-343.

Chen, F., C. N. Hancock, et al. (2006). "Characterization of ATP-independent ERK inhibitors identified through in silico analysis of the active ERK2 structure." Bioorg Med Chem Lett **16**(24): 6281-7.

Chen, F., A. D. Mackerell, Jr., et al. (2008). "Using Caenorhabditis elegans as a model organism for evaluating extracellular signal-regulated kinase docking domain inhibitors." J Cell Commun Signal **2**(3-4): 81-92.

Chen, Z., T. B. Gibson, et al. (2001). "MAP kinases." Chem Rev **101**(8): 2449-76.

Chilcott, C. N. and D. J. Ellar (1988). "Comparative toxicity of Bacillus thuringiensis var. israelensis crystal proteins in vivo and in vitro." J Gen Microbiol **134**(9): 2551-8.

Chow, E., G. J. Singh, et al. (1989). "Binding and aggregation of the 25-kilodalton toxin of Bacillus thuringiensis subsp. israelensis to cell membranes and alteration by monoclonal antibodies and amino acid modifiers." Appl Environ Microbiol **55**(11): 2779-88.

Cohen, S., R. Cahan, et al. (2007). "Specific targeting to murine myeloma cells of Cyt1Aa toxin from Bacillus thuringiensis subspecies israelensis." J Biol Chem **282**(39): 28301-8.

Cohen, S., O. Dym, et al. (2008). "High-resolution crystal structure of activated Cyt2Ba monomer from Bacillus thuringiensis subsp. israelensis." J Mol Biol **380**(5): 820-7.

Cohen, Y., M. Xing, et al. (2003). "BRAF mutation in papillary thyroid carcinoma." Journal of the National Cancer Institute **95**(8): 625-7.

Collier, R. J. and J. A. Young (2003). "Anthrax toxin." Annu Rev Cell Dev Biol **19**: 45-70.

Corry, B., D. Jayatilaka, et al. (2005). "A flexible approach to the calculation of resonance energy transfer efficiency between multiple donors and acceptors in complex geometries." Biophys J **89**(6): 3822-36.

Crickmore, N., D. R. Zeigler, et al. (1998). "Revision of the nomenclature for the Bacillus thuringiensis pesticidal crystal proteins." Microbiol Mol Biol Rev **62**(3): 807-13.

Cuadrado, A. and A. R. Nebreda (2010). "Mechanisms and functions of p38 MAPK signalling." Biochem J **429**(3): 403-17.

Davies, H., G. R. Bignell, et al. (2002). "Mutations of the BRAF gene in human cancer." Nature **417**(6892): 949-54.

DeSilva, D. R., E. A. Jones, et al. (1998). "Inhibition of mitogen-activated protein kinase kinase blocks T cell proliferation but does not induce or prevent anergy." J Immunol **160**(9): 4175-81.

Dimitri, C. A., W. Dowdle, et al. (2005). "Spatially separate docking sites on ERK2 regulate distinct signaling events in vivo." Curr Biol **15**(14): 1319-24.

Drobniewski, F. A. and D. J. Ellar (1988). "Toxin-membrane interactions of *Bacillus thuringiensis* d-endotoxin." Biochem Soc. Trans. **16**: 38-40.

Du, J., B. H. Knowles, et al. (1999). "Biochemical characterization of Bacillus thuringiensis cytolytic toxins in association with a phospholipid bilayer." Biochem J **338 (Pt 1)**: 185-93.

Dudley, D. T., L. Pang, et al. (1995). "A synthetic inhibitor of the mitogen-activated protein kinase cascade." Proc Natl Acad Sci U S A **92**(17): 7686-9.

Duncia, J. V., J. B. Santella, 3rd, et al. (1998). "MEK inhibitors: the chemistry and biological activity of U0126, its analogs, and cyclization products." Bioorg Med Chem Lett **8**(20): 2839-44.

Dunlop, J., H. B. McIlvain, et al. (2005). "Characterization of novel aryl-ether, biaryl, and fluorene aspartic acid and diaminopropionic acid analogs as potent inhibitors of the high-affinity glutamate transporter EAAT2." Mol Pharmacol **68**(4): 974-82.

Enslen, H. and R. J. Davis (2001). "Regulation of MAP kinases by docking domains." Biol Cell **93**(1-2): 5-14.

Fantz, D. A., D. Jacobs, et al. (2001). "Docking sites on substrate proteins direct extracellular signal-regulated kinase to phosphorylate specific residues." J Biol Chem **276**(29): 27256-65.

Favata, M. F., K. Y. Horiuchi, et al. (1998). "Identification of a novel inhibitor of mitogen-activated protein kinase kinase." J Biol Chem **273**(29): 18623-32.

Federici, B. A. (1998). "Cyt1Aa protein of *Bacillus thuringiensis* is toxic to the Cottonwood Leaf Beetle, *Chrysomela scripta*, and suppresses high levels of resistance to Cry3Aa." Appl Environ Microbiol **64**(11): 4368-4371.

Federici, B. A., Hyun-Woo Park, Yuko Sakano (2006). Insecticidal Protein Crystals of *Bacillus thuringiensis*. Microbiology Monographs, Springer Berlin/Heidelberg. **1/2006:** 195-236.

Federici, B. A., H. W. Park, et al. (2003). "Recombinant bacteria for mosquito control." J Exp Biol **206**(Pt 21): 3877-85.

Ferrell, J. E., Jr. and R. R. Bhatt (1997). "Mechanistic studies of the dual phosphorylation of mitogen-activated protein kinase." J Biol Chem **272**(30): 19008-16.

Flaherty, K. T., I. Puzanov, et al. "Inhibition of mutated, activated BRAF in metastatic melanoma." N Engl J Med **363**(9): 809-19.

Galanis, A., S. H. Yang, et al. (2001). "Selective targeting of MAPKs to the ETS domain transcription factor SAP-1." J Biol Chem **276**(2): 965-73.

Gao, F., N. Bren, et al. (2005). "Agonist-mediated conformational changes in acetylcholine-binding protein revealed by simulation and intrinsic tryptophan fluorescence." J Biol Chem **280**(9): 8443-51.

Gavin, A. C., A. Ni Ainle, et al. (1999). "A p90(rsk) mutant constitutively interacting with MAP kinase uncouples MAP kinase from p34(cdc2)/cyclin B activation in Xenopus oocytes." Mol Biol Cell **10**(9): 2971-86.

Geoghegan, K. F. (1996). "Improved method for converting an unmodified peptide to an energy-transfer substrate for a proteinase." Bioconjug Chem **7**(3): 385-91.

Gingrich, R. E., N. Allan, et al. (1974). "Bacillus thuringiensis: laboratory tests against four species of biting lice (Mallophaga: Trichodectidae)." J Invertebr Pathol **23**(2): 232-6.

Goldberg, L. J., and Margalit, J. (1977). "A bacterial spore demonstrating rapid larvicidal activity against Anopheles sergantii, Uranotaenia ungguiculata, Culex univitattus, Aedes aegypti, and Culex pipines." Mosquito News **37**: 355-358.

Grochulski, P., L. Masson, et al. (1995). "Bacillus thuringiensis CryIA(a) insecticidal toxin: crystal structure and channel formation." J Mol Biol **254**(3): 447-64.

Gryczynski, I., W. Wiczk, et al. (1988). "Lifetime distributions and anisotropy decays of indole fluorescence in cyclohexane/ethanol mixtures by frequency-domain fluorometry." Biophys Chem **32**(2-3): 173-85.

Guex, N. and M. C. Peitsch (1997). "SWISS-MODEL and the Swiss-PdbViewer: an environment for comparative protein modeling." Electrophoresis **18**(15): 2714-23.

Haider, M. Z. and D. J. Ellar (1989). "Mechanism of action of Bacillus thuringiensis insecticidal delta-endotoxin: interaction with phospholipid vesicles." Biochim Biophys Acta **978**(2): 216-22.

Hammarstrom, P., M. Persson, et al. (1999). "Structural mapping of an aggregation nucleation site in a molten globule intermediate." J Biol Chem **274**(46): 32897-903.

Hancock, C. N., A. Macias, et al. (2005). "Identification of novel extracellular signal-regulated kinase docking domain inhibitors." Journal of medicinal chemistry **48**(14): 4586-95.

Hasselbacher, C. A., E. Rusinova, et al. (1995). "Environments of the four tryptophans in the extracellular domain of human tissue factor: comparison of results from absorption and fluorescence difference spectra of tryptophan replacement mutants with the crystal structure of the wild-type protein." Biophys J **69**(1): 20-9.

Haugland, R. P. (2002). Handbook of fluorescent probes and research products.

Hicks, L. D., J. L. Hyatt, et al. (2009). "Improved, selective, human intestinal carboxylesterase inhibitors designed to modulate 7-ethyl-10-[4-(1-piperidino)-1-piperidino]carbonyloxycamptothecin (Irinotecan; CPT-11) toxicity." J Med Chem **52**(12): 3742-52.

Hingorani, S. R., M. A. Jacobetz, et al. (2003). "Suppression of BRAF(V599E) in human melanoma abrogates transformation." Cancer Res **63**(17): 5198-202.

Hoffman, D., P. Luthy, R. Hutter, and V. Pliska (1988). "Binding of the d-endotoxin of *Bacillus thuringiensis* to brush-border membrane vesicles of the cabbage butterfly (*Pieris brassiacae*)." Eur J Biochem **173**: 85-91.

Hofte, H. and H. R. Whiteley (1989). "Insecticidal crystal proteins of Bacillus thuringiensis." Microbiol Rev **53**(2): 242-55.

Hong, S. K., S. Yoon, et al. (2009). "Noncatalytic function of ERK1/2 can promote Raf/MEK/ERK-mediated growth arrest signaling." J Biol Chem **284**(48): 33006-18.

Hu, Y. J., Y. Liu, et al. (2005). "Interaction of colchicine with human serum albumin investigated by spectroscopic methods." Int J Biol Macromol **37**(3): 122-6.

Humphrey, W., A. Dalke, et al. (1996). "VMD: visual molecular dynamics." J Mol Graph **14**(1): 33-8, 27-8.

Ibarra, J. E. and B. A. Federici (1986). "Isolation of a relatively nontoxic 65-kilodalton protein inclusion from the parasporal body of Bacillus thuringiensis subsp. israelensis." J Bacteriol **165**(2): 527-33.

Jacobs, D., D. Glossip, et al. (1999). "Multiple docking sites on substrate proteins form a modular system that mediates recognition by ERK MAP kinase." Genes Dev **13**(2): 163-75.

Jameson, D. M., E. Gratton, et al. (1987). "Intrinsic fluorescence of elongation factor Tu in its complexes with GDP and elongation factor Ts." Biochemistry **26**(13): 3894-901.

Karasarides, M., A. Chiloeches, et al. (2004). "B-RAF is a therapeutic target in melanoma." Oncogene **23**(37): 6292-8.

Keyse, S. M. (2000). "Protein phosphatases and the regulation of mitogen-activated protein kinase signalling." Curr Opin Cell Biol **12**(2): 186-92.

Knowles, B. H., and D. J. Ellar (1987). "Colloid-osmotic lysis is a general feature of the mechanism of action of *Bacillus thuringiensis* delta-endotoxins with different insect specificity." Biochim. Biophys. Acta **924**: 509-518.

Knowles, B. H., M. R. Blatt, et al. (1989). "A cytolytic delta-endotoxin from Bacillus thuringiensis var. israelensis forms cation-selective channels in planar lipid bilayers." FEBS Lett **244**(2): 259-62.

Knowles, B. H. and D. J. Ellar (1988). "Differential specificity of two insecticidal toxins from Bacillus thuringiensis var. aizawai." Mol Microbiol **2**(1): 153-7.

Knowles, B. H. a. D. J. E. (1987). "Colloid-osmotic lysis is general feature of the mechanism of action of Bacillus thuringiensis delta-endotoxins with different insect specificity." Biochim Biophys Acta **924**: 509-518.

Kohno, M. and J. Pouyssegur (2006). "Targeting the ERK signaling pathway in cancer therapy." Ann Med **38**(3): 200-11.

Kolch, W. (2000). "Meaningful relationships: the regulation of the Ras/Raf/MEK/ERK pathway by protein interactions." Biochem J **351 Pt 2**: 289-305.

Koni, P. A. and D. J. Ellar (1993). "Cloning and characterization of a novel Bacillus thuringiensis cytolytic delta-endotoxin." J Mol Biol **229**(2): 319-27.

Kosinski-Collins, M. S. and J. King (2003). "In vitro unfolding, refolding, and polymerization of human gammaD crystallin, a protein involved in cataract formation." Protein Sci **12**(3): 480-90.

Krieg, A. F. (1971). "Concerning alpha-endotoxin produced by vegetative cells of Bacillus thuringiensis and Bacillus cereus." J. Invertebrate Pathol. **17**: 134-135.

Lakowicz, J. R. (1999). Principles of Fluorescence Spectroscopy. New York, Springer.

Lakshmikanth, G. S., K. Sridevi, et al. (2001). "Structure is lost incrementally during the unfolding of barstar." Nat Struct Biol **8**(9): 799-804.

Lasagna, M., E. Gratton, et al. (1999). "Apohorseradish peroxidase unfolding and refolding: intrinsic tryptophan fluorescence studies." Biophys J **76**(1 Pt 1): 443-50.

Lee, T., A. N. Hoofnagle, et al. (2004). "Docking motif interactions in MAP kinases revealed by hydrogen exchange mass spectrometry." Mol Cell **14**(1): 43-55.

Lenormand, P., C. Sardet, et al. (1993). "Growth factors induce nuclear translocation of MAP kinases (p42mapk and p44mapk) but not of their activator MAP kinase kinase (p45mapkk) in fibroblasts." J Cell Biol **122**(5): 1079-88.

Lewis, T. S., P. S. Shapiro, et al. (1998). "Signal transduction through MAP kinase cascades." Adv Cancer Res **74**: 49-139.

Li, J., P. A. Koni, et al. (1996). "Structure of the mosquitocidal delta-endotoxin CytB from Bacillus thuringiensis sp. kyushuensis and implications for membrane pore formation." J Mol Biol **257**(1): 129-52.

Li, J. D., J. Carroll, et al. (1991). "Crystal structure of insecticidal delta-endotoxin from Bacillus thuringiensis at 2.5 A resolution." Nature **353**(6347): 815-21.

Li, X., Nevels, K. J., Gryczynski, Z., Gryczynski, I., Pusztai-Carey, M., Xie, D., and Butko, P. (2009). "A Molecular Dynamics Model of the Bt Toxin Cyt1A And Its Validation by Resonance Energy Transfer." Biophysical Chemistry **(under revision)**.

Lyons, J. F., S. Wilhelm, et al. (2001). "Discovery of a novel Raf kinase inhibitor." Endocr Relat Cancer **8**(3): 219-25.

Macias AT, Mia MY, et al. (2005). "Lead validation and SAR development via chemical similarity searching; application to compounds targeting the pY+3 site of the SH2 domain of p56lck. ." J Chem Inf Model **45**: 1759-1766.

MacKenzie, S. J., G. S. Baillie, et al. (2000). "ERK2 mitogen-activated protein kinase binding, phosphorylation, and regulation of the PDE4D cAMP-specific phosphodiesterases. The involvement of COOH-terminal docking sites and NH2-terminal UCR regions." J Biol Chem **275**(22): 16609-17.

Manceva, S., Pusztai-Carey M, Russo PS, Butko P. (2005). "A Detergent-like Mechanism of Action of the Cytolytic Toxin Cyt1A from Bacillus thuringiensis var. israelensis." Biochemistry **44**(2): 589-597.

Martin, M. C., L. A. Allan, et al. (2008). "The docking interaction of caspase-9 with ERK2 provides a mechanism for the selective inhibitory phosphorylation of caspase-9 at threonine 125." J Biol Chem **283**(7): 3854-65.

Murphy, L. O., S. Smith, et al. (2002). "Molecular interpretation of ERK signal duration by immediate early gene products." Nat Cell Biol **4**(8): 556-64.

Nikiforova, M. N., E. T. Kimura, et al. (2003). "BRAF mutations in thyroid tumors are restricted to papillary carcinomas and anaplastic or poorly differentiated carcinomas arising from papillary carcinomas." J Clin Endocrinol Metab **88**(11): 5399-404.

Ohori, M., T. Kinoshita, et al. (2005). "Identification of a selective ERK inhibitor and structural determination of the inhibitor-ERK2 complex." Biochem Biophys Res Commun **336**(1): 357-63.

Paris, M., J. P. David, et al. "Fitness costs of resistance to Bti toxins in the dengue vector Aedes aegypti." Ecotoxicology **20**(6): 1184-94.

Park, H., D. K. Bideshi, et al. (1999). "Differential enhancement of Cry2A versus Cry11A yields in Bacillus thuringiensis by use of the cry3A STAB mRNA sequence." FEMS Microbiol Lett **181**(2): 319-27.

Park, H. W., D. K. Bideshi, et al. (2005). "Recombinant larvicidal bacteria with markedly improved efficacy against culex vectors of west nile virus." Am J Trop Med Hyg **72**(6): 732-8.

Pearson, G., F. Robinson, et al. (2001). "Mitogen-activated protein (MAP) kinase pathways: regulation and physiological functions." Endocr Rev **22**(2): 153-83.

Polychronopoulos, S., M. Verykokakis, et al. (2006). "The transcriptional ETS2 repressor factor associates with active and inactive Erks through distinct FXF motifs." J Biol Chem **281**(35): 25601-11.

Polzien, L., A. Baljuls, et al. (2011). "BAD Contributes to RAF-mediated Proliferation and Cooperates with B-RAF-V600E in Cancer Signaling." The Journal of biological chemistry **286**(20): 17934-44.

Poulikakos, P. I., C. Zhang, et al. "RAF inhibitors transactivate RAF dimers and ERK signalling in cells with wild-type BRAF." Nature **464**(7287): 427-30.

Pratz, K. W., E. Cho, et al. "A pharmacodynamic study of sorafenib in patients with relapsed and refractory acute leukemias." Leukemia **24**(8): 1437-44.

Promdonkoy, B. and D. J. Ellar (2003). "Investigation of the pore-forming mechanism of a cytolytic delta-endotoxin from Bacillus thuringiensis." Biochem J **374**(Pt 1): 255-9.

Promdonkoy, B., A. Rungrod, et al. (2008). "Amino acid substitutions in alphaA and alphaC of Cyt2Aa2 alter hemolytic activity and mosquito-larvicidal specificity." J Biotechnol **133**(3): 287-93.

Ptitsyn, O. B., R. H. Pain, et al. (1990). "Evidence for a molten globule state as a general intermediate in protein folding." FEBS Lett **262**(1): 20-4.

Ren, J., S. Lew, et al. (1997). "Transmembrane orientation of hydrophobic alpha-helices is regulated both by the relationship of helix length to bilayer thickness and by the cholesterol concentration." Biochemistry **36**(33): 10213-20.

Robbins, D. J. and M. H. Cobb (1992). "Extracellular signal-regulated kinases 2 autophosphorylates on a subset of peptides phosphorylated in intact cells in

response to insulin and nerve growth factor: analysis by peptide mapping." Mol Biol Cell **3**(3): 299-308.

Robbins, D. J., E. Zhen, et al. (1993). "Regulation and properties of extracellular signal-regulated protein kinases 1 and 2 in vitro." J Biol Chem **268**(7): 5097-106.

Roberts, P. J. and C. J. Der (2007). "Targeting the Raf-MEK-ERK mitogen-activated protein kinase cascade for the treatment of cancer." Oncogene **26**(22): 3291-310.

Roux, P. P. and J. Blenis (2004). "ERK and p38 MAPK-activated protein kinases: a family of protein kinases with diverse biological functions." Microbiol Mol Biol Rev **68**(2): 320-44.

Rubinfeld, H., T. Hanoch, et al. (1999). "Identification of a cytoplasmic-retention sequence in ERK2." The Journal of biological chemistry **274**(43): 30349-52.

Samworth, C. M., M. Degli Esposti, et al. (1988). "Quenching of the intrinsic tryptophan fluorescence of mitochondrial ubiquinol--cytochrome-c reductase by the binding of ubiquinone." Eur J Biochem **171**(1-2): 81-6.

Sangcharoen, A., W. Tepanant, et al. (2009). "Investigation of the unfolding pathway of Bacillus thuringiensis Cyt2Aa2 toxin reveals an unfolding intermediate." J Biotechnol **141**(3-4): 137-41.

Satoh, Y., Y. Kobayashi, et al. "Deletion of ERK1 and ERK2 in the CNS causes cortical abnormalities and neonatal lethality: Erk1 deficiency enhances the impairment of neurogenesis in Erk2-deficient mice." J Neurosci **31**(3): 1149-55.

Schindler, J. F., J. B. Monahan, et al. (2007). "p38 pathway kinases as anti-inflammatory drug targets." J Dent Res **86**(9): 800-11.

Schneider, J. M., C. I. Barrett, et al. (1984). "lac Repressor cysteine-140 reacts selectively with a fluorescent probe bound to the core-headpiece interface." Biochemistry **23**(10): 2221-6.

Sebesra, K. a. H. S. (1970). "The specificity of inhibition of DNA-dependent RNA polymerase *Bacillus thuringiensis* exotoxin." FEBS Lett **8**: 233-235.

Sellman, B. R., B. L. Kagan, et al. (1997). "Generation of a membrane-bound, oligomerized pre-pore complex is necessary for pore formation by Clostridium septicum alpha toxin." Mol Microbiol **23**(3): 551-8.

Sellman, B. R., S. Nassi, et al. (2001). "Point mutations in anthrax protective antigen that block translocation." J Biol Chem **276**(11): 8371-6.

Shao, Z. (2001). "Effects of the 20-Kilodalton Helper Protein on Cry1Ac Production and Spore Formation in Bacillus thuringiensis." Appl Environ Microbiol **67**(12): 5362-5369.

Shapiro, P. S., A. M. Whalen, et al. (1999). "Extracellular signal-regulated kinase activates topoisomerase IIalpha through a mechanism independent of phosphorylation." Mol Cell Biol **19**(5): 3551-60.

Sharma, A., N. R. Trivedi, et al. (2005). "Mutant V599EB-Raf regulates growth and vascular development of malignant melanoma tumors." Cancer Res **65**(6): 2412-21.

Sheridan, D. L., Y. Kong, et al. (2008). "Substrate discrimination among mitogen-activated protein kinases through distinct docking sequence motifs." J Biol Chem **283**(28): 19511-20.

Sillen, A., S. Verheyden, et al. (2003). "Mechanism of fluorescence and conformational changes of the sarcoplasmic calcium binding protein of the sand worm Nereis diversicolor upon Ca2+ or Mg2+ binding." Biophys J **85**(3): 1882-93.

Smith, J. A., C. E. Poteet-Smith, et al. (1999). "Identification of an extracellular signal-regulated kinase (ERK) docking site in ribosomal S6 kinase, a sequence critical for activation by ERK in vivo." J Biol Chem **274**(5): 2893-8.

Solit, D. B. and N. Rosen "Resistance to BRAF inhibition in melanomas." N Engl J Med **364**(8): 772-4.

Tabashnik, B. E. (1994). "Evolution of resistance to Bacillus thuringiensis." Annu Rev. Entomol **39**: 47-79.

Tanoue, T., M. Adachi, et al. (2000). "A conserved docking motif in MAP kinases common to substrates, activators and regulators." Nat Cell Biol **2**(2): 110-6.

Tanoue, T., R. Maeda, et al. (2001). "Identification of a docking groove on ERK and p38 MAP kinases that regulates the specificity of docking interactions." The EMBO journal **20**(3): 466-79.

Tanoue, T., R. Maeda, et al. (2001). "Identification of a docking groove on ERK and p38 MAP kinases that regulates the specificity of docking interactions." Embo J **20**(3): 466-79.

Tanoue, T. and E. Nishida (2003). "Molecular recognitions in the MAP kinase cascades." Cell Signal **15**(5): 455-62.

Thomas, W. E. and D. J. Ellar (1983). "Bacillus thuringiensis var israelensis crystal delta-endotoxin: effects on insect and mammalian cells in vitro and in vivo." J Cell Sci **60**: 181-97.

Thomas, W. E. and D. J. Ellar (1983). "Mechanism of action of Bacillus thuringiensis var israelensis insecticidal delta-endotoxin." FEBS Lett **154**(2): 362-8.

Tiriveedhi, V. and P. Butko (2007). "A fluorescence spectroscopy study on the interactions of the TAT-PTD peptide with model lipid membranes." Biochemistry **46**(12): 3888-95.

Toho, A. a. K. A. (1983). "Dissolution and degradation of Bacillus thuringiensis d-endotoxins by gut juice protease of the silkworm Bombyx mori." Appl Environ Microbiol **45**: 576-580.

Ullrich, A. and J. Schlessinger (1990). "Signal transduction by receptors with tyrosine kinase activity." Cell **61**(2): 203-12.

Valeur, B. (2002). Molecular Fluorescence: Principles and Applications. Weinheim, Wiley-VCH.

van der Goot, F. G., F. Pattus, et al. (1994). "The cytolytic toxin aerolysin: from the soluble form to the transmembrane channel." Toxicology **87**(1-3): 19-28.

Van Der Meer, B. W., G. Coker, et al. (1994). Resonance Energy Transfer: Theory and Data, VCH Publishers, INC.

Van Rie, J., S. Jansens, et al. (1989). "Specificity of Bacillus thuringiensis delta-endotoxins. Importance of specific receptors on the brush border membrane of the mid-gut of target insects." Eur J Biochem **186**(1-2): 239-47.

Van Rie, J., S. Jansens, et al. (1990). "Receptors on the brush border membrane of the insect midgut as determinants of the specificity of *Bacillus thuringiensis* d-endotoxins." Appl Environ Microbiol **56**(5): 1378-1385.

Walker, B., M. Krishnasastry, et al. (1992). "Assembly of the oligomeric membrane pore formed by Staphylococcal alpha-hemolysin examined by truncation mutagenesis." J Biol Chem **267**(30): 21782-6.

Wan, P. T., M. J. Garnett, et al. (2004). "Mechanism of activation of the RAF-ERK signaling pathway by oncogenic mutations of B-RAF." Cell **116**(6): 855-67.

Ward, E. S., D. J. Ellar, et al. (1988). "Single amino acid changes in the Bacillus thuringiensis var. israelensis delta-endotoxin affect the toxicity and expression of the protein." J Mol Biol **202**(3): 527-35.

Wilhelm, S. M., C. Carter, et al. (2004). "BAY 43-9006 exhibits broad spectrum oral antitumor activity and targets the RAF/MEK/ERK pathway and receptor tyrosine kinases involved in tumor progression and angiogenesis." Cancer Res **64**(19): 7099-109.

Wirth, M. C., J. A. Jiannino, et al. (2005). "Evolution of resistance toward Bacillus sphaericus or a mixture of B. sphaericus+Cyt1A from Bacillus thuringiensis, in the mosquito, Culex quinquefasciatus (Diptera: Culicidae)." J Invertebr Pathol **88**(2): 154-62.

Xie, J., P. Butko, et al. (2005). "Molecular dynamics simulations of the cytolytic toxin Cyt1A in solution." IEEE Trans Nanobioscience **4**(3): 235-40.

Yamamoto, T. and R. E. McLaughlin (1981). "Isolation of a protein from the parasporal crystal of Bacillus thuringiensis var. Kurstaki toxic to the mosquito larva, Aedes taeniorhynchus." Biochem Biophys Res Commun **103**(2): 414-21.

Yang, Y. and C. Han "GDNF stimulates the proliferation of cultured mouse immature Sertoli cells via its receptor subunit NCAM and ERK1/2 signaling pathway." BMC Cell Biol **11**: 78.

Yoon, S. and R. Seger (2006). "The extracellular signal-regulated kinase: multiple substrates regulate diverse cellular functions." Growth Factors **24**(1): 21-44.

Zhang, F., A. Strand, et al. (1994). "Atomic structure of the MAP kinase ERK2 at 2.3 A resolution." Nature **367**(6465): 704-11.

Zhang, J., T. Oashi, et al. (2011). "Chemical control of a signaling crossroad: ATP-independent ERK2 inhibitors targeting substrate docking domains."

Zhang, J., B. Zhou, et al. (2003). "A bipartite mechanism for ERK2 recognition by its cognate regulators and substrates." J Biol Chem **278**(32): 29901-12.

Zhong, S., A. T. Macias, et al. (2007). "Computational identification of inhibitors of protein-protein interactions." Curr Top Med Chem **7**(1): 63-82.

Zhou, B., L. Wu, et al. (2001). "Multiple regions of MAP kinase phosphatase 3 are involved in its recognition and activation by ERK2." J Biol Chem **276**(9): 6506-15.

Zhou, T. J., L. G. Sun, et al. (2006). "Crystal structure of the MAP3K TAO2 kinase domain bound by an inhibitor staurosporine." Acta Biochim Biophys Sin (Shanghai) **38**(6): 385-92.

Zuniga, A., J. Torres, et al. (1999). "Interaction of mitogen-activated protein kinases with the kinase interaction motif of the tyrosine phosphatase PTP-SL provides substrate specificity and retains ERK2 in the cytoplasm." J Biol Chem **274**(31): 21900-7.